UNIVERSITY OF TWENTE.

CEM MSc Thesis

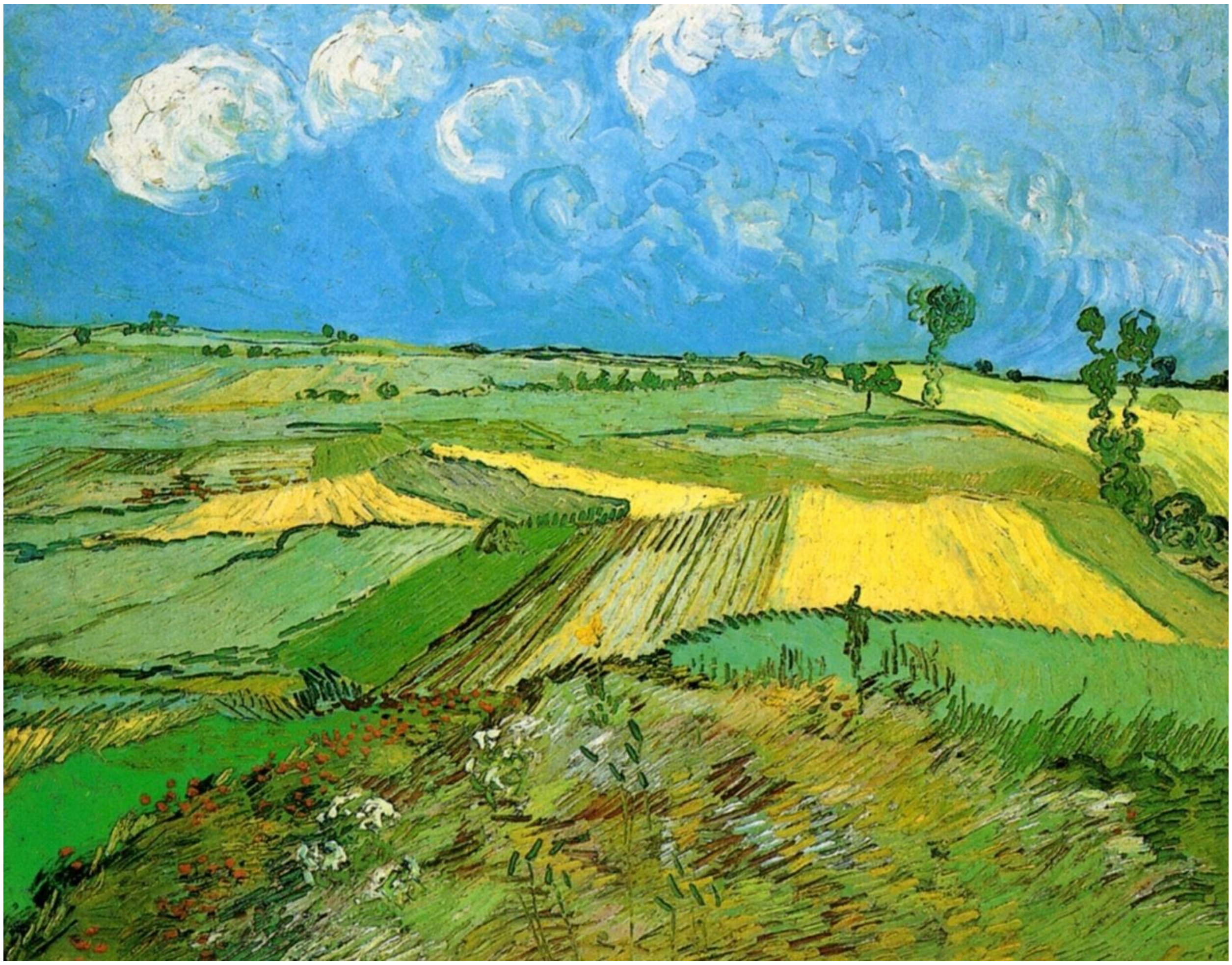

Impacts of climate change on drought in the Meuse basin

A new method to assess the impacts of climate change on drought based on output of regional climate models

Author:
H. Houtenbos

Supervisors:
Prof. dr. ir. A.Y. Hoekstra
Dr. ir. M.J. Booij

September 19, 2013

Colophon

Author: H. Houtenbos
Institute: University of Twente

Supervisors: Prof. dr. ir. A.Y. Hoekstra
University of Twente
Department of Water Engineering and Management

Dr. ir. M.J. Booij
University of Twente
Department of Water Engineering and Management

Date: August 29, 2013

Cover photo: Wheat Fields at Auvers Under Clouded Sky – Vincent van Gogh – 1890

Summary

In recent years it has become clear how vulnerable even industrialized and economically well-off regions like Europe can be to drought, when several severe and prolonged water deficit periods cause major environmental, social and economic problems. This seems to continue and can worsen when considering the possible impact of climate change in the 21st century. Climate impact studies on drought are obviously done to get a better understanding of the possible impact of a changed climate on drought, but also to identify different ways of analyzing drought. For many regions it is well established what the possible impact is, however mostly at a large spatial scale and with a high level of uncertainty.

This study tries to reduce this uncertainty and uses projections at a small spatial scale (±25km). The main purpose is twofold: to identify new methods to assess the impacts of climate change on drought and to apply these methods to a case study: the Meuse basin. Drought will be assessed by applying the Standardized Precipitation Index (SPI) on different time scales. A different time scale will relate to a different type of drought; from meteorological, agricultural and hydrological to extreme long-lasting events. Each type of drought relates to different physical conditions. For example meteorological drought can be seen as a significant deviation from the 'normal' of meteorological variables such as precipitation. The assessment is based on the output of thirteen high resolution Regional Climate Model (RCM) runs driven by five different Global Climate Models (GCMs). Only the A1B SRES emission scenario is used as climatic forcing. It is known that RCMs have difficulty with simulating spatial structures and this is assessed in this study specifically for drought. Other drought indicators were developed and applied to identify and quantify the number of events and its characteristics.

There is inherent uncertainty in these projections and related conclusions. Probably the most important source of uncertainty lies in the lack of using multiple emission scenarios in the impact analysis. Basically these emission scenarios are different storylines that could enfold in the 21st century. Furthermore, for most indicators and most RCMs the projection shows a large error between the simulated value and the observed one. I.e. the climate models have difficulty simulating drought. The impacts of climate change is expected to be larger then presented in this report. This is because the used drought identification method only incorporates precipitation, while it is known that other factors will influence the occurrence and the characteristics of drought. The main other factor is evapotranspiration which is largely determined by temperature. It is very likely that temperature will increase (globally) in the 21st century.

Overall it seems that the RCMs simulate a more temporal variable climate than observed. The spatial structure of drought frequencies in the basin is not simulated well by the RCMs. The best performing RCM run, in simulating the spatial structure of drought, had a small to significant (15%) average error for different time scales. For each drought indicator used in this study a weighted average is calculated based on the error of each RCM run. This weighted average is used to identify the main trend of the projection in future periods. In this way the quality of the RCM run (for that specific drought indicator) is taken into account.

Based on this weighted average it was found that for most time scales there will be a significant increase (range between +7% and +44%) in the number of drought events. Each time scale is denoted with a different number (1, 3, 6 or 12) reflecting the number of aggregated monthly precipitation values used in the SPI calculation.

For meteorological drought (SPI-1) it was found that the average duration increases (11%), the average deficit increases (40%) and the average intensity increases as well (28%). The variation in this characteristics changes even more than the average values. Meteorological drought will affect a larger area than the historical period. For agricultural drought (SPI-3) the average duration increases (14%), the average deficit increases (50%) and the average intensity increases as well (40%). The variation in this characteristics changes even more than the average values. Agricultural drought will affect a larger area than the historical period. For hydrological drought (SPI-6) the average duration does not increase significantly (less than 10%), the average deficit increases (34%) and the average intensity increases as well (27%). The variation in this characteristics changes even more than the average values. This type of drought will affect a larger area than the historical period. For extreme hydrological drought events (SPI-12) the average duration increases (12%), the average deficit increases (40%) and the average intensity increases as well (22%). The variation in this characteristics changes even more than the average values. Extreme drought will affect a larger area than the historical period.

Preface

This master thesis concludes the final part of my master Water Engineering and Management (WEM) at the University of Twente, Enschede. This thesis presents research concerning a climate impact study on drought in the Meuse basin. The research consisted mainly of programming and discussing the possibilities of the drought indicators. The main aim of this was to go from multiple European-wide precipitation datasets into ultimately the results as presented in this report. This research was carried out in the WEM-department of this university.

At first the main difficulty was to use the datasets since it was, for me, in an unknown format. It could be used by multiple programs and ironically it was specially constructed to make it easier for the researcher. It was another challenge to reduce these large datasets to the Meuse basin. The first step towards results was constructing the SPI method in Matlab and secondly to construct a script that could transform these SPI series into drought events. One major and important part of this research was constructing different drought statistics; how can drought and the change in drought be described? Eventually the statistics were reduced to what was seen as best fitting for this research. Another important part, and the more interesting one, was interpreting and discussing the results. Particular projections with the same climate model and the relation between different drought indicators were interesting. This gave, personally, a lot of interesting insight in how drought is constructed.

During this research project I was supervised by Arjen Hoekstra and Martijn Booij. I would like to thank my supervisors for their guidance and support. Martijn gave a lot of detailed feedback and was always willing to discuss new results. Each new result was greeted with a lot of enthusiasm. Arjen supervision was more focused on the overview of the process and the end product. Each meeting he provided the needed critical questions.

I would like to thank the roommates in the WEM graduation room. The coffee breaks, lunch walks and exchange of experiences provided the needed recreation and insight in the graduation process. Last but not least I am thankful to all friends and family for their support.

Hildemar Houtenbos

Enschede, September 2013

Table of contents

List of figures

List of tables

Chapter 1 Introduction

This chapter presents the outline of this research. Section 1.1 provides a description of the background of this research. Section 1.2 describes the state-of-the-art with respect to climate impact studies on drought. Section 1.3 defines the problem that this research will address. Section 1.4 presents the research objectives and questions. Section 1.5 summarizes the research strategy and provides an outline of the thesis.

1.1 Background

Drought is a phenomenon that can affect society and the environment. As Palmer (1965) states various people have different concerns which depend on the effects of a drought. According to a report from EEA (1999), European Environment Agency, it is shown that in recent years it has become clear how vulnerable even industrialized and economically well-off regions like Europe can be to drought, when several severe and prolonged water deficit periods cause major environmental, social and economic problems. This seems to continue: for example in Europe there was an exceptional drought in 2003 which was estimated to have cost 8.7 billion euro's (EEA, 2010). A potentially significant impact of climate change over many regions will be changes in the frequency and characteristics of droughts (Blenkinsop and Fowler, 2007).

The key factors to drought occurrence and drought severity are precipitation and evapotranspiration (Blenkinsop and Fowler, 2007). Therefore if climate change results in changes in one or both of these factors it can be expected that drought occurrence and its severity will change as well. Precipitation and evapotranspiration are part of the hydrological cycle and one of the key features of global climate change will be perturbations to the hydrological regime across Europe (Blenkinsop and Fowler, 2007). It is also expected that climate change can affect mean precipitation and its variability (Trenberth et al., 2003). A change in the precipitation mean and variability obviously influence the occurrence and severity of drought. According to a study by IPCC (2007) changes in temperature, radiation, atmospheric humidity, and wind speed will affect the amount of evaporation which can exaggerate effects of decreased precipitation on surface water and run-off. Evaporation is closely related to temperature (Thornthwaite, 1948). A study by Lenderink et al. (2007) suggests temperature and evaporation increase when imposing future climate boundary conditions on Europe. A study by Vicente-Serrano et al. (2010) suggests that temperature will play a major role in determining future drought severity. A similar conclusion by Wang et al. (2011) is drawn stressing the importance of temperature for drought. Furthermore according to a study by Schär et al. (2004) an increase in variability of temperature implies an increase in extremes climatic conditions.

Drought indices have been developed to objectively assess drought conditions and different kinds of drought. Looking only at meteorological drought, the departure from normal of meteorological variables that induces drying of the surface (Liu et al., 2012), it can be stated that duration, intensity and total deficit should be assessed. Liu et al. (2012) concluded that more drought indices from ecological and socioeconomic perspectives should be investigated and inter-compared to provide a more complete picture of drought risks and its potential impacts on the nature-human coupled system. A drought can also be characterized by its frequency and spatial extent (Blenkinsop and Fowler, 2007).

1.2 Assessing impacts of climate change on drought

When assessing the impact of climate change at a high spatial resolution it is preferred to use Regional Climate Models (RCMs) to properly simulate the important variables. Climate models range from very simple zero order models (providing a single global average) to more complex three-dimensional general climate models (GCMs). These GCMs can provide boundary conditions for RCMs. There have been numerous studies done to assess the impact of climate change on drought. In Europe the PRUDENCE project has set a new standard for interdisciplinary climate change research (Christensen et al., 2007). This project is the predecessor of the ENSEMBLES project which applies the same methodology. The main methodology of this project is to use multiple RCMs driven by multiple GCMs with multiple scenarios (greenhouse gas and aerosol emissions) to assess the change in climate at high spatial resolutions (around 50 km or less). By using this methodology a range of possible projections can be calculated and analyzed. The use of RCMs adds value to the projection, because it shows a higher level of detail (shape, vegetation and soil characteristics) and it describes smaller-scale atmospheric processes, which lead to the formation of mesoscale weather phenomena (Feser et al., 2011). For example Wang et al. (2011) used RCM projections based on three GCMs and two scenarios as input for SPI (a drought index to identify drought events) calculations and found that different combinations resulted in different changes in drought intensity, duration and frequency. Wang et al. (2011) stated that the different projections based on different GCM-RCM combinations are probably due to different model structures and parameterizations. Given the sensitivity of the climate system in central Europe, the value of using a multi-model ensemble to represent the uncertainty is evident (Lenderink et al., 2007). Maule et al. (2012) state that a realistic reproduction of observations, coupled with an understanding of why the RCMs perform well or have limitations, are essential prerequisites for using the RCMs in climate change projections.

In (climate impact) studies concerning drought the temporal and spatial variability as well as the spatial structure is not always assessed. More importantly there is no preferred way of assessing the temporal and spatial variability and the spatial structure to the authors knowledge. Min et al. (2003) assessed the temporal variability of SPI by applying a wavelet analysis and quantified the temporal extent of SPI values. Santos et al. (2010) applied a spectral analysis to SPI series and identified periodical signals. There are multiple ways to assess the spatial variability and the spatial structure. Santos et al. (2010) applied a principal component analysis (PCA) to the SPI series to assess the spatial variability and spatial structure. Livada and Assimakopoules (2007) calculated correlation values between SPI series of different rainfall stations to assess the spatial variability. Bonaccorso et al. (2003) applied a PCA to SPI series of Sicily and identified which part of the island show coherent climatic variability (assessing the spatial structure). Lloyd-Hughes and Saunders (2002) assess the spatial structure of drought by plotting the mean duration of (extreme) events and (complementary) the number of drought events for Europe. Overall it can be stated that multiple options have been applied to assess the temporal and spatial variability as well as the spatial structure in drought studies.

1.3 Problem definition

The background section showed the importance of assessing the impact of climate change on drought. However there is not one preferred way of doing this. The mentioned studies in the previous section showed the importance of using multiple emission-GCM-RCM combinations to assess the uncertainty of climate change and its impacts. Furthermore it is difficult to simulate the climate of a relatively small river basin. In particular the spatial structure of climate is hard to simulate. This research will emphasize the temporal and spatial variability and the spatial structure of drought in the basin. The variability relates to the correlation of drought along time and space, while the spatial structure relates to the difference of drought along the basin, i.e. which parts of the basin are subject to more drought events. The problem definition is twofold; firstly what is an appropriate method to assess the impact of climate change on drought at river basin scale. And secondly what can such method reveal for the basin: i.e. assessing the impact of climate change on drought in the basin.

For this study the Meuse basin is chosen since it is an important river for the Netherlands and has been the subject of many studies. A study by De Wit et al. (2007) is useful for this research since it is reveals the relation between meteorological conditions and low-flows for the Meuse river. The Standardized Precipitation Index (SPI) is applied in this study to identify drought events. This index can be applied at different time scales to assess different types of drought. The main reasons to use the SPI method, over other indices, is that the SPI method provides good results (Paulo et al., 2012), its simplicity (Lloyd-Hughes and Saunders, 2002) and it can be used on different time scales to identify different drought types.

1.4 Research objective and questions

Based on the problem definition the following objective of this research is:

> *Develop and apply a method to assess the impacts of climate change on drought in the Meuse basin at different time scales*

A schematic overview of the research is shown in Figure 1-1 and with each step a research question is formulated. To accomplish the research objective the following questions are formulated.

1. How can drought be assessed in a suitable way for climate impact analysis?
2. How well are the climate model simulations in simulating drought?
3. What are the impacts of climate change on drought in the Meuse basin?

1.5 Research strategy and thesis outline

The research questions guide the research and based on these questions the following conceptual model is made (Figure 1-1). Chapter 3 describes the SPI method, its limitations, and modifications of this method to appropriately apply the impact analysis (question 1). The drought assessment (for observed and RCMs, historical period) is based on the SPI method and drought statistics that analyze the SPI results (question 2). The impact analysis (question 3) is based on the difference between drought assessment based on the historical simulation and the simulation of the future period.

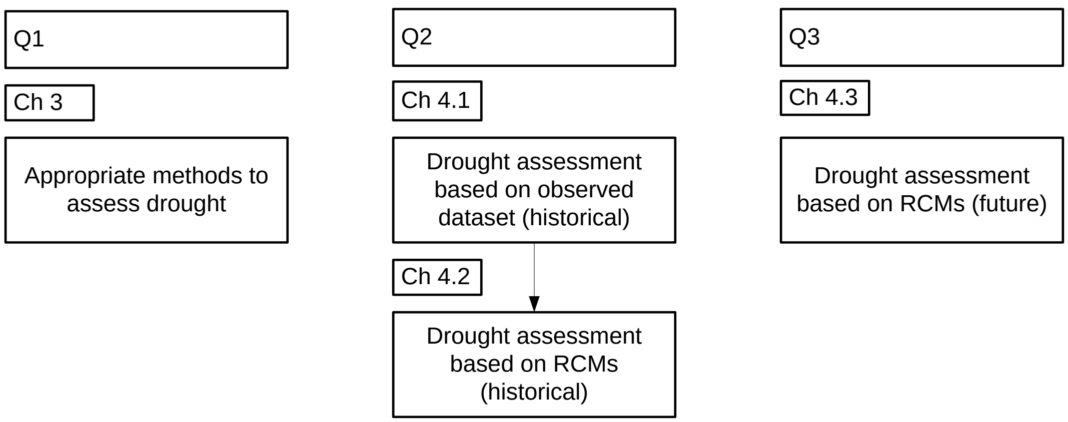

Figure 1-1 Schematic overview of research. The research questions are denoted with a Q.

Chapter 2 Study area and data

In this chapter the study area (section 2.1) and the data (section 2.2) are discussed. Relevant characteristics of the study area are described. Furthermore a preliminary selection is made of the available data sets (RMCs) in section 2.2.2. This is done based on the spatial resolution and period covered by these RCMs.

2.1 Study area

The Meuse basin covers parts of France, Luxembourg, Belgium, Germany and the Netherlands and covers approximately 33.000 km^2 (de Wit et al., 2007; Pfister et al., 2004). There is a maximum altitude of just below 700 m above sea level according to de Wit et al. (2007). The Meuse basin as defined in this research is the Meuse basin upstream of the place Borgharen, the Netherlands. The catchment area of the Meuse upstream of Borgharen is approximately 21.000 km^2.

The average annual precipitation ranges from 1,000 to 1,200 mm in the Ardennes (de Wit et al, 2007). Monthly precipitation displays little seasonal variation (de Wit et al., 2007). According to Pfister et al. (2004) the spatial distribution pattern of rainfall in the Meuse basin clearly reflects the differences in elevation. To interpret the SPI results it is important to know the common precipitation patterns for the basin. Furthermore a plot of elevation of the basin will provide information to better understand the SPI results. The Meuse basin defined in this research is presented in Figure 2-1. The figure shows that the part upstream of the Netherlands is considered in this research (a). The figure shows also the elevation in this area (b). Figure 2-2 shows the seasonal precipitation values. The elevation and precipitation patterns are clearly related. The figure supports the known observations of this basin: a relation between elevation and spatial distribution of precipitation and little seasonal variation.

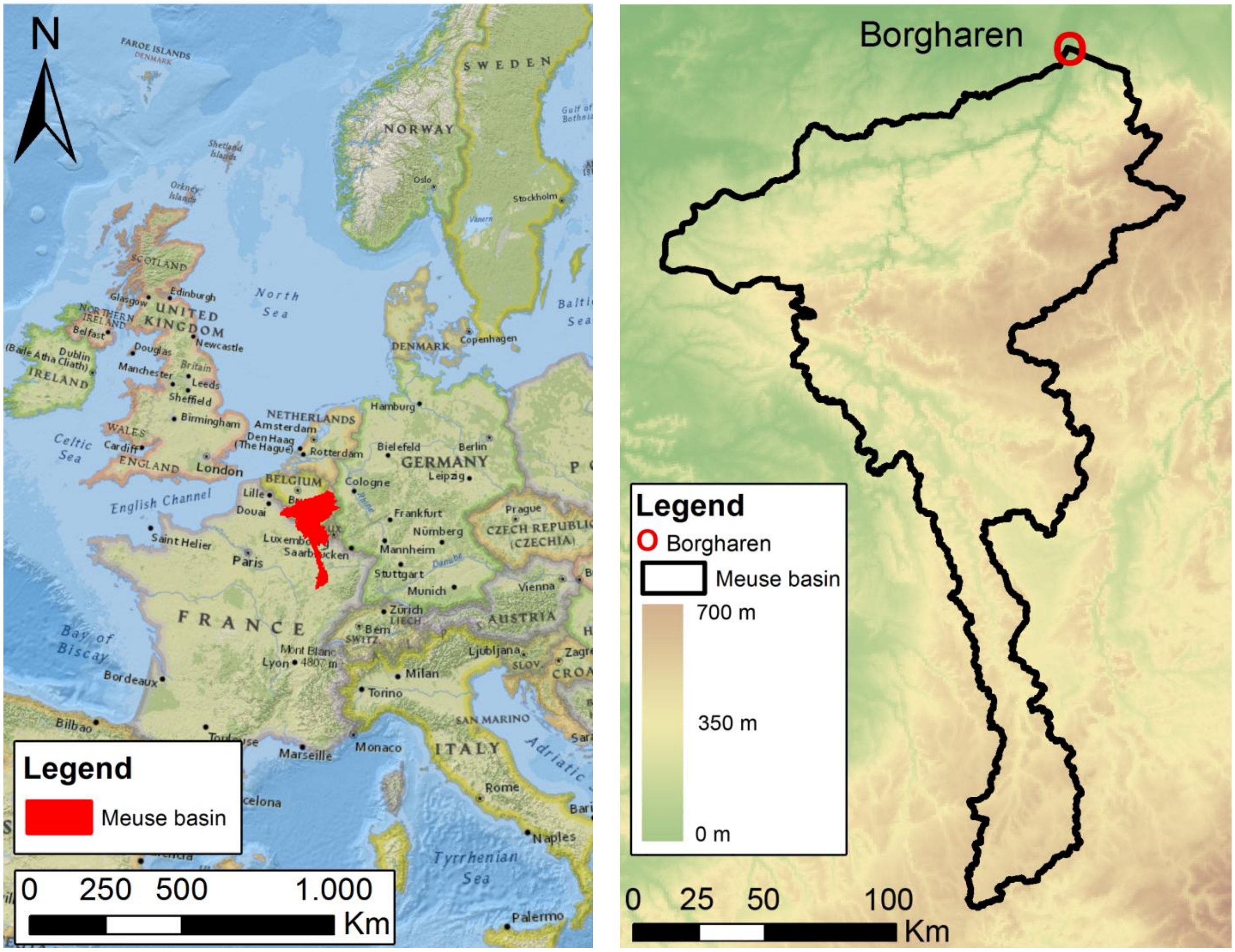

Figure 2-1 Meuse basin topography (left) and elevation map (right).

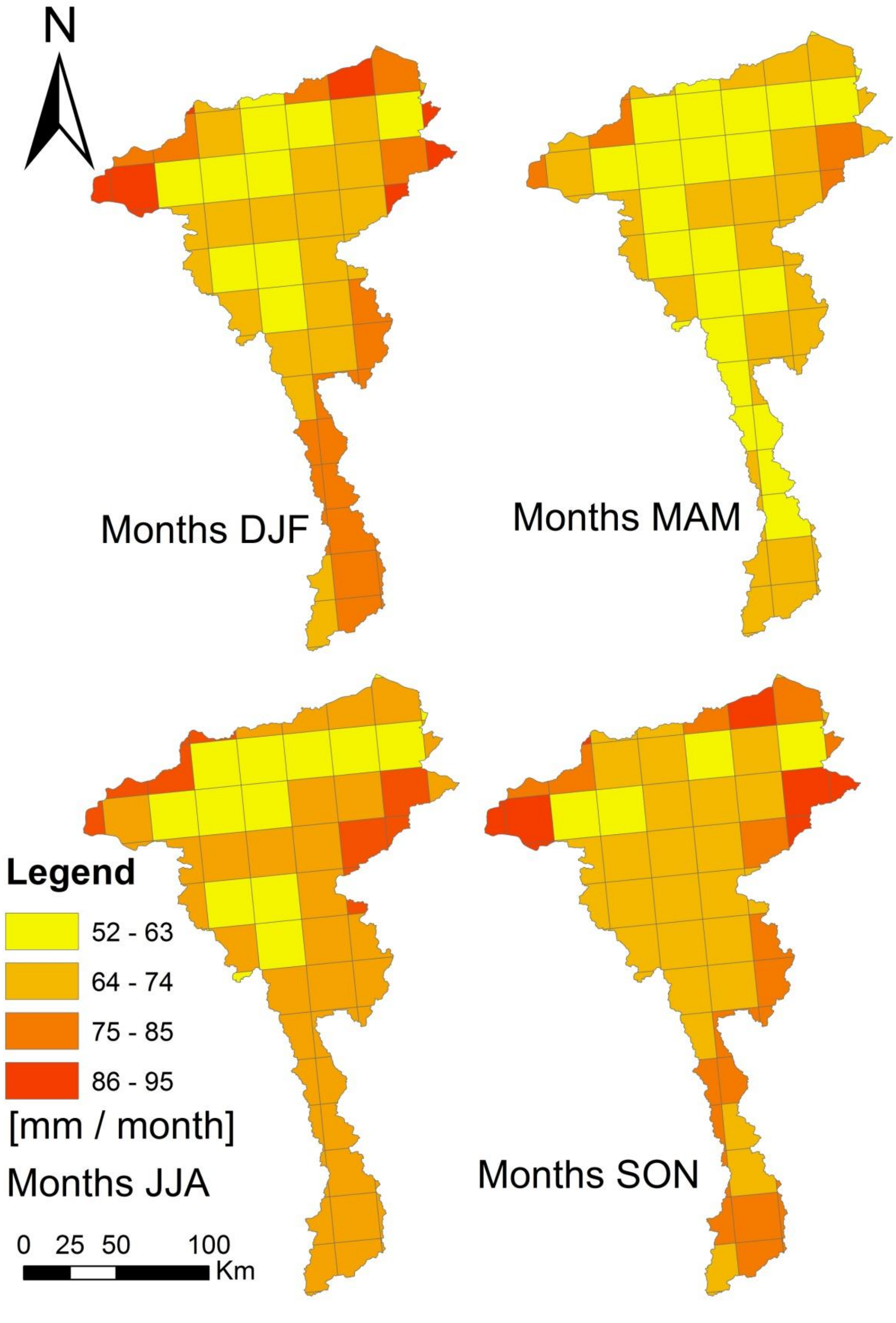

Figure 2-2 Average precipitation for different seasons (DJF = December, January, February, MAM = March, April, May, JJA = June, July, Augustus and SON = September, October, November)

2.2 Data

This section will describe the data as used in this research. The observed dataset is given in section 2.2.1 and the RCM simulations (historical and future periods) are described in section 2.2.2.

2.2.1 Observed data set

The observed data set is from the EU-FP6 project ENSEMBLES and the data providers in the ECA&D project. An earlier version of this data set was presented by Haylock et al. (2008) which can be used as reference. They stated that the data set consists of grid values representing the best estimate average of the grid square observations. The dataset E-OBS version 7.0 which was released in September 2012 is used in this study. This is a high resolution dataset concerning multiple variables including precipitation. The data file based on a 0.22 degrees rotated grid concerning the best estimate of daily precipitation is used. The dataset covers a period from 01-01-1950 until 30-06-2012. The data set is made on a 0.22 degree rotated pole grid, with the North Pole artificially projected at 39.25N, 162W. The rotation provides the grid cells to vary less in size than on a regular grid over the whole projection.

The dataset is based on point observations and interpolated to grid values. The interpolation inherently provides additional uncertainty in the values in the dataset. A study by Nikulen et al. (2011) concerning the performance of ENSEMBLES RCM stated that the uncertainties in the E-OBS dataset potentially contribute to the difference between observed and simulated variables. These uncertainties can arise from the number of observational stations combined with the orography. Obviously the uncertainties are larger for a lower number of stations and a more complex orography. To summarize Table 2-1 shows the characteristics of the observed dataset.

Table 2-1 Overview observed dataset

Institute	Version	Dataset	Period covered
ECA&D	7.0	E-OBS gridded dataset	1950/01/01- 2012/06/30

2.2.2 RCM simulations

The RCM simulations that will be used in this research have been retrieved from the ENSEMBLES project. The ENSEMBLES data used in this work was funded by the EU FP6 Integrated Project ENSEMBLES (Contract number 505539) whose support is gratefully acknowledged. Each RCM simulation covers a historic period and a future projection. An overview of all these runs is provided in appendix E. In this section a preliminary selection is made.

As stated in chapter 1 it is preferred to include multiple scenarios in climate impact analysis. The RCM runs all use the A1B scenario. Using these datasets the effect of uncertainty in emissions is neglected. Therefore the outcome of the impact analysis neglects this uncertainty and the results should be interpreted in this perspective.

The ENSEMBLES final report (Kjellström et al., 2011) indicates that it is important to fully sample the range of GCM uncertainty especially for projections around 2100 and for periods closer to the present more RCMs should be sampled. This is because of the relative importance of the climate model on different distant future periods. De Wit et al. (2007) found that the lateral forcing of the GCMs strongly influence the results for the Meuse basin.

The preliminary selection is based on two criteria. First to make the results based on the different datasets intercomparable, obviously the same period should be sampled. Secondly a higher spatial resolution of these projections is preferred. The selection is based on the highest possible resolution (around 25 km or 0.22 d and the availability of the data set for future periods. From a SPI perspective at least 30 years should be covered to properly calculate SPI values (Guttman, 1998). It is decided to create three periods of 30 consecutive years each; one historical period for the validation phase and two future periods for assessing midterm and long term climate change impacts. Only runs that can cover these periods are considered in further analysis:

- 1971 - 2000
- 2021 - 2050
- 2066 - 2095

Table 2-2 shows the 13 RCM projections which are included in this research. To assess the influence of the GCM on the RCM projection it is interesting to look for projections with the same RCM and different GCMs. The influence of the RCM can be assessed in a similar manner. Table 2-2 introduces a numbering for the 13 RCMs to keep the reference to each dataset short.

Table 2-2 All considered RCMs. For convenience the RCMs are numbered and this numbering will be used throughout this report (RCM with nr.1 is called RCM-1). The period covered is noted with an asterisk for two RCMs: the run goes up to the 11th month of the last year, instead of the 12th for all the other simulations.

Nr.	Institute	Scenario	Driving GCM	RCM	Period covered
1	CNRM	A1B	ARPEGE_RM5.1	Aladin	1950-2100
2	KNMI	A1B	ECHAM5-r3	RACMO	1951-2100
3	SMHI	A1B	ECHAM5-r3	RCA	1950-2099
4	SMHI	A1B	HadCM3Q3	RCA	1950-2098*
5	MPI	A1B	ECHAM5-r3	REMO	1951-2100
6	C4I	A1B	HadCM3Q16	RCA3	1951-2099
7	ETHZ	A1B	HadCM3Q0	CLM	1950-2098*
8	HC	A1B	HadCM3Q0	HadRM3Q0	1951-2100
9	HC	A1B	HadCM3Q3	HadRM3Q3 (low sensitivity)	1951-2100
10	HC	A1B	HadCM3Q16	HadRM3Q16 (high sensitivity)	1951-2100
11	DMI	A1B	ARPEGE	HIRHAM	1950-2099
12	DMI	A1B	ECHAM5-r3	DMI-HIRHAM5	1951-2100
13	ICTP	A1B	ECHAM5-r3	RegCM	1951-2100

Chapter 3 Methods

In this chapter the methods as applied in this research will be described. Section 3.1 describes how drought will be characterized. The technical procedures of applying this index (the SPI method) and its limitations are discussed in section 3.2. Section 3.3 describes how the SPI can be modified to compare different locations or periods and how the SPI can be spatially aggregated to basin level. Analyzing the SPI results involves different techniques which are discussed in section 3.4. These techniques together form the new method to analyze the impact of climate change on drought based on RCMs.

3.1 Drought definition

A drought index can be used to identify drought events. A drought event can be described by its impact, duration and spatial extent. Drought assessment consists of describing the drought events given a certain location and period. In other words to get an understanding of what kind of drought events are normal and what is extreme all the events over a certain period are described and analyzed. This will be done in section 3.4 (drought assessment).

However, there are multiple perspectives on drought and thus multiple definitions. The most common classification is the meteorological, hydrological, agricultural and socio-economic perspective (Wilhite and Glantz, 1985) as cited by Wilhite (2011). For climate impact studies the meteorological drought perspective is the most easy to apply and probably the most reliable. This is because the other perspectives need additional information (change in agriculture, socio-economic situation) and/or additional transformation (hydrologic model) and thus additional assumptions for the future scenarios. The climate models provide meteorological information and it would be preferred to use only this output for the drought assessment.

For the drought identification the standardized precipitation index (SPI) is applied. This is mainly because the index has been proven to give good and reliable results. Another important factor is that it only requires (monthly) precipitation which is a direct output of the RCM runs. Another great advantage of this index is its simplicity which makes it easier to interpret the results. The main downside of this index is the lack of input (temperature, wind speed, etc.) known to be important for drought.

Since the SPI can be applied with different time scales, different types of drought can be assessed. Section 3.2.3 will describe how the different time scales probably relate to different types or definitions of drought. For the sake of interpretation it assumed that the used time scales relate to certain drought types as presented in Table 3-1. A time scale stands for the amount of months of precipitation the aggregation is based on. A different time scale relates to different physical conditions (soil water, agricultural problems or water level of the river) in the river basin.

Table 3-1 The time scales and the related SPI and drought type

Time scale	SPI	Drought type
1-month	SPI-1	Meteorological
3-months	SPI-3	Agricultural
6-months	SPI-6	Hydrological
12-months	SPI-12	Extreme hydrological

Drought characteristics like intensity and severity are known in the literature next to total deficit and duration. The total deficit is simply the sum of the intensities during the event (each month has an intensity or SPI value). Severity is similar: the total deficit divided by the duration equals the severity of the drought event. Intensity is interesting since this reflects the ‘extremeness’ of the event, the lowest SPI value of that event. To keep the drought assessment short severity is not taken into account. This is seen as the least interesting characteristic since it is based on deficit and duration which is taken into account.

3.2 SPI method

The SPI method has been developed by McKee et al. (1993) and can be used at multiple time scales. This index converses precipitation values by calculating the probability distribution of these precipitation values into standardized values. These values have an average of zero and a standard deviation of one.

3.2.1 SPI procedure

The recommended methodology as described by WMO (2012) to apply the SPI is as follows. For each location (a precipitation station or in this case a grid cell) and for each month of the precipitation series (minus the possible lag due to the time scale) a SPI index value is calculated. For each time scale the aggregation of precipitation values is different. For SPI-12 the last 11 months and the month in question is aggregated for that particular month. For SPI-1 there is no real aggregation since the original monthly precipitation values are used. To these aggregated values a probability density function (PDF) is fitted. Based on this function the non-exceedance probabilities are calculated which are transformed into standard normal variable values: i.e. SPI values (see Eq. (3.1)). Basically in this way the aggregated precipitation values are transformed into values that reveal what the probability is of that value. I.e. what is normal and what is extreme for that particular climate (location and period).

$$SPI_{i,k} = \mathrm{F}^{-1}(\mathrm{p})$$
$$p = F(x) = \frac{1}{\sqrt{2\pi}} \int_{-\infty}^{\mathrm{t}} \mathrm{e}^{-\frac{1}{2}\mathrm{x}_{\mathrm{i,k}}^{2}}\, dt \qquad \text{Eq. (3.1)}$$

Where

$$\mathrm{x}_{\mathrm{i,k}}\text{: the non} - \text{exceedance probability for ith grid cell, kth month}$$

The non-exceedance probabilities range between 0 and 1. These values are transformed into SPI values by taking the inverse of these probabilities using the corresponding mean and standard deviation of the PDF. In this way the mean is zero and a value of one (or minus one) means a deviation of the mean of one standard deviation. In this research this will mean that for each grid cell (i) and each month (k) an aggregated precipitation value ($x_{i,k}$) can be transformed into a SPI value based on the mean of that grid cell and the standard deviation. Appendix A presents the full procedure of the SPI calculation.

3.2.2 Limitations SPI method

When applying the SPI method it should be considered that the method inherently has some limitations considering the method itself, its application and what the method does not assess. Since the SPI has been widely applied a number of limitations of the method and therefore its results have been found. It should be noted that SPI values are standardized values and therefore typically have a range from 2.00 to -2.00. A SPI value of ≤ -1 has an occurrence probability of 15.9 % and a value of ≤ -2 has a probability of 2.3% (Lloyd-Hughes and Saunders, 2002).

Guttman (1999) stated that the number of observations of the precipitation data is related to the bounds of the SPI value. The SPI value represents a certain probability of occurrence. The amount of used data (observations) indicates to what extent the SPI method can assess extreme events. An earlier study of Guttman (1998) stated that the probability estimates can be considered to be a function of sample size. The less observations the more inaccurate the estimation of more extreme probabilities becomes. Agnew (2000) stated that in dry lands (a climate with a lot of zero monthly precipitation values) it is difficult to calculate precipitation averages with any certainty and it has been suggested that the use of the thirty-year averaging period is questionable. However the value of the SPI will change if different lengths of precipitation data are used (Wu et al., 2005), due to the changes in shape and scale parameters of the gamma distribution. Therefore when applying the SPI method the same length of precipitation data and a minimum of 30 continuous years data set should be used.

The method assumes that a suitable probability distribution can be fitted to the precipitation data. This is not necessarily the case according to Lloyd-Hughes and Saunders (2002). However they also concluded that the 2-parameter gamma distribution seems to be the most appropriate approach to describe monthly precipitation over Europe and to calculate the SPI index. However it is open for discussion if the gamma distribution should be used all the time (Guttman, 1998). Sienz et al. (2012) studied the implications of using different probability distributions and state that the gamma function should not be used but a Weibull type when applying the SPI. The SPI procedure involves determining the shape of the probability density distribution function. Certain shape parameters need to be calculated to determine this shape. Different statistical tools are available to determine these parameters. Since there is debate over the preferred probability density distribution function it remains also uncertain which tools should be applied. Comparability is limited since no uniform method of calculating SPI is known. Hayes et al. (2011) stated that a comprehensive user manual for the SPI should be developed. As stated earlier WMO (2012) provides a user manual. However the study of Sienz et al. (2012) state that the Weibull type is preferred whiles the gamma function is prescribed in this manual. Another observation concerning the probability density function is about the extreme (SPI) values that are calculated. There are common problems in fitting the tails of the distribution function and therefore Dubrovsky et al. (2009) state that SPI values outside of the range of (-2 and +2) should be used with care.

Applying the SPI method should also include assessing the ‘normal’ rainfall distribution of de study area. For example Hayes et al. (1999) stated when calculating SPI values based on one or three month(s) for areas with normally low seasonal precipitation totals a small variance in precipitation can result in misleadingly low SPI values. A similar conclusion is drawn by Lloyd-Hughes and Saunders (2002) warning for misleading results. Agnew (2000) stated that SPI method takes no account of impacts.

An important limitation is the standardized nature of the index (Lloyd-Hughes and Saunders, 2002) is that drought events identified by the SPI, when considered over a long time period, will occur with the same frequency at all locations. The standardization introduces problems when comparing droughts between different periods (same location) or different locations (same period). When comparing between different periods (as the impact analysis in this research) the SPI should not be applied. This is because the standardization will cause a similar distribution of SPI values in the classification categories of the SPI for both periods (Lloyd-Hughes and Saunders, 2002). However there is a solution proposed by Dubrovsky et al. (2009) to overcome this limitation. Dubrovsky et al. (2009) state that future drought conditions need to be expressed in present-day climate. The SPI is basically transformed into a relative SPI based on the present-day climate rather than the future period. This is done by using the probability distribution functions of the present-day period (1971-2000) to calculate the SPI values for the future period (2021-2050 or 2067-2098). Comparing locations based on SPI obviously results is a similar problem and a similar solution can be applied. Using a reference set the relative SPI can be applied to compare locations. The reference set could be based on one location and using this location to compare the other locations to that one. The relative temporal and relative spatial SPI will be defined and applied in this research (see section 3.3 for more information).

3.2.3 Interpreting SPI results

The SPI can be calculated on different time scales and each time scale relates to different physical mechanisms related to drought. The SPI method is applied at multiple time scales to get a comprehensive view of drought events. A time scale of 1 month reflects short-term conditions. A larger time scale is associated with droughts with long-term impacts. WMO (2012) stated that the SPI can be calculated based on 1 month up to a time scale of 72 months. It is decided to look into three periods of 30 years and because of the length of this period the SPI up to 12 months is calculated. This is based on the sample size becoming too small and therefore the statistical confidence of the probability estimates on the extremes (wet and drought) becoming weak (Guttman, 1998). The time scale has implications concerning the length of the SPI series. For each time scale the input is the same (360 monthly precipitation values) however a different time scale results in a different length of the SPI series. For example for SPI-1 the 360 precipitation values can be transformed into 360 SPI values. However for SPI-12 the first 12 precipitation values are used to calculate the first SPI value. The SPI-12 series has therefore 360 – 11 (349) values for each period. It is not known for the Meuse basin how the different SPIs relate to physical conditions and type of drought. However based on the studies presented here, Table 3-1 is made.

1-month SPI

The results based on the 1-month SPI reflect the short-term conditions of drought. WMO (2012) state that the results can be closely related to meteorological drought, soil moisture and crop stress during the growing season. However interpreting the results can be misleading unless the climatology is understood. As stated by WMO (2012) if the rainfall during a month is normally low the SPI can fluctuate largely even if the departure from the mean is relatively small. Lee and Kim (2012) stated that soil moisture conditions respond to precipitation anomalies on a relatively short scale. In this report the 1-month SPI is interpreted as a time scale that reflects meteorological drought.

3-month SPI

The 3 month SPI of a certain month uses the precipitation values of the considered month and the two previous months to calculate the SPI value. The results based on the 3-month SPI reflect short-term conditions and can provide misleading results in a similar manner as the 1-month SPI. Bussay et al. (1998) and Szalai and Szinell (2000) found that agricultural drought in Hungary was related to SPIs with time scales of 2 to 3 months. Myronidis et al. (2012) found moderate correlation values between the lake's water level and SPI-3. This was lake Dorian in the north of Greece with a surface area of about 40 km^2 and an average depth of 10 m. The study stated that intense drought phenomena strongly affect the water level of Lake Doiran. In this report the 3-month SPI is interpreted as a time scale that reflects agricultural drought.

6-month SPI

The 6-month SPI indicates seasonal to medium-term trends in precipitation. WMO (2012) state that SPI-6 can be very effective in showing drought over seasons. Bussay et al. (1998) and Szalai and Szinell (2000) found that for Hungary the stream flow was best described by SPIs with time scales from 2 to 6 months. They also found a strong relation between ground water level and SPI with time scales of 5 to

24 months. In this report the 6-month SPI is interpreted as a time scale that reflects hydrological drought.

12-month SPI

The 12-month SPI reflects long-term conditions of drought. WMO (2012) state that this time scale can be related to stream flows and reservoir levels. Lee and Kim (2012) stated that stream flow and reservoir storage reflect longer-term precipitation anomalies. De Wit et al. (2007) showed that multi-seasonal droughts are generating critical low-flows for the river Meuse. In this report the 12-month SPI is interpreted as a time scale that reflects extreme hydrological drought.

The resulting SPI values can be further analyzed and interpreted. Each SPI value relates to a certain probability. For example a SPI value of zero represent a precipitation value that is 'normal' for that period and a SPI value of -2 or less can be considered extreme since such a value or lower has a probability of 2.3 %. Table 3-2 shows these relations between the SPI value and the probability of occurrence of the SPI value.

Table 3-2 Range of SPI values, their category and their probability of occurrence (based on Lloyd-Hughes and Saunders, 2002)

SPI value	Category	Probability [%]
2.00 or more	Extremely wet	2.3
1.50 to 1.99	Severely wet	4.4
1.00 to 1.49	Moderately wet	9.2
0 to 0.99	Mildly wet	34.1
0 to -0.99	Mildly drought	34.1
-1.00 to -1.49	Moderate drought	9.2
-1.50 to -1.99	Severe drought	4.4
-2 or less	Extreme drought	2.3

3.3 SPI modifications

Some modifications are made to the original SPI. This was done to be able to compare over time, location and to identify drought at a higher spatial level (river basin). To compare over time or location the original SPI is made relative based upon a reference point. The reference point is a presumed different climate (different location or period) where the precipitation is also presumed to be different. The SPI basin is based on the SPI series of the cells covering the basin.

3.3.1 Relative temporal SPI

The reference point for the relative temporal SPI is the historical climate. The difference for the relative temporal SPI is to use the historical probability density function parameters that describe the fit to calculate the SPI for the future period. In this way the difference in meteorological conditions (i.e. climate change) is taken into account for the SPI values. The future monthly precipitation values are fitted to the historical probability density function. In this way extreme future precipitation values, extreme compared to historical values, will result in extreme SPI values. When a *new* probability density function was constructed for the future period this same extreme future precipitation values will result in 'normal' SPI values due to the standardization. The relative temporal SPI is abbreviated to rtSPI in this report.

3.3.2 Relative spatial SPI

For the relative spatial SPI the reference set is the average of the probability parameter values off all the cells describing the basin. This will identify which cell is more (or less) drought prone compared to the average: i.e. the normal of the basin. The average is weighted with the area size of the cell. The relative spatial SPI is only used to calculate the drought frequency of each cell. The frequency values can be plotted over the Meuse basin to reveal observed spatial patterns. The relative spatial SPI is abbreviated to rsSPI in this report.

3.3.3 SPI basin calculation

There are 63 grid cells that overlay the Meuse basin. The SPI for the whole basin is calculated by considering the area covered by each cell:

$$SPI_{basin} = \sum_{i=1}^{n=63} SPI_{cell(i)} * (A_{cell(i)} / A_{basin}) \qquad \text{Eq. (3.2)}$$

In this equation $SPI_{cell(i)}$ is the SPI time series of $cell(i)$. Each cell represents a part of the basin and the relative importance of each time series is based on the area of the basin covered by that cell $A_{cell(i)}$ and the total area of the Meuse basin A_{basin}.

3.4 Drought assessment based on SPI

Multiple drought statistics are designed to quantify drought characteristics. The input for these statistics is the results of the SPI and its modifications. Interesting values are the number of events, average duration, deficit and intensity of the events. This is a quick way to analyze what type of drought is observed or simulated. All the drought statistics will be discussed in this section. The drought statistics are:

- Number of drought events
- Characteristics of drought events
- Drought frequency basin plot
- Deficit-duration relationship
- Temporal correlogram
- Spatial correlogram

To get an intuitive understanding the following plot (Figure 3-1) is made. Figure 3-1 gives an impression how a SPI series is used to identify and describe drought events. Figure 3-1 shows (part of) the basin SPI-12 series based on observed precipitation values. The first values (blue ones) show first positive values (relative wet but normal conditions) and then change into negative values. As soon as a SPI value changes from above -1 to below this number a drought events begins (red bars). As long as the SPI value does not reach a positive value the drought continues. The duration of this drought event is the number of red bars. The deficit is the sum of all red values (the length of each red bar). The frequency is the duration of all drought events in that series divided by the amount of SPI values in that series.

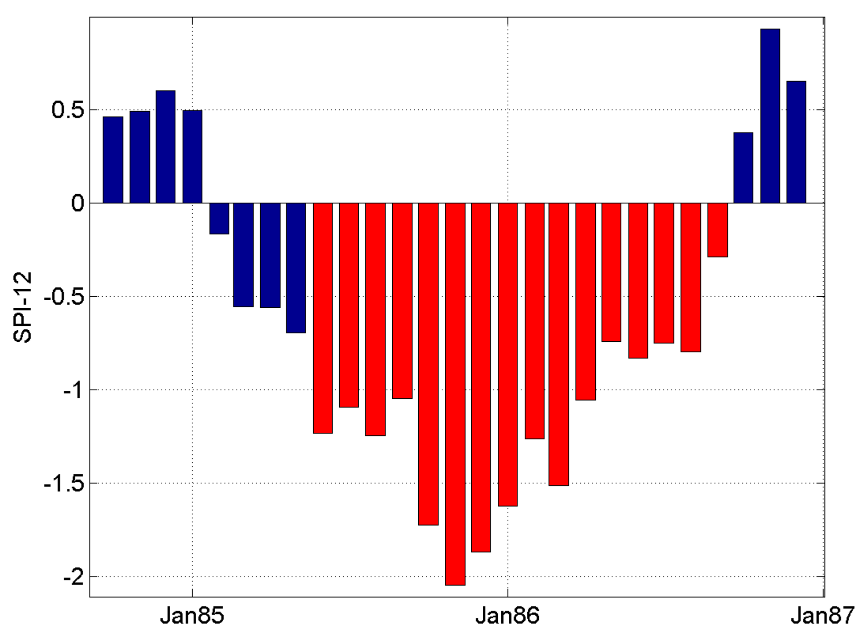

Figure 3-1 Part of observed SPI-12 series. The bars represent SPI values for each month. The red ones indicate a drought event.

3.4.1 Number of drought event, its characteristics and frequency basin plot

The number and characteristics of drought events reveals what type of drought events (range of values for drought characteristics: duration, deficit and intensity) are to be expected and how variable these characteristics are. The number of drought events can be easily derived once the SPI series are calculated. For all drought events identified the average in drought characteristics (duration, deficit and intensity) can be calculated as well. To assess the variability in these characteristics the standard deviation is calculated. The standard deviation is calculated by:

$$s = \left[\frac{1}{n-1}\sum_{i=1}^{n}(x_i - \bar{x})^2\right]^{1/2} \qquad \text{Eq. (3.3)}$$

Where x_i stands for the value of that characteristic (duration, deficit or intensity) of the ith event. n stands for the total number of events. The drought frequency is based on the sum of duration of all drought events divided by the length of that series.

For each cell in the basin the relative spatial SPI is utilized to calculate the drought frequency that reflects the difference of drought along the basin. Since the relative spatial SPI is based on the basin average the drought frequency reflect which areas are subject to more or less drought events than the basin 'normal'. This will reveal the spatial structure of drought in the basin.

For the RCM assessment the weighted-average absolute error is calculated for each time scale to reveal which RCM simulates the spatial structure in the basin well. The weighting is based on the area covered by that cell. For each cell an absolute error is calculated. Based upon this absolute error the best performing RCM is used for the impact analysis, all the other RCMs are not used in the impact analysis for this specific indicator.

3.4.2 Deficit-duration relationship

The deficit and duration relationship reveals what type of drought events are to be expected. For all drought events (cell and basin based) a plot can be made a long duration and deficit. This will reveal, visually, the relationship of these two characteristics.

For the assessment and impact analysis the relationship and difference (or change) in this relationship is quantified. For the assessment the difference is an error in simulation. Calculating the error in simulating this relationship is done by calculating the absolute mean error of the simulation and the observation for each duration value:

$$E_{abs} = |def_{OBS} - def_{RCM}| \qquad \text{Eq. (3.4)}$$

For some duration values there are no events for one datasets (RCM or EOBS) and consequently no absolute error can be calculated. To summarize the error in the simulation the sum of the weighted errors is calculated. The weighted error is the sum of absolute error in relation with the mean number of events the error is based on. In this way an error based on a few events becomes less important than one based on a lot of events. Overall there are a lot of low duration events and this number quickly drops with a high duration value. The weighted error is formulated as:

$$E_w = \sum_{i=1}^{n=\max dur} E_{abs,i} * \frac{(\frac{N_{events\_OBS,i} + N_{events\_RCM,i}}{2})}{N_{all\_events}} \qquad \text{Eq. (3.5)}$$

The second term determines the weight based on the number of drought events for that particular duration (i) along all the drought events (both observed and RCM) considered in this equation. For the impact analysis the change is calculated by first calculating for each duration value:

$$C_{rel} = def_{OBS} - def_{RCM} \qquad \text{Eq. (3.6)}$$

The value for the change in deficit and duration is calculated by weighted summing (similar to Eq. (3.13)) the change between historical simulation and the future (a positive value equals a larger deficit in the future for the same duration in the historical period). The value is based on a summation where positive values can compensate negative values.

3.4.3 Temporal and spatial correlation

The temporal and spatial correlogram are used to identify the temporal and spatial variability in the SPI series. The correlation (and thus variability) of SPI series can be examined with a correlogram. For the temporal correlation a plot of autocorrelation values at different lags (shift of the series over time) is made. The correlation values are calculated by:

$$\hat{R}_{xy(\tau)} = \frac{[\sum_{t=1+\tau}^{n} y_t * y_{t+\tau} - (n-\tau)\bar{Y}_t\bar{Y}_{t-\tau}]/(n-\tau-1)}{[\sum_{t=1}^{n}(y_t - \bar{Y})^2]/(n-1)} \qquad \text{Eq. (3.7)}$$

Where n is the length of the time series and the lag τ is the number of intervals between points. y_t is the observed value at t and $\bar{Y}$ the mean of the dataset.

The spatial correlation is analyzed by calculating for each cell the correlation in SPI-series with all the other cells. Combined with the distance between each combination a correlogram can be made. Only unique combinations are used (comparing cell 1 with 2 gives the same result as comparing 2 with 1). With 63 cells ($i = 63$) this will result in $\frac{i^2-63}{2} = 1953$ unique combinations. The correlation value for each combination is calculated with:

$$\hat{R}_{xy} = \frac{\sum_{i=1}^{n}[(x_i - \bar{X})(y_i - \bar{Y})]}{\sqrt{\sum_{i=1}^{n}(x_i - \bar{X})^2 \sum_{i=1}^{n}(y_i - \bar{Y})^2}} \qquad \text{Eq. (3.8)}$$

In this equation there is no lag since only the spatial correlation is relevant. All the unique combinations of the SPI series of other cells x_i are compared with one cell y_i^*. The distance calculations are based on longitude and latitude values.

Correlation length calculation

The temporal and spatial patterns can be described by calculating the correlation length. This is a certain length (in months or km's) which is a characteristic of the correlation over time or space. To calculate this value an exponential function is fitted through the correlation dataset. Based on this fit the correlation length is calculated. For the temporal and the spatial correlation the relationships are estimated with an exponential function:

$$F_{exp} = e^{-\frac{t}{\tau}} \qquad \text{Eq. (3.9)}$$

t stands for the lag in time or space. When there is no lag (t=0) the fit should and is showing an correlation of one. The term τ stands for the correlation length: when $t = \tau$ the value F_{exp} is reduced by a factor e (i.e. a correlation of 0.368). The correlation length is a descriptive value of the relation of SPI values over time of space. It can be interpreted as the temporal or spatial extent over which the SPI values are significantly positively related to each other.

For the temporal correlation the number of correlation values considered for the fit is based on the time scale of the SPI series and the correlation values itself. The time scale is related to physical conditions and temporal variations. Based on this it is decided that correlation values up to twice the time scale will be considered. For example the SPI-3 is based on three months of precipitation and from a physical point of view it is interesting if there is a temporal correlation up to 6 months. When the correlation values are below a certain limit the values will not be considered for the fit. This seems logical because the correlation length should be based on relevant (positive) correlation values since the correlation length is an indicator of the positive correlation. The limit is on a 95 % significance level and can be estimated by:

$$\pm 2/\sqrt{N} \qquad \text{Eq. (3.10)}$$

Based on this significance level it can be expected that 5% of the correlation values are outside of the confidence limit suggesting a significant correlation when actually there is no significant correlation. The confidence level is for all the SPI-series around 0.05 (N ranges from 349 to 360). In this way the correlation series is reduced to positive significant values suitable for the exponential fit.

Significance and strength of fit

The exponential fit can be analyzed based on the goodness-of-fit and the significance of the fit. The goodness of fit or strength of the fit is assessed by the r^2value. The better the exponential regression the closer the value of r^2 is to one. However since an exponential function is used to fit through the dataset a linearization is needed to use the r^2 as a measurement of goodness-of-fit. The significance of the fit is assessed by the F-test (Haan, 2002). The r^2 and F values are presented in Appendix B. The resulting drought indicator is the correlation length (τ) for both temporal and spatial correlation.

3.4.4 Impact analysis

For the impact analysis there is a weighted average constructed based on the error found in the RCM assessment. The RCM assessment consists of comparing the drought statistics based on the observed dataset and the output of the RCMs. This is input for a weighted average of all RCMs in the impact analysis. For each statistic and each time scale there is a different error and therefore a different weighting of each RCM. The lowest rank will result in a first ranking and thus a weighting of 13.4 %, see Table 3-3. The weights are linearly distributed with a minimum of 2% for the worst RCM. In this way the weighted average is related to the quality of the RCM. For each drought statistic and each time scale the ranking is different, since the error is different.

Table 3-3 The weighting of RCMs in the impact analysis

Rank	Weight [%]
1	13.4
2	12.4
3	11.5
4	10.5
5	9.6
6	8.6
7	7.7
8	6.7
9	5.8
10	4.8
11	3.9
12	2.9
13	2.0

Chapter 4 Results

In this chapter all the results are presented. Section 4.1 provides the observed drought of the historical period 1971-2000. This provides information for assessing the quality of the RCMs to simulate drought in the Meuse basin which is described in section 4.2. For each SPI and statistics a weighted average is calculated. This average and the individual projections indicate the possible impact of climate change on drought for different statistics for two future periods, 2021-2050 and 2066-2095, which are described in section 4.3.

4.1 Observed historical drought

This section will firstly present how observed historical drought is identified and quantified by the SPI. Furthermore the same statistics as will be used in section 4.2 and 4.3 will be presented based on the observed dataset. The concluding remarks will discuss the statistics and tries to find consistency in the results.

4.1.1 SPI basin

To get an understanding how a SPI series might look like (at different time scales) the SPI series of the Meuse basin are plotted for the historical period. Figure 4-1 the presents the SPI basin series based on the observed dataset. This gives an impression about how the different SPIs temporally differ and when in this period what kinds of droughts are identified. For example an extreme long-term drought event can be identified by SPI-12 around 1976, with an extreme trough in September of that year. This corresponds with known droughts in the history of the Meuse basin and parts of Western Europe (Sheffield et al., 2009). It can be noticed that the larger the time scale the less the values vary. This indicates that a larger time scale is more predictable than a smaller one. Another result is that a short term wet period can occur during a long term drought event (SPI-12 drought event around 1976 and at the same time some positive peaks (wet events) in SPI-1).

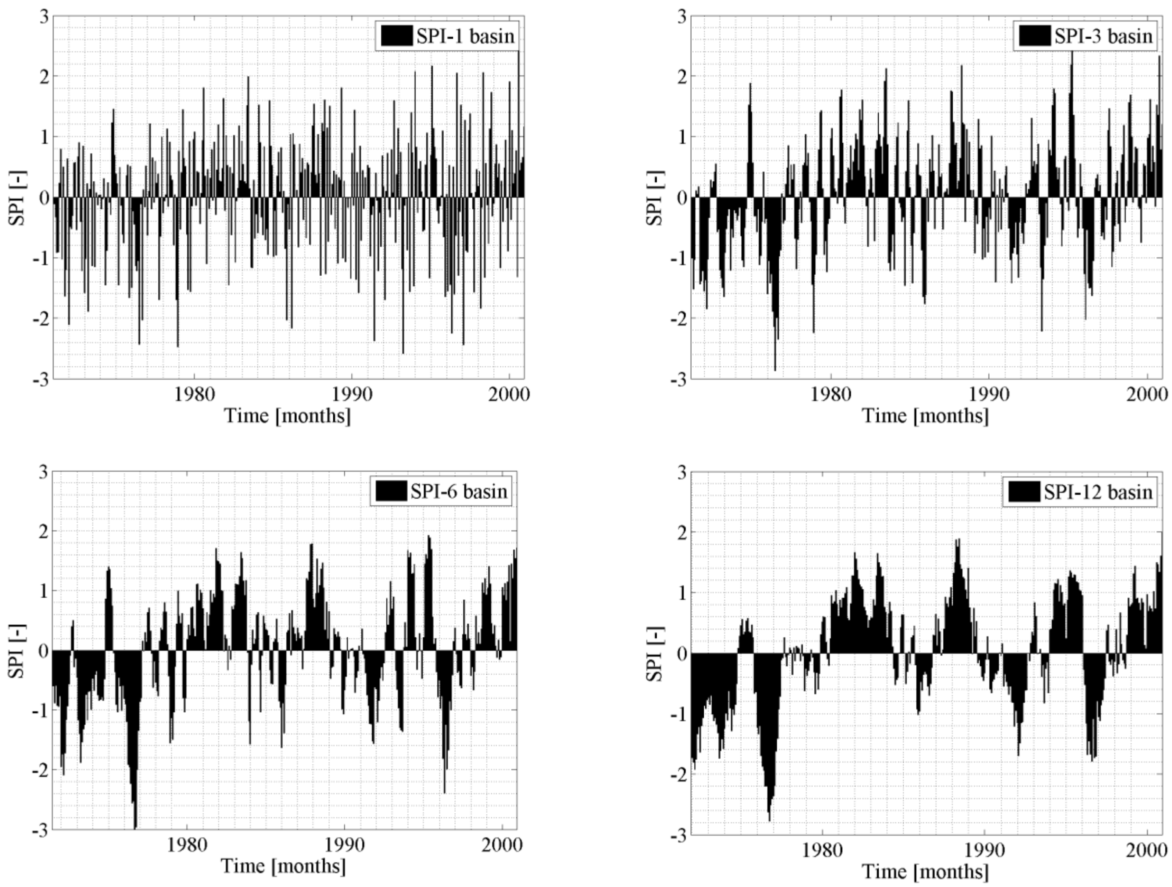

Figure 4-1 All SPI basin series based on the observed dataset.

4.1.2 Driest month

Figure 4-2 shows SPI values of the months with the lowest SPI basin value during the observed period, i.e. the driest month. For each time scale this is a different month. However it can be noticed that these months for SPI-3, -6 and -12 are around the end of 1976 or beginning of 1977 and are therefore probably related to each other. The plots reveal how an extreme drought event is spatially structured over the basin for that month. There is a different spatial pattern visible for all four plots. Based on these plots it seems that drought is spatially correlated but that each drought event is spatially differently structured. However the plot is a snapshot and does not represent all drought events. Another observation is that SPI-12 does not show extreme values like the other time scales.

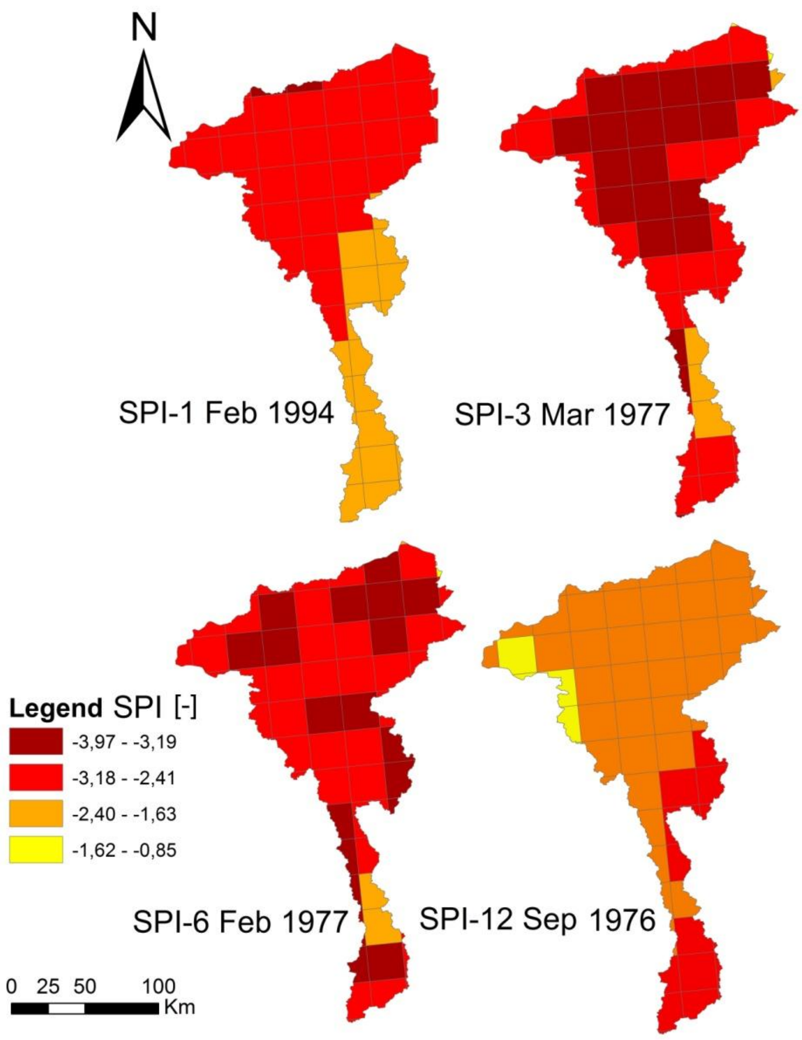

Figure 4-2 Driest months for four time scales based on observed dataset. The darker (red) values show a lower value (more extreme) than the light color (yellow).

4.1.3 Table of drought events

Table 4-1 presents the number of basin drought events identified with the SPI and their distribution as a function of duration. It is clear that the larger the time scale the lower the number of drought events identified. Table 4-2 shows that the larger the time scales are the longer the average duration is. This could be explained by the variability of the larger time scales; the variability is lower for a larger time scale and therefore a drought event is likely to continue. The different (temporal) variability of different time scales can be intuitively explained by the SPI basin plots and quantitatively by the temporal correlation length (see section 4.1.6). A larger time scale has a lower variability; i.e. when the SPI-12 value is below minus one it is unlikely that the next month the value will be above zero. Most SPI-1 droughts have a duration of 1 month and SPI-1 clearly has a high variability that causes this. The small range in average intensity and its variation can probably be largely explained by the standardization nature of the SPI: all SPI values have a certain probability of occurrence (see section 3.2.3). Therefore the most extreme month in a drought event (intensity) has a probability that is largely determined by the method itself.

Table 4-1 Distribution of drought events based on observed dataset (basin events).

	Duration [months]	Observed
SPI-1	**All**	**47**
	1	28
	2	12
	3 and longer	7
SPI-3	**All**	**17**
	1,2,3	8
	4 to 7	5
	8 and longer	4
SPI-6	**All**	**11**
	1 to 4	7
	5 to 8	1
	9 and longer	3
SPI-12	**All**	**4**
	1 to 8	2
	9 to 16	1
	17 and longer	1

Table 4-2 Drought characteristics of drought events based on observed dataset (cell events).

	Ave. duration [month]	St.dev. duration [month]	Ave. deficit [-]	St.dev. deficit [-]	Ave. intensity [-]	St.dev. intensity [-]
SPI-1	1.81	1.46	-2.25	1.51	-1.65	0.51
SPI-3	5.21	4.32	-5.65	5.08	-1.67	0.53
SPI-6	7.83	7.13	-9.28	9.72	-1.79	0.62
SPI-12	19.62	16.31	-21.37	20.43	-1.75	0.48

4.1.4 Drought frequency plots

The relative spatial SPI (rsSPI) is only used to calculate the drought frequencies for all cells in the river basin. These drought frequencies will reveal the spatial structure of drought inside the basin. Figure 4-3 shows the drought frequency based on the rsSPI. To interpret these plots it can be useful to look at the average precipitation for different seasons over the basin (Figure 2-1). Since for the rsSPI the same probability density function is used, the drought frequencies based on the rsSPI are mainly determined by the input: precipitation values. For most SPIs there is a clear spatial pattern that relates to the difference in elevation and precipitation. The more elevated the area, the more precipitation and thus the fewer droughts occurs. SPI-12 is the exception where it seems that a reverse relation is shown; the higher areas are subject to more droughts compared to the lower regions. This is difficult to explain looking at the precipitation pattern. Maybe this could be explained by the fact that SPI values between minus one and zero can be part of a drought event, but are not necessarily. It depends if it is preceded with a SPI value below minus one (start of drought event). For SPI-12 there are few drought events with a high average duration and therefore one drought event not identified because the threshold is not reached will influence the drought frequency quite largely.

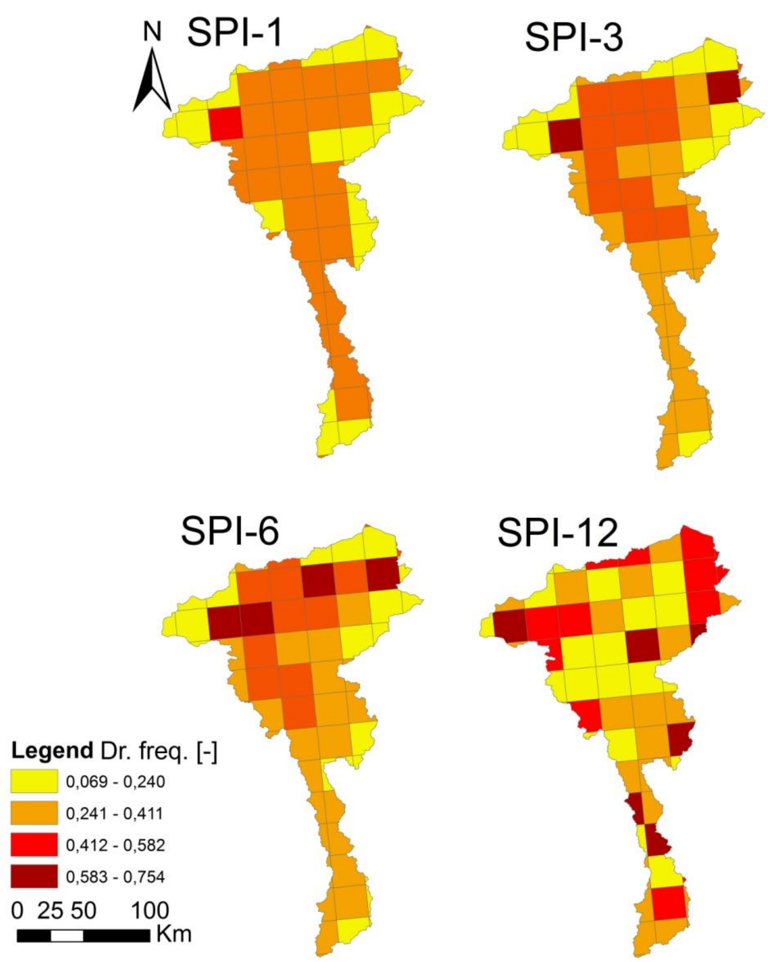

Figure 4-3 Drought frequencies for four time scales for the Meuse basin based on observed dataset.

4.1.5 Deficit-duration relations

Each drought event is plotted by its deficit and duration in Figure 4-4. For SPI-1 cell events there is a maximum in duration found of 13 months and a maximum of around -13 for the deficit. For SPI-12 there are extreme cell events identified with a duration of more than 100 months (more than 8 years) and a deficit of around -120. This is a confirmation of Table 4-2 where it was noticed that a larger time scale relates to a higher average duration and a higher deficit value. Another observation is that for each SPI the relation between deficit and duration seems to be linear. For each SPI, there seems to be an increase in deficit of one, for each month in duration. This seems to be confirmed by Table 4-2 where the average (and standard deviation) is similar for duration and deficit for all time scales. Furthermore the difference in basin and cell drought events can be analyzed. The relation between duration and deficit for cell events seems to be similar to basin events for all time scales. However based on these plots it seems that cell events are more variable: for the same duration value there is more variation in deficit for the cell events than the basin events. This could be caused by the fact that there are a lot more cell events than drought events. Another observation is the lower maximum in duration for the basin events compared to the cell events. It seems unlikely that this can be explained by just the higher number of events. This is probably related to the difference in spatial scale. It is more unlikely that a drought event occurs at a larger spatial scale (basin) than a smaller spatial scale (cell).

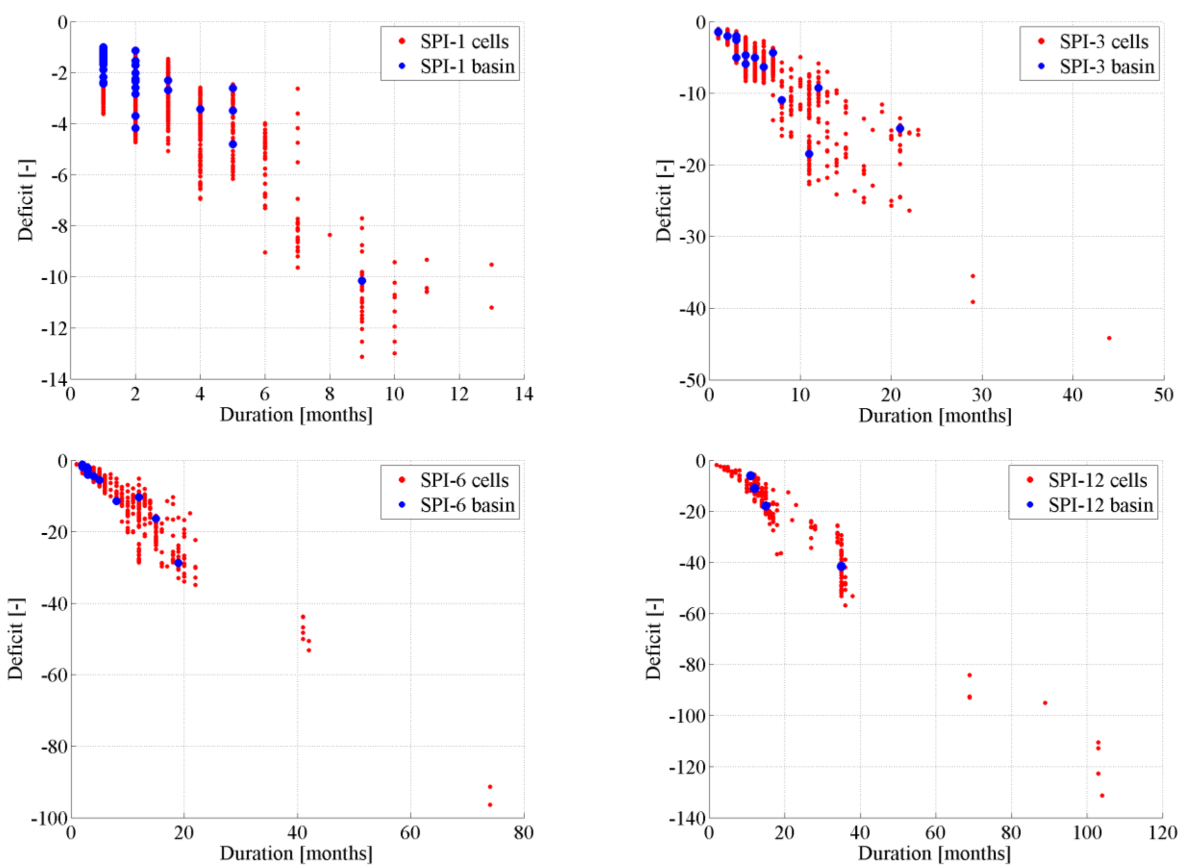

Figure 4-4 Deficit as a function of duration based on observed dataset for four time scales and for basin and cell events.

4.1.6 Temporal correlogram

Figure 4-5 shows the correlation values for different lags for the three SPIs of the basin and the exponential fit of these series. The temporal correlogram shows for different time scales the temporal variability of that SPI. As was noticed by the SPI basin plots the larger the time scale the lower the temporal variability. This plot confirms this observation. The variability of each SPI series can be largely explained by how these values are constructed. For example for the SPI-1 series, the next SPI value is based on a different dataset (precipitation next month for 30 years) and therefore a different probability density function (PDF). The correlation of precipitation in one month and the next is for all 12 months probably low. This is related to why the correlation length of the SPI-1 is not calculated. This is further explained in appendix C. The SPI-12 is the SPI series based on the largest aggregation of precipitation values. Therefore the next SPI value is based on a similar dataset (1 of 12 values is different) and therefore also a similar PDF.

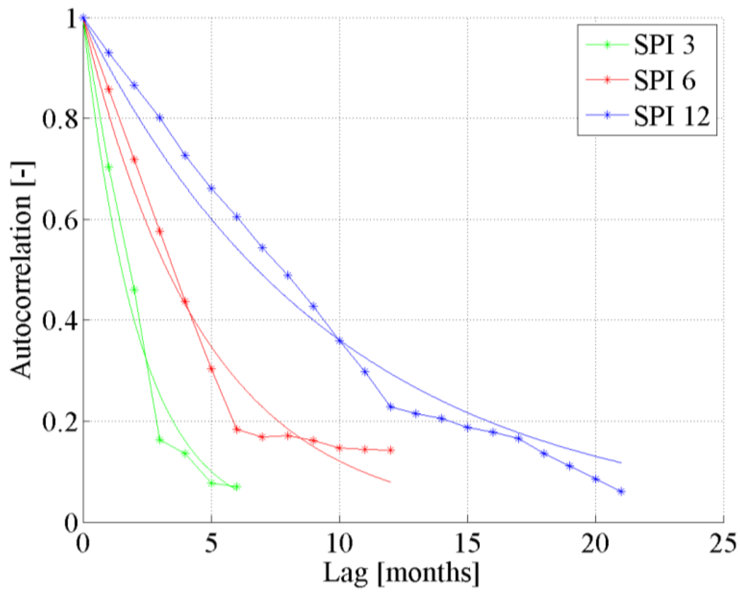

Figure 4-5 Temporal correlogram SPI-basin, for SPI-3, -6 and -12 based on observed dataset.

The correlation length is based on the exponential fit. Table 4-3 shows the correlation length based on these fits. It can be interpreted as the temporal extent where the SPI values are significantly positively related to each other.

Table 4-3 Temporal correlation length based on observed dataset.

	Temporal correlation length [months]
SPI-3	2.2
SPI-6	4.7
SPI-12	9.8

4.1.7 Spatial correlogram

Figure 4-6 shows the spatial correlograms based on the combination of all cells. For each combination a certain correlation value and the distance between the cells is calculated. The spread of data points shows that an exponential function fits well and the r^2 value confirms this. The correlation length is shown in Table 4-4. It can be interpreted as the spatial extent where the SPI values are significantly positively related to each other It seems that short term drought conditions (SPI-1 and SPI-3) are a bit less spatially correlated than long term drought conditions (SPI-6 and SPI-12). However the main conclusion is that for each SPI the correlation length is a multitude of the maximum width of the river basin. The plots show that the greatest distance between cells is around 350 km, while the observed correlation lengths are all above 750 km (range between 760 and 947 km). This implies that the correlation length is an extrapolated value and thus is subject to a higher uncertainty than when it was in range of the data points.

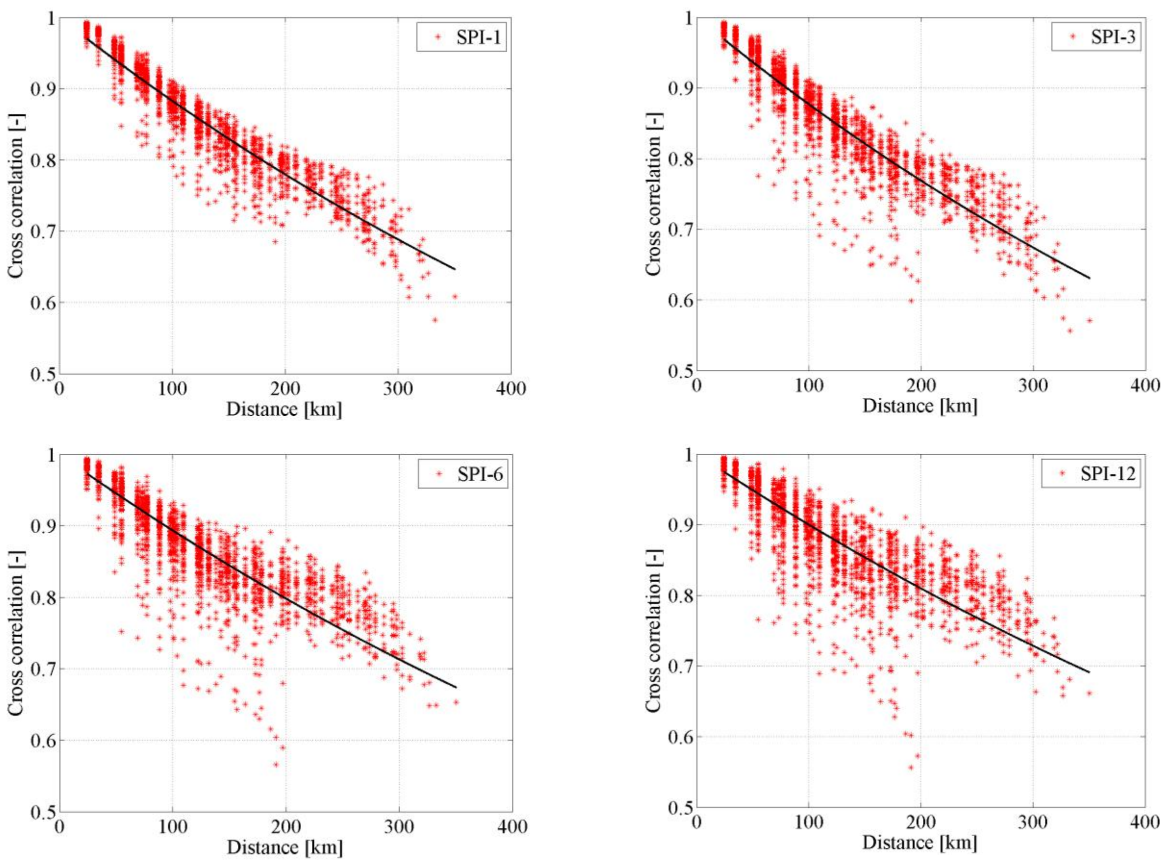

Figure 4-6 Spatial correlogram with exponential fit for all time scales based on observed dataset.

Table 4-4 Spatial correlation length based on observed dataset.

	Observed correlation length [km]
SPI-1	803
SPI-3	760
SPI-6	887
SPI-12	947

4.1.8 Concluding remarks

Based on the previous sections the following statements can be made:

- The larger the time scale, the larger the temporal correlation (i.e. the lower the temporal variability).
- The larger the time scale, the less drought events are observed.
- The larger the time scale, the higher the average and standard deviation in duration.
- The larger the time scale, the higher the average and standard deviation in deficit.
- For all the time scales there is a similar average and standard deviation in intensity.
- For all time scales, except SPI-12, there is a clear relation between the spatial precipitation pattern and the drought frequency pattern in the river basin
- For all time scales there was a (rough) linear relationship between duration and deficit.
- For all time scales the spatial correlation is larger than the basin length, indicating a homogenous basin for each month in SPI values.

The different temporal variability for different time scales is obviously largely explained by the aggregation of precipitation values of consecutive months. For larger time scales this will result in less variable input values. With less variable input values for the SPI calculation, the SPI values will be less variable as well. The difference in temporal variability for the different SPIs is probably causing the difference in average and maximum drought duration and deficit for the different SPIs. Larger time scales have a higher average and maximum in duration and deficit.

There is quite a strong relation between deficit and duration for all time scales. The difference in temporal variability probably also explains the difference in number of drought events. For a 30 year period there were 47 SPI-1 events, 17 SPI-3 events, 11 SPI-6 events and four SPI-12 events identified. In other words it is very likely that an increase in temporal variability will result in an increase in the number of the events and these events will have a lower average and a lower standard deviation in duration and deficit. Temporal variability seems not to be related to the spatial correlation or the intensity of the drought events.

The drought frequency plots show a clear spatial structure for all SPIs that correspond with the precipitation, except for SPI-12. There is no obvious explanation for this, since for the other time scales it seems to be explained by the precipitation pattern which is the same for each SPI. However this precipitation pattern does not to seem influence SPI-12 in the same way.

4.2 RCM assessment

The RCM assessment consists of comparing the drought statistics based on the observed dataset and the output of the RCMs. This is input for a weighted average of all RCMs in the impact analysis. For each statistic and each time scale there is a different error and therefore a different weighting of each RCM.

4.2.1 Number of drought events

Table 4-5 shows how all the identified drought events are distributed based as a function of duration. Overall SPI-1 drought events are simulated quite well. The total number is for most RCMs (exceptions are RCM-1, RCM-9 and RCM-10) in the range of the observed number of drought events. The exceptions also show a totally different distribution of events as a function of duration. For example RCM-1 simulates most events in the highest category (3 and longer) instead of simulating most events in the 1-month category.

SPI-3 drought events are overall overestimated. For the highest category (8 months and longer) there is a large underestimation by half of the RCMs. RCM-1, RCM-7 and RCM-11 performed well for the SPI-3 drought events.

SPI-6 drought events are mostly well simulated, only RCM-10 largely overestimates the number of events. RCM-5, RCM-7 and RCM-9 show a significant different distribution than observed. RCM-8 underestimates the number in the longest category.

SPI-12 events are overestimated by all RCMs. However RCM-4, RCM-9 and RCM-10 show a similar number of drought events (5 instead of 4 events). In particular RCM-4 performs extremely well, only one event in the shortest category is simulated more than observed. All the other RCMs have a relative large overestimation (around +100%) in the total number of events and /or a significant different distribution.

Table 4-5 The number of drought events as a function of duration, based on observed and 13 RCM output datasets.

	Duration [months]	Observed	RCM-1	RCM-2	RCM-3	RCM-4	RCM-5	RCM-6
SPI-1	**All**	**47**	**28**	**40**	**37**	**43**	**39**	**40**
	1	28	5	14	14	20	13	17
	2	12	11	14	10	9	15	12
	3 and longer	7	12	12	13	14	11	11
SPI-3	**All**	**17**	**20**	**20**	**21**	**22**	**20**	**21**
	1,2,3	8	13	12	12	12	11	10
	4 to 7	5	3	6	6	8	6	10
	8 and longer	4	4	2	3	2	3	1
SPI-6	**All**	**11**	**9**	**14**	**15**	**12**	**12**	**13**
	1 to 4	7	3	7	8	6	1	4
	5 to 8	1	3	3	5	3	9	6
	9 and longer	3	3	4	2	3	2	3
SPI-12	**All**	**4**	**7**	**9**	**11**	**5**	**9**	**11**
	1 to 8	2	3	7	9	3	8	9
	9 to 16	1	3	1	2	1	0	2
	17 and longer	1	1	1	0	1	1	0

	Duration [months]	RCM-7	RCM-8	RCM-9	RCM-10	RCM-11	RCM-12	RCM-13
SPI-1	**All**	**39**	**38**	**25**	**31**	**39**	**39**	**44**
	1	13	16	8	0	22	16	18
	2	15	7	0	21	6	14	17
	3 and longer	11	15	17	10	11	9	9
SPI-3	**All**	**19**	**18**	**27**	**28**	**18**	**20**	**22**
	1,2,3	10	8	11	11	9	8	14
	4 to 7	6	10	16	12	6	12	6
	8 and longer	3	0	0	5	3	0	2
SPI-6	**All**	**13**	**11**	**15**	**21**	**12**	**13**	**13**
	1 to 4	2	8	10	16	6	5	4
	5 to 8	9	3	0	1	2	6	6
	9 and longer	2	0	5	4	4	2	3
SPI-12	**All**	**7**	**10**	**5**	**5**	**8**	**8**	**9**
	1 to 8	6	10	0	5	6	7	8
	9 to 16	0	0	5	0	2	1	1
	17 and longer	1	0	0	0	0	0	0

4.2.2 Characteristics of drought events

Duration

For each RCM the average duration and the standard deviation based on all cell events is shown in Table 4-6. These are different events than in Table 4-5 since these are all drought events identified by all the cells, rather than based on the basin. The main difference is that basin drought events tend to be more 'extreme' (longer and more deficit) than cell drought events. The reason to use the cell based events is because of the fact that there are a lot more cell based events than basin based and thus the statistics are more robust.

The average for SPI-1 events is overestimated by all RCMs. RCM-1 and RCM-10 show the highest overestimation. For SPI-3 events all RCMs underestimate the average. RCM-11 seems to perform the best. For SPI-6 most RCMs are close to the observed value. RCM-1 overestimates the most; RCM-8 underestimates the most. For SPI-12 events all RCMs underestimate the average duration. RCM-8 is estimating the lowest value. RCM-1 performs the best.

Looking at the standard deviation it can be noticed that for SPI-1 it is simulated well by all RCMs. The worst simulation, RCM-1, overestimates the standard deviation by 27 %. For SPI-3 all RCMs underestimate the standard deviation. The best RCMs are RCM-1 and RCM-11 (both driven by GCM ARPEGE). The worst estimation was made by RCM-8. For SPI-6 RCM-1 simulates the standard deviation very well. All the other RCMs significantly underestimate the value, where RCM-8 simulates the worst value. For SPI-12 all RCMs largely underestimates the standard deviation. The best estimation is made by RCM-4 which underestimates by around 40 %.

Table 4-6 Average duration in months based on observed and 13 RCM output dataset, cell based events, 1971-2000. The standard deviation is presented between the brackets.

	Observed	**RCM-1**	**RCM-2**	**RCM-3**	**RCM-4**	**RCM-5**	**RCM-6**
SPI-1	1.8 (±1.5)	2.6 (±1.9)	2.2 (±1.5)	2.1 (±1.2)	2.1 (±1.6)	2.0 (±1.2)	2.1 (±1.4)
SPI-3	5.2 (±4.3)	4.4 (±3.5)	4.0 (±2.5)	3.6 (±2.4)	4.4 (±3.1)	4.2 (±2.8)	4.5 (±2.4)
SPI-6	7.8 (±7.1)	9.4 (±7.0)	6.9 (±4.0)	6.0 (±3.4)	6.8 (±4.6)	7.1 (±3.3)	6.7 (±3.5)
SPI-12	19.6 (±16.3)	15.9 (±8.5)	12.2 (±9.3)	10.5 (±7.2)	14.8 (±10.3)	12.1 (±9.7)	10.1 (±8.4)
	RCM-7	**RCM-8**	**RCM-9**	**RCM-10**	**RCM-11**	**RCM-12**	**RCM-13**
SPI-1	2.0 (±1.2)	2.3 (±1.4)	2.4 (±1.3)	2.9 (±1.4)	2.1 (±1.7)	2.0 (±1.3)	2.0 (±1.4)
SPI-3	4.2 (±2.8)	3.6 (±1.3)	3.3 (±1.9)	4.5 (±2.2)	4.9 (±3.5)	3.9 (±2.3)	4.1 (±2.6)
SPI-6	7.1 (±3.3)	4.9 (±2.4)	6.9 (±5.8)	6.0 (±4.0)	7.6 (±4.8)	6.4 (±3.8)	6.9 (±4.6)
SPI-12	11.8 (±9.5)	7.4 (±5.6)	13.4 (±5.0)	11.0 (±2.8)	12.2 (±7.6)	12.9 (±8.6)	10.9 (±6.8)

Deficit

Table 4-7 shows the observed and simulated average deficit and the standard deviation of all cell based events. For SPI-1 events all RCMs overestimate the average deficit, but for most RCMs this is not a large overestimation. The largest errors are made by RCM-1, RCM-9 and RCM-10. For the SPI-3 events most RCMs underestimate the average deficit but not by much. RCM-11 performs the best in this case. For the SPI-6 events all RCMs underestimate the average except for RCM-1. Most estimates are near the observed value, the two worst performing RCMs are RCM-8 and RCM-10. For SPI-12 all RCM underestimate the average deficit. The worst performing RCM is RCM-8, RCM-1 performs the best.

For SPI-1 events the RCMs perform overall well for the standard deviation. The worst RCMs are RCM-1 and RCM-9. For SPI-3 events all RCMs underestimate the standard deviation. The three worst performing RCMs are RCM-8, RCM-9 and RCM-10. These simulations are made with a Hadley RCM. For SPI-6 RCM1 performs by far the best. All the other RCMs underestimate the value. RCM-8 performs the worst. For SPI-12 all RCMs largely underestimate the value.

Table 4-7 Average deficit [-] based on observed and 13 RCM output dataset, cell based events, 1971-2000. The standard deviation is presented between the brackets.

	Observed	**RCM-1**	**RCM-2**	**RCM-3**	**RCM-4**	**RCM-5**	**RCM-6**
SPI-1	-2.3 (±1.5)	-3.2 (±2.3)	-2.7 (±1.3)	-2.4 (±1.3)	-2.5 (±1.5)	-2.4 (±1.3)	-2.5 (±1.3)
SPI-3	-5.7 (±5.1)	-4.9 (±4.2)	-4.9 (±3.4)	-4.3 (±3.0)	-4.9 (±3.7)	-4.8 (±3.4)	-5.1 (±2.9)
SPI-6	-9.3 (±9.7)	-10.6 (±9.5)	-7.7 (±4.6)	-6.8 (±4.5)	-7.4 (±6.4)	-7.8 (±4.6)	-7.8 (±4.3)
SPI-12	-21.4 (±20.4)	-17.5 (±12.1)	-12.9 (±10.3)	-11.0 (±9.0)	-16.7 (±13.8)	-12.3 (±10.1)	-10.8 (±9.3)
	RCM-7	**RCM-8**	**RCM-9**	**RCM-10**	**RCM-11**	**RCM-12**	**RCM-13**
SPI-1	-2.4 (±1.3)	-2.7 (±1.5)	-3.1 (±2.4)	-3.5 (±1.5)	-2.6 (±1.9)	-2.4 (±1.4)	-2.4 (±1.4)
SPI-3	-4.8 (±3.5)	-4.1 (±1.9)	-3.8 (±2.1)	-4.8 (±2.1)	-5.7 (±4.5)	-4.5 (±2.8)	-4.7 (±3.2)
SPI-6	-7.8 (±4.7)	-5.0 (±2.7)	-6.8 (±5.5)	-5.7 (±4.2)	-8.6 (±6.6)	-7.1 (±4.7)	-7.5 (±5.4)
SPI-12	-12.0 (±10.1)	-7.7 (±5.6)	-13.2 (±6.8)	-11.7 (±4.6)	-13.4 (±10.0)	-13.6 (±10.7)	-11.9 (±8.6)

Intensity

Table 4-8 shows the observed and simulated average intensity for all SPIs. For the SPI-1 events the averages are really close to each other. There are no large deviations from the observed values. This is the same for SPI-3, SPI-6 and SPI-12 events. The observed and simulated results are all showing values around -1.7. The maximum is -1.8 and the minimum -1.5. In other words there is little variation in the results. As was mentioned in section 4.1.3 the SPI method is probably related to this close range in average intensity and the standard deviation.

For all time scales the standard deviation is simulated quite well. Significantly different results are shown by RCM-10: particular low values for SPI-3, -6 and -12.

Table 4-8 Average intensity [-] based on observed and 13 RCM output dataset, cell based events, 1971-2000. The standard deviation is presented between the brackets.

	Observed	**RCM-1**	**RCM-2**	**RCM-3**	**RCM-4**	**RCM-5**	**RCM-6**
SPI-1	-1.6 (±0.51)	-1.7 (±0.56)	-1.8 (±0.58)	-1.6 (±0.51)	-1.7 (±0.52)	-1.7 (±0.56)	-1.7 (±0.57)
SPI-3	-1.7 (±0.53)	-1.7 (±0.53)	-1.8 (±0.54)	-1.8 (±0.52)	-1.6 (±0.43)	-1.7 (±0.52)	-1.7 (±0.48)
SPI-6	-1.8 (±0.62)	-1.8 (±0.62)	-1.8 (±0.54)	-1.7 (±0.44)	-1.6 (±0.45)	-1.7 (±0.49)	-1.8 (±0.48)
SPI-12	-1.7 (±0.48)	-1.8 (±0.68)	-1.7 (±0.44)	-1.7 (±0.41)	-1.8 (±0.57)	-1.7 (±0.49)	-1.7 (±0.36)
	RCM-7	**RCM-8**	**RCM-9**	**RCM-10**	**RCM-11**	**RCM-12**	**RCM-13**
SPI-1	-1.7 (±0.56)	-1.7 (±0.52)	-1.7 (±0.63)	-1.8 (±0.49)	-1.7 (±0.60)	-1.6 (±0.48)	-1.6 (±0.46)
SPI-3	-1.7 (±0.53)	-1.6 (±0.40)	-1.7 (±0.49)	-1.6 (±0.31)	-1.8 (±0.52)	-1.7 (±0.52)	-1.7 (±0.46)
SPI-6	-1.7 (±0.50)	-1.6 (±0.43)	-1.6 (±0.39)	-1.5 (±0.25)	-1.7 (±0.51)	-1.7 (±0.48)	-1.7 (±0.46)
SPI-12	-1.7 (±0.50)	-1.6 (±0.45)	-1.7 (±0.40)	-1.5 (±0.33)	-1.7 (±0.55)	-1.7 (±0.43)	-1.7 (±0.50)

4.2.3 Drought frequency pattern

Figure 4-7 shows how RCM-1 simulates the drought frequency pattern in the river basin. In this section all the RCMs are compared to the observed pattern. For each time scale the best performing RCM was RCM-1. Visually comparing the observed pattern (Figure 4-3) and Figure 4-7 it can be noticed that for SPI-1 similar values and a similar pattern is visible. For SPI-3 and SPI-6 there are similar values simulated but a more spatially variable pattern is shown. For SPI-12 there was an unexpected observed pattern. The simulation seems more logical; the lower areas have less precipitation and thus a higher drought frequency (since drought is now defined relative to the basin average). The average error in drought frequency is 0.05, 0.09, 0.12 and 0.15 for respectively SPI-1, -3, -6 and -12. Considering the range for drought frequency values (between 0 and 1) an average absolute error of 0.15 seems significant.

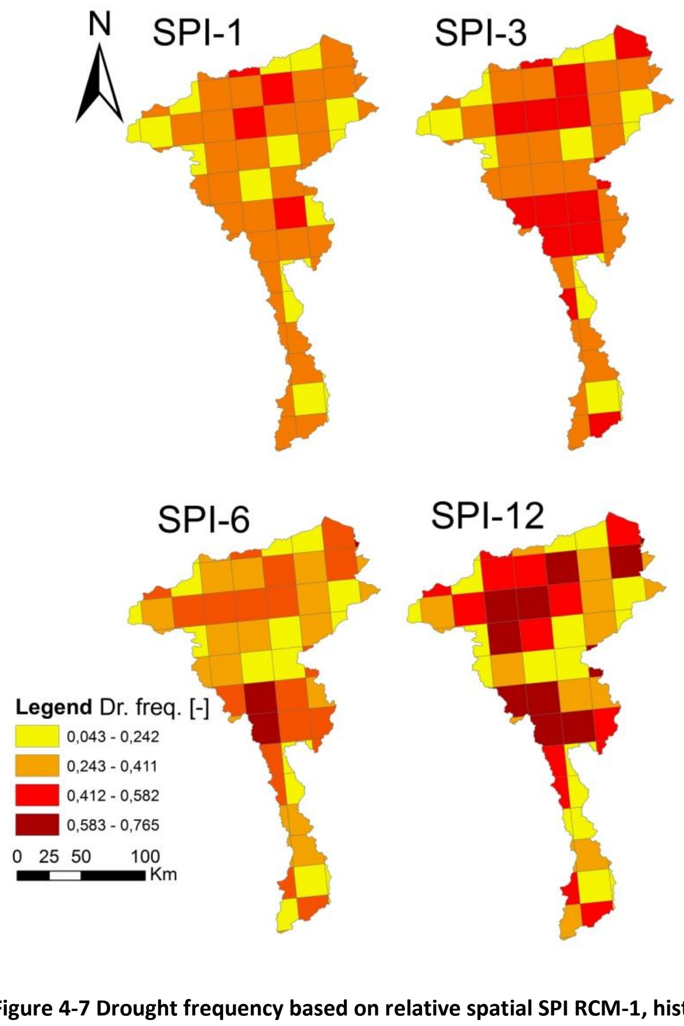

Figure 4-7 Drought frequency based on relative spatial SPI RCM-1, historical period

4.2.4 Deficit and duration error

Table 4-9 shows the relative errors in the deficit-duration relation for all RCMs. This relative error is based on the absolute difference between observed and simulated average deficit for each duration value. In appendix D an example deficit duration plot of one RCM is shown for all time scales. This can be helpful when interpreting the results in Table 4-9.

It is established in section 4.1.3 that the smaller the time scale, the shorter and higher the number of events is. This can be seen as the main factor causing the difference in relative error for different SPIs. The smaller the time scale, the higher the number of events and the shorter the events are and thus the less variability in deficit. For all SPIs and all RCMs the relative error was below 3%. This seems a particular low value that can be (partly) explained by the input and how the weighting is done.

Another factor that relates to this low error value is that extreme events are most of the time not taken into account since there is no corresponding event in the other dataset. This is quite important for the assessment since the more extreme events are more important than the less extreme ones. However the relation is overall simulated quite well. Section 4.2.2 showed how well the duration and deficit is simulated. The average and standard deviation of both characteristics were largely underestimated for SPI-12 by all RCMs. In combination with section 4.2.1, where it was established that most RCMs simulated more events for SPI-12, but less extreme events, it can be stated that most likely there are not a lot of extreme events not taken into account. In other words it is very likely that there is not a great error for any RCM for the deficit-duration relationship. This is probably related to the high correlation between these characteristics.

Table 4-9 The relative error in simulating the deficit [%]

	SPI-1	SPI-3	SPI-6	SPI-12
RCM-1	0.24	1.12	1.44	2.85
RCM-2	0.28	0.87	1.40	1.64
RCM-3	0.14	0.69	1.07	1.95
RCM-4	0.14	0.79	1.16	2.45
RCM-5	0.10	0.60	1.25	2.39
RCM-6	0.22	0.98	1.42	1.77
RCM-7	0.10	0.53	1.17	2.46
RCM-8	0.26	0.67	1.09	1.82
RCM-9	0.45	0.91	1.57	1.98
RCM-10	0.49	0.60	0.92	2.64
RCM-11	0.21	0.90	0.97	1.78
RCM-12	0.16	0.83	1.27	2.43
RCM-13	0.17	0.63	1.13	2.58

4.2.5 Temporal correlation length

Table 4-10 shows the observed values and the difference in temporal correlation length between observed and simulated. For SPI-3 the temporal correlation length is simulated quite well. The highest overestimation is made by RCM-10 (+0.71 months), the highest underestimation is made by RCM-9 (-0.71 months). These are (relatively) quite large errors, however most RCMs are close to the observed value.

For SPI-6 it can be noticed that most RCMs underestimate the value, except for RCM-1. RCM-1 simulates by far the best of all RCMs for SPI-6. RCM-8 performs the worst with an underestimation of 2 months. For SPI-12 all RCMs underestimate the correlation length. RCM-8 performs again the worst with an underestimation of 6.32 months. RCM-1 performs the best with an underestimation of 1.17 months.

An underestimation of the temporal correlation can be interpreted as an overestimation of the temporal variability; i.e. the SPI values change more quickly and drought events have a higher probability to end and to start again. This will probably result in more drought events. It is uncertain how the average duration and its standard deviation will be affected. But based on the observed drought and the difference between the SPIs and their type of drought it can be expected that an overestimation of the temporal variability will result in an underestimation of the average duration and deficit. Section 4.2.2 showed the average and standard deviation of duration of all drought events for all RCMs. Looking at RCM-8 for SPI-12 (the largest underestimation of the temporal correlation) it can be noticed that the average duration is the lowest of all simulations and that the standard deviation in duration is one of the lowest of all simulations. Section 4.2.1 shows that RCM-8 simulates the most events of all simulations. This indicates that the temporal variability is related in the way as expected with the number of drought events and the kind of droughts. The goodness-of-fit and the strength of the fit are based on the r^2 and the F value respectively. These values can be found in appendix B. For SPI-3 10/13 RCMs showed significant fits, for SPI-6 this is 8/13 and for SPI-12 this is 11/13.

Table 4-10 Observed values and error in temporal correlation length [months]

	SPI-3	SPI-6	SPI-12
Observed	2.18	4.74	9.82
RCM-1	0.26	0.32	-1.17
RCM-2	0.01	-1.38	-3.35
RCM-3	-0.42	-1.23	-3.26
RCM-4	0.12	-1.06	-2.38
RCM-5	-0.23	-0.77	-1.48
RCM-6	-0.07	-1.43	-3.69
RCM-7	-0.24	-0.82	-1.74
RCM-8	-0.02	-2.00	-6.32
RCM-9	-0.71	-0.69	-3.92
RCM-10	0.71	-1.00	-3.22
RCM-11	-0.28	-1.03	-2.39
RCM-12	-0.41	-1.46	-2.04
RCM-13	-0.26	-0.94	-2.88

4.2.6 Spatial correlation length

The observed spatial relation showed a quite constant high spatial correlation for each SPI. Table 4-11 shows the error in correlation lengths of each simulation and SPI. For SPI-1 there are large under- and overestimations. With an observed value of around 800 km an underestimation of 367 km (RCM-8) is quite large. The largest overestimation is made by RCM-1 with 289 km.

For the other SPIs it can be noticed that RCM-1 largely overestimates the spatial correlation length. RCM-10 seems to highly overestimate the correlation length for all SPIs except for SPI-1. RCM-5 and RCM-8 largely underestimates the spatial correlation length for all SPIs. For all SPIs there is a rather equally spread of under- and overestimation. This can be seen as positive since the weighted average will be around the observed value. An overestimation of the spatial correlation length can be interpreted as an overestimation of the spatial extent of the drought events. The goodness-of-fit and the strength of the fit are based on the r^2 and the F value respectively. These values can be found in appendix B. The fits were all significant, but not always very strong: RCM-10 for SPI-6 and -12 showed a value of 0.46 and 0.28 respectively for the r^2. However all the other fits were equal or above 0.5 and most above 0.8. This indicates that most fits were strong.

Table 4-11 Observed values and error in spatial correlation length [km]

	SPI-1	SPI-3	SPI-6	SPI-12
Observed	803	760	887	947
RCM-1	289	514	498	628
RCM-2	30	-12	-139	-318
RCM-3	81	50	-112	-131
RCM-4	-39	130	64	77
RCM-5	-255	-275	-424	-523
RCM-6	60	50	-20	-99
RCM-7	-255	-274	-421	-524
RCM-8	-367	-434	-508	-733
RCM-9	280	47	-279	-167
RCM-10	-83	486	912	886
RCM-11	-158	-7	-141	-102
RCM-12	-232	-179	-349	-309
RCM-13	-225	-225	-369	-457

4.2.7 Summary of results and discussion

Based on the previous sections the following statements can be made:

- For each SPI, except SPI-1, most RCMs tend to overestimate the number of drought events
- For each SPI, except SPI-1, most RCMs underestimate:
    - the average duration
    - the variation in duration
    - the average deficit
    - the variation in deficit
- For each SPI the average intensity and its variation are simulated well.
- For each SPI most RCMs simulate the spatial variation inside the basin not well.
- Based on one RCM (RCM-1; the best performing RCM for drought frequency pattern), it seems that the spatial variation inside the basin is better simulated for smaller time scales.
- For each SPI the deficit-duration relation seems to be simulated well by all RCMs.
- For SPI-3 the temporal correlation length is simulated well, for SPI-6 and SPI-12 most RCMs underestimate the correlation.
- For each SPI the spatial correlation was simulated well by some RCMs.

The main conclusion that can be drawn is that RCMs have difficulty in simulating the observed drought. There was not one RCM that really performed well for all assessment criteria. Overall it seems that RCMs simulate a more temporally variable climate than observed. The higher variability (assessed by the temporal correlation length) is probably the main factor contributing to more drought events. The simulated drought events are less extreme (lower duration and deficit) and the variation in duration and deficit is lower. The relation between a higher temporal variability and an increase in number of events and less extreme events is confirmed in this section.

For the SPI-1 events there is an underestimation of the number of events. This is probably related to the higher average duration and also a higher average deficit. The simulated temporal variability is probably lower than observed, but this was not quantified with the temporal correlation length. The spatial structure was simulated quite well by RCM-1 for all time scales. However, RCM-1 was one of the RCMs that largely overestimate the spatial correlation length for all time scales. This seems a contradicting result. Apparently the spatial correlation is not related with the spatial structure. The spatial structure is mostly dependent on the precipitation pattern, while the spatial correlation is not. The spatial correlation is based on SPI; i.e. standardized precipitation values, and therefore does not necessarily reflect the spatial structure of precipitation.

Possible errors in the RCM simulation can only be explained by how the RCMs simulate the precipitation. This since only (monthly) precipitation is used as input for the SPI calculations. There could be a precipitation bias in the used GCM and/or RCM. This can be examined by looking at research addressing the particular GCM or RCM and how it simulates precipitation. This will be done in discussion section (Chapter 5). However the SPI standardizes the precipitation values and therefore the difference in absolute values (observed vs. simulated) is not the main problem. The variability is the main issue here. The temporal variability can be differently simulated than observed and maybe more importantly the variability in precipitation for each individual month. The first variability will result in a different temporal variability of the SPI values and thus result in a different type of drought events. The latter variability largely determines the probability density function and thus the SPI values.

Influence of GCM and RCM on results

RCM-11 and RCM-12 (same RCM but different GCM) show similar values for the number of events but a different distribution. For all the other statistics similar values were obtained or similar trends. This suggests that the RCM determines most of the results when analyzing meteorological drought. However the other RCMs with the same RCM and a different GCM did not show this relation.

RCM-2, -3, -5, -12 and -13 (different RCM but same GCM) show similar values in number of events but a different distribution. The drought characteristics and temporal correlation was quite similar. The large difference lies in the spatial correlation. This suggests that the RCM determines the spatial correlation length more than the GCM. However the other RCMs with the same RCM and a different GCM did not show this relation. However the other RCMs with a different RCM and the same GCM did not show this relation. Based upon the previous paragraphs it seems that the applied RCM or driving GCM is not largely influencing the simulations of the historical period.

4.3 Impact of climate change on drought

The impact analysis is carried out by comparing the results for the future period (2021-2050 or 2066-2095) with the historical period (1971-2000). In the plots these periods are indicated by the last year, of the respective period. To indicate the simulated trend a line based on the average of all RCM simulations is plotted. For each statistic the average is a weighted average based on the RCM assessment, except for the drought frequency of the basin.

Table 4-12 shows for each RCM run the driving GCM and applied RCM. For the 13 RCM projections five different GCMs and 11 different RCMs are applied. Each GCM has a unique symbol (or marker) to identify the driving GCM for each RCM projection. In combination with a color all the projections have a unique code. The color relates to the used RCM, except for the RCMs with white as their color. Some RCM runs use the same RCM (they only differ in GCM). These RCM runs are colored red, blue or green and each color relates to the same RCM (RCA3 (red)) or to similar RCMs (the Hadley RCMs (blue) and HIRHAM and DMI-HIRHAM both are green). The difference in the Hadley GCMs is their parameterization and response to radiative forcing (Kjellström et al. 2011). These groups can indicate the influence of the used GCM on the drought impact results. There are five RCM runs that use the ECHAM5-r3 GCM. These RCM runs all have a square as the symbol. In this way the influence of the RCM can be investigated. For the historical period the observed value (the yellow point) is shown in the figures and indicates how well the RCMs perform by comparing with the simulated value.

Table 4-12 The GCM-RCM matrix; symbols and color identification for all RCM runs

	GCM	ARPEGE	ECHAM5-r3	HadCM3Q0	HadCM3Q3	HadCM3Q16
RCM	Color/ Symbol	○	□	▷	◇	▽
Aladin	White	RCM-1				
RACMO	Orange		RCM-2			
RCA#	Red		RCM-3		RCM-4	RCM-6
REMO	Cyan		RCM-5			
CLM	White			RCM-7		
HadRCM3Q0	Blue			RCM-8		
HadRCM3Q3					RCM-9	
HadRCM3Q16						RCM-10
HIRHAM	Green	RCM-11				
DMI-HIRHAM			RCM-12			
RegCM	White		RCM-13			

4.3.1 Change in number of drought events

Figure 4-8 shows the number of drought events based on the SPI basin. For the SPI-1 drought events it can be noticed that all RCMs underestimate the number of drought events (see section 4.2.1). On average there is a small increase simulated. The spread in results remains similar for all periods.

The SPI-3 drought events show an obvious increase in the number of events. For the SPI-6 drought events the spread in results increases for the future periods. The weighted average shows an increase in the number of events. The number of SPI-12 drought events is overestimated by all RCMs. The spread in the possible number of events increases and one RCM projects no basin drought events for the last period. On average there is a slight decrease and a slight increase for respectively period 2050 and 2095.

Focusing on particular RCMs it can be noticed that RCM-8 shows an increase in number of drought events for all SPIs and that RCM-3 shows the largest decrease in the number of events. For all the SPIs it can be noticed that the RCMs with GCM ECHAM5-r3 (denoted with a square) show the lowest number of drought event for the future periods. This indicates that this GCM is projecting a more wet climate than the other GCMs.

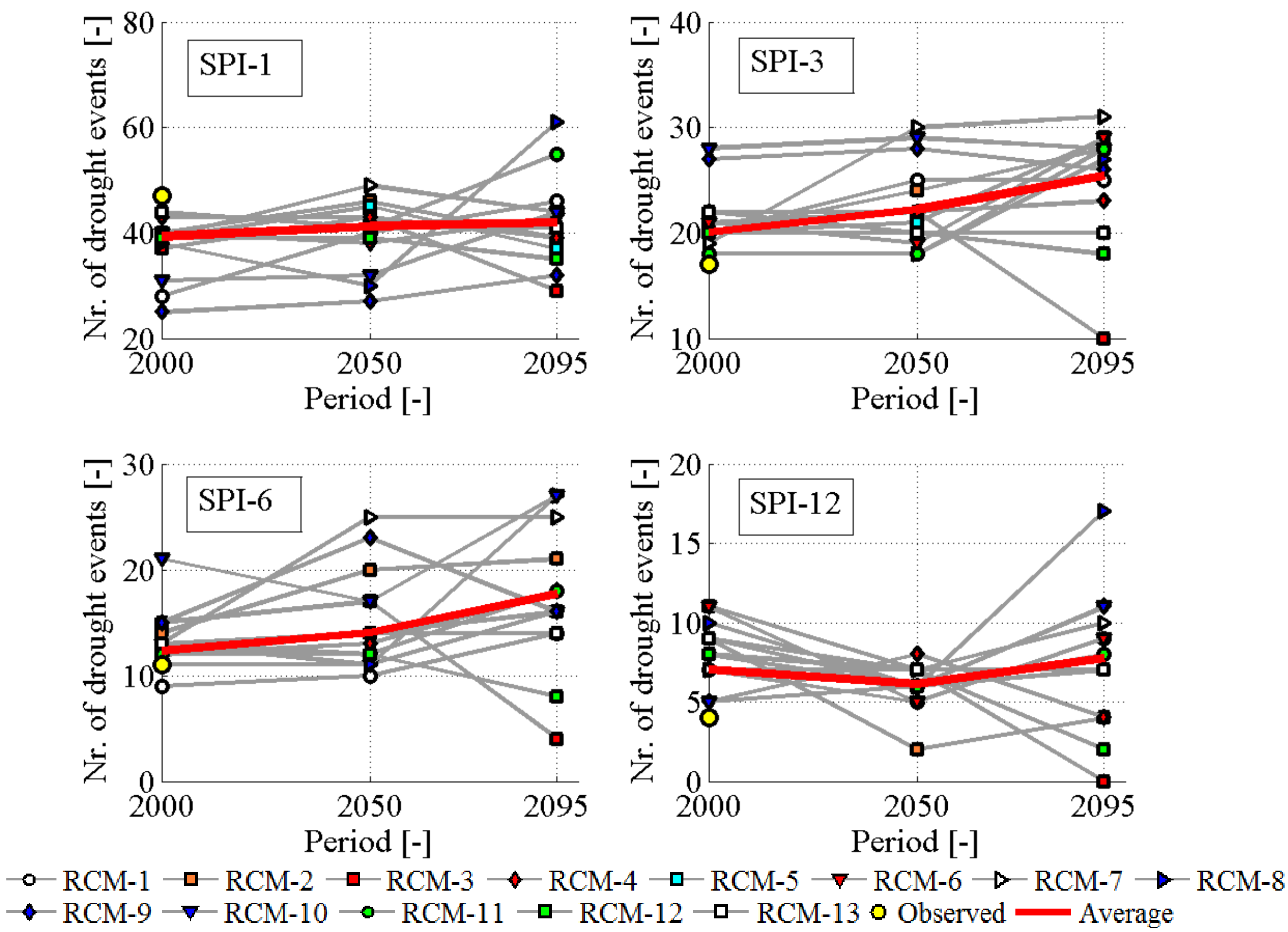

Figure 4-8 Number of drought events, for 2000 (observed and simulated), 2050 (simulated) and 2095 (simulated) with weighted average of simulations.

4.3.2 Change in drought event characteristics

The drought events considered are the cell based events. Next to duration the other event characteristics that are considered are total deficit (sum of SPI values) and intensity (lowest SPI value of an event).

Duration

Figure 4-9 shows the change in average duration of drought events. The average duration is overestimated for SPI-1 and underestimated for SPI-3 and SPI-12 by all RCMs. For SPI-6 there is a good representation of the average duration as most results are close to the observed value (see section 4.2). For all SPIs there is an increase projected for the 2095 period. The average duration decreases for SPI-1, SPI-3 and SPI-6 for the 2050 period and increase (compared to the historical period) in the 2095 period. Most of the RCMs with the GCM ECHAM5-r3 (denoted with a square) are projecting below average for all SPIs. The Hadley RCMs (blue ones) all show an above average estimation for SPI-1.

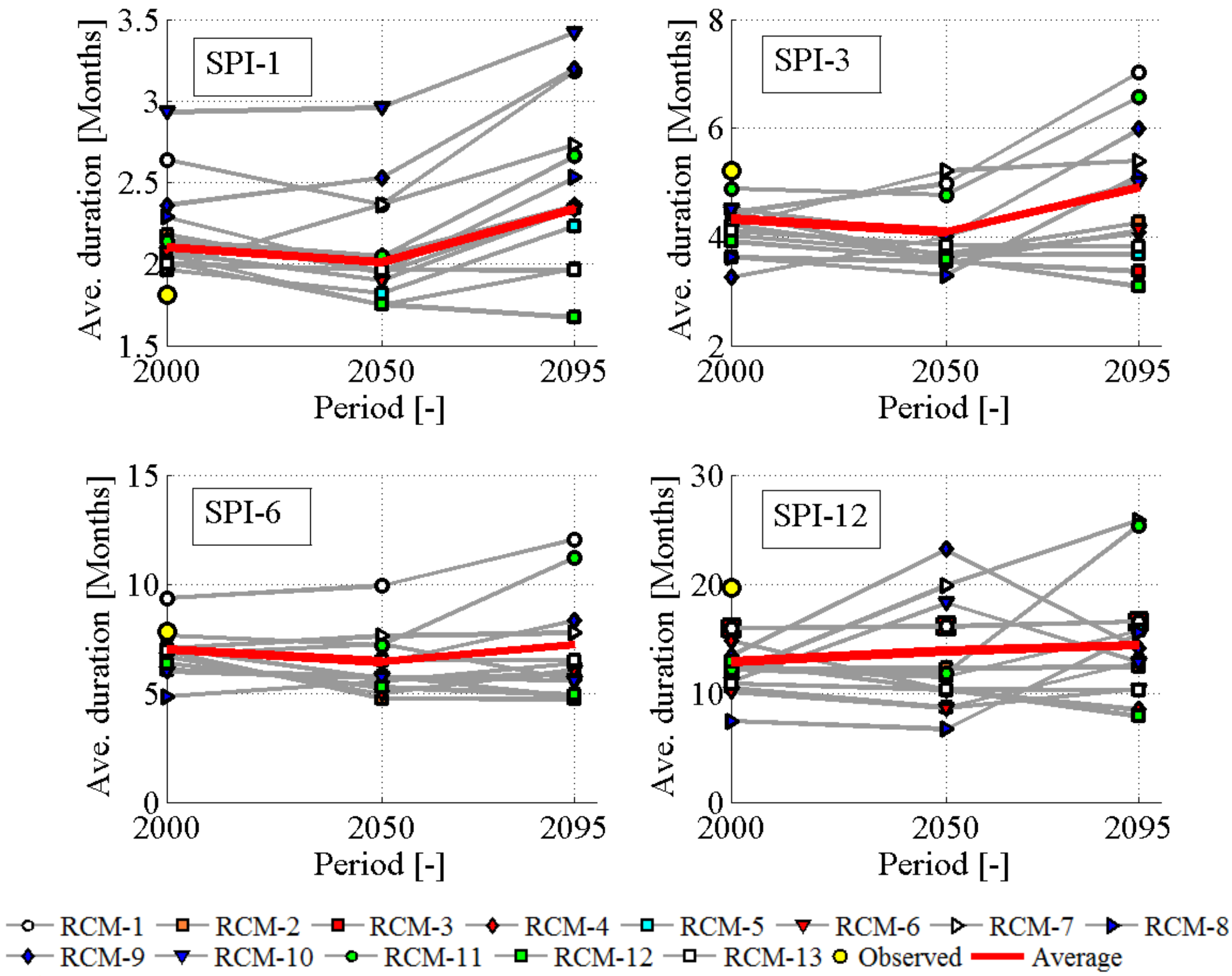

Figure 4-9 Average duration of drought events, for 2000 (observed and simulated), 2050 (simulated) and 2095 (simulated) with weighted average of simulations.

Figure 4-10 shows the change in the standard deviation of duration. For all SPIs, except for SPI-1, the RCMs underestimate the standard deviation. For SPI-1 there is an overall good simulation of the standard deviation. See section 4.2 for more information.

There is a small to large increase on average in standard deviation for all time scales. In combination with a small to large increase in average duration for the different SPIs (see Figure 4-9), it can be concluded that an increase in extreme long drought events for all time scales is projected in the future. Especially for SPI-1 for the 2066-2095 there is a large increase in average duration and its standard deviation.

RCM-7 seems to simulate strange results for most SPIs (except for SPI-1); there are extremely high values simulated for the two future periods. In combination with the fact that RCM-7 simulated the observed value well this will have a quite large influence on the weighted average value.

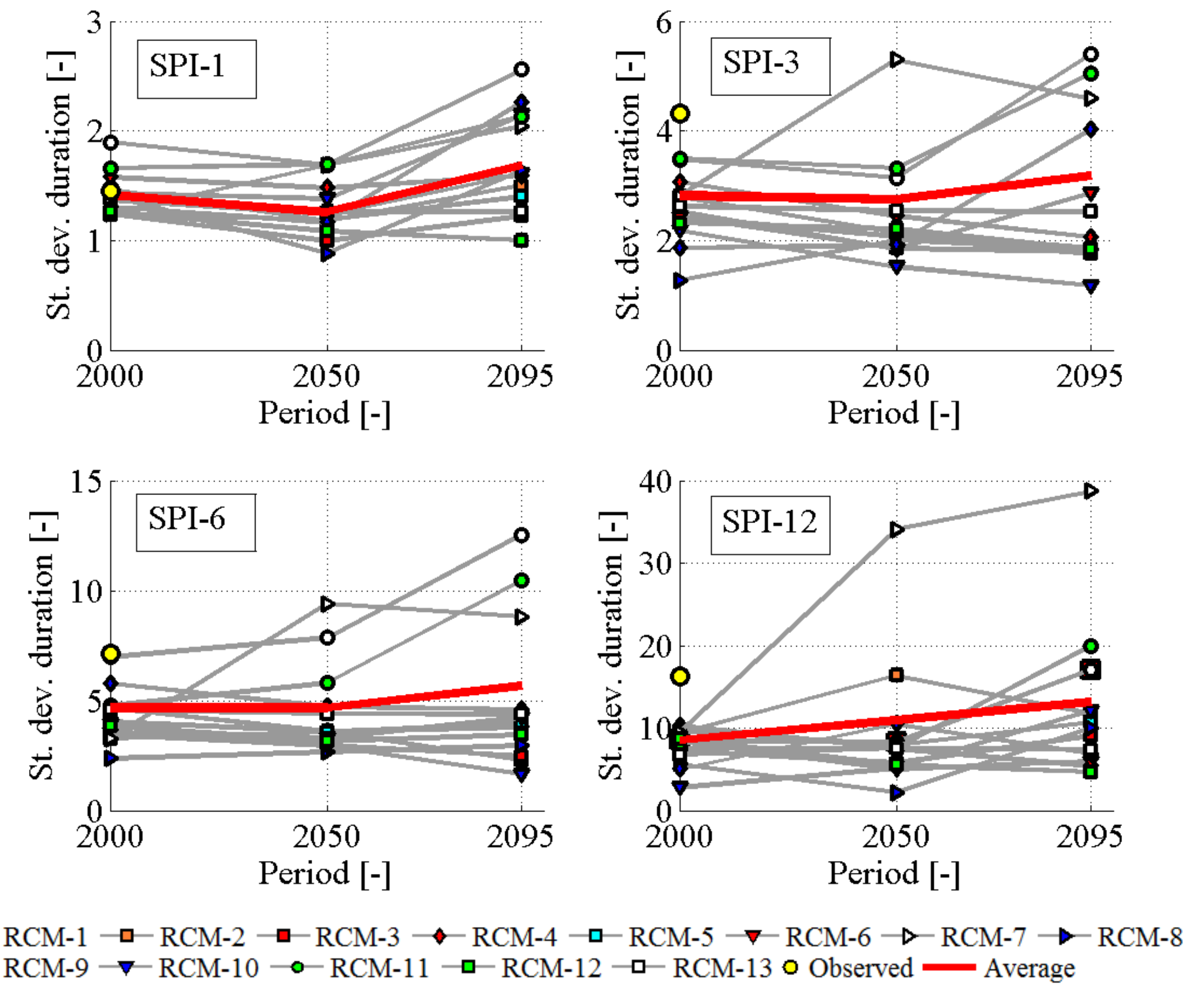

Figure 4-10 Standard deviation of duration of drought events, for 2000 (observed and simulated), 2050 (simulated) and 2095 (simulated) with weighted average of simulations.

Deficit

Figure 4-11 shows the change in average deficit of all RCMs. Deficit is by definition a negative value. A lower value for the deficit means a higher deficit. For SPI-1 the RCMs overestimate the average deficit and a large increase in the range of values for the future periods can be noticed. The average of the RCMs shows that the average deficit will increase for all SPIs. For SPI-3 the RCMs underestimate the observed value. Most RCMs tend to show an increase in deficit which corresponds with the weighted average. For SPI-6 there is an overall good simulation of the observed value. Most RCMs shows an increase in deficit for the two future periods. For SPI-12 the simulations underestimate quite largely the observed value and the projections for the two future periods show an increased range of values. The first statement indicates the lack of quality in the simulations (both historical and future periods) the latter statement indicates the large range of possible outcomes. Combined it should be noted that for this case no strong conclusion can be drawn.

RCM-10 shows the largest increase for SPI-1 events in average deficit. RCM-7 simulates one of the largest increases in average deficit for most SPIs. For SPI-6 the RCMs with GCM ARPEGE (green) show the largest increase in average deficit.

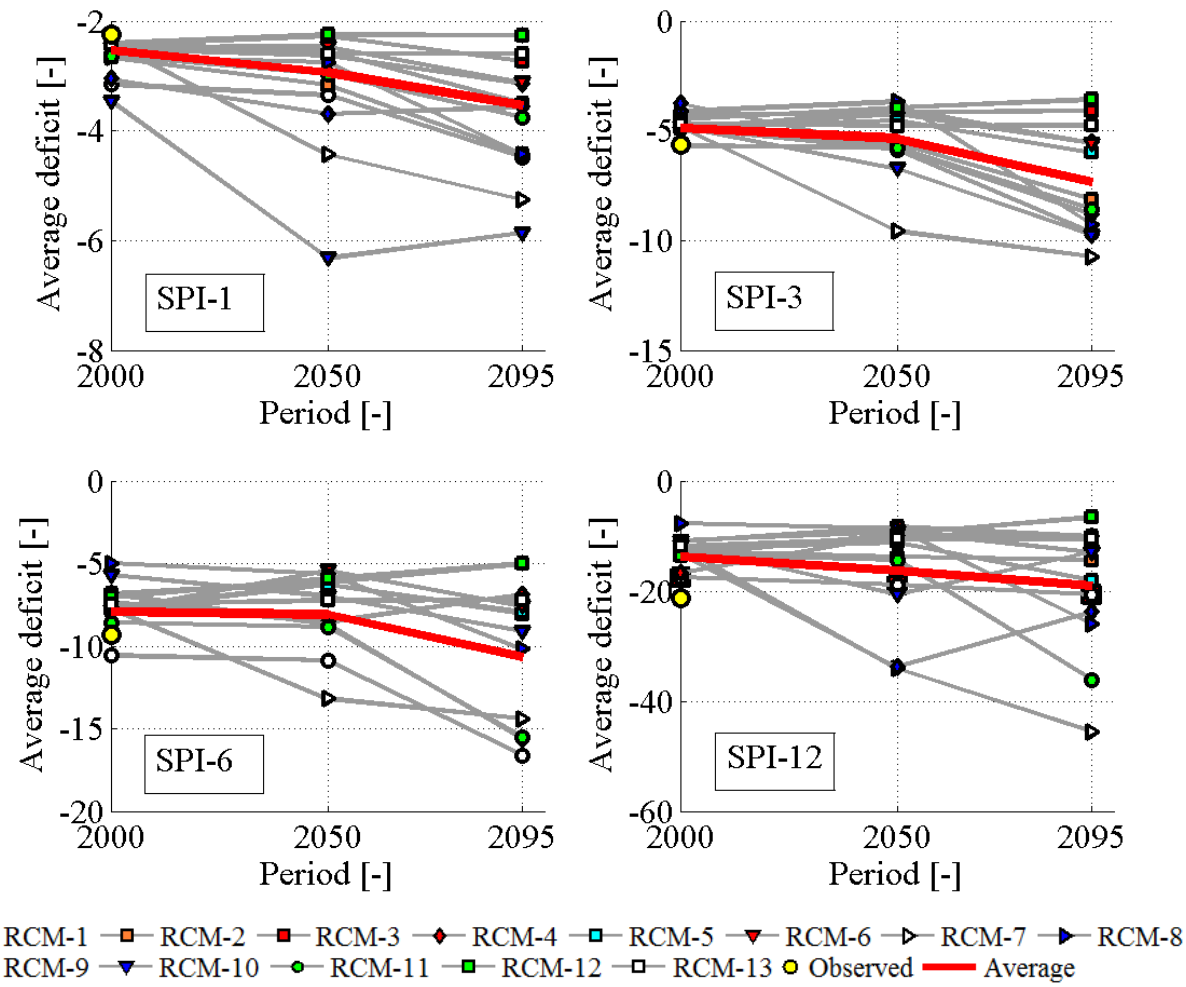

Figure 4-11 Average deficit of drought events, for 2000 (observed and simulated), 2050 (simulated) and 2095 (simulated) with weighted average of simulations.

Figure 4-12 shows the change in the standard deviation of the deficit. The standard deviation for SPI-1 drought events is simulated quite well, for the other SPIs the RCMs underestimate the deviation. See section 4.2 for more information.

On average the standard deviation of the deficit increases for all time scales. This indicates similar to the increase in variation in duration an increased chance of extreme events. RCM-7 shows oddly high changes for all SPIs. RCM-10 shows a similar strange high change for SPI-1.

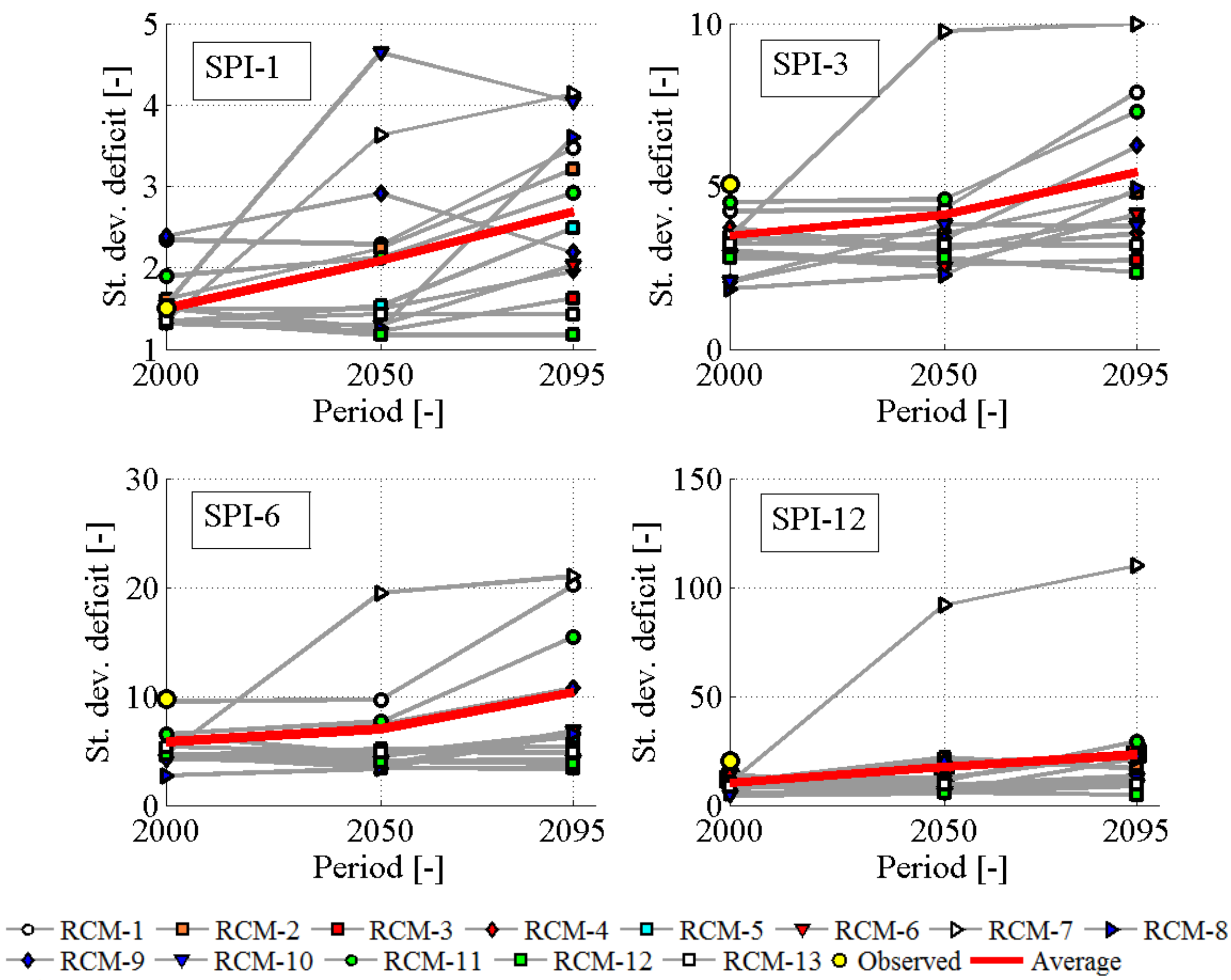

Figure 4-12 Standard deviation of deficit of drought events, for 2000 (observed and simulated), 2050 (simulated) and 2095 (simulated) with weighted average of simulations.

Intensity

Figure 4-13 shows the change in average intensity (the lowest SPI value of a drought event). For all SPIs the observed value is simulate well and the weighted average shows an increase in intensity (a lower value, thus a higher intensity). The spread in results for all SPIs considerably increases in the future periods. RCM-7 shows the largest changes in average intensity for all SPIs.

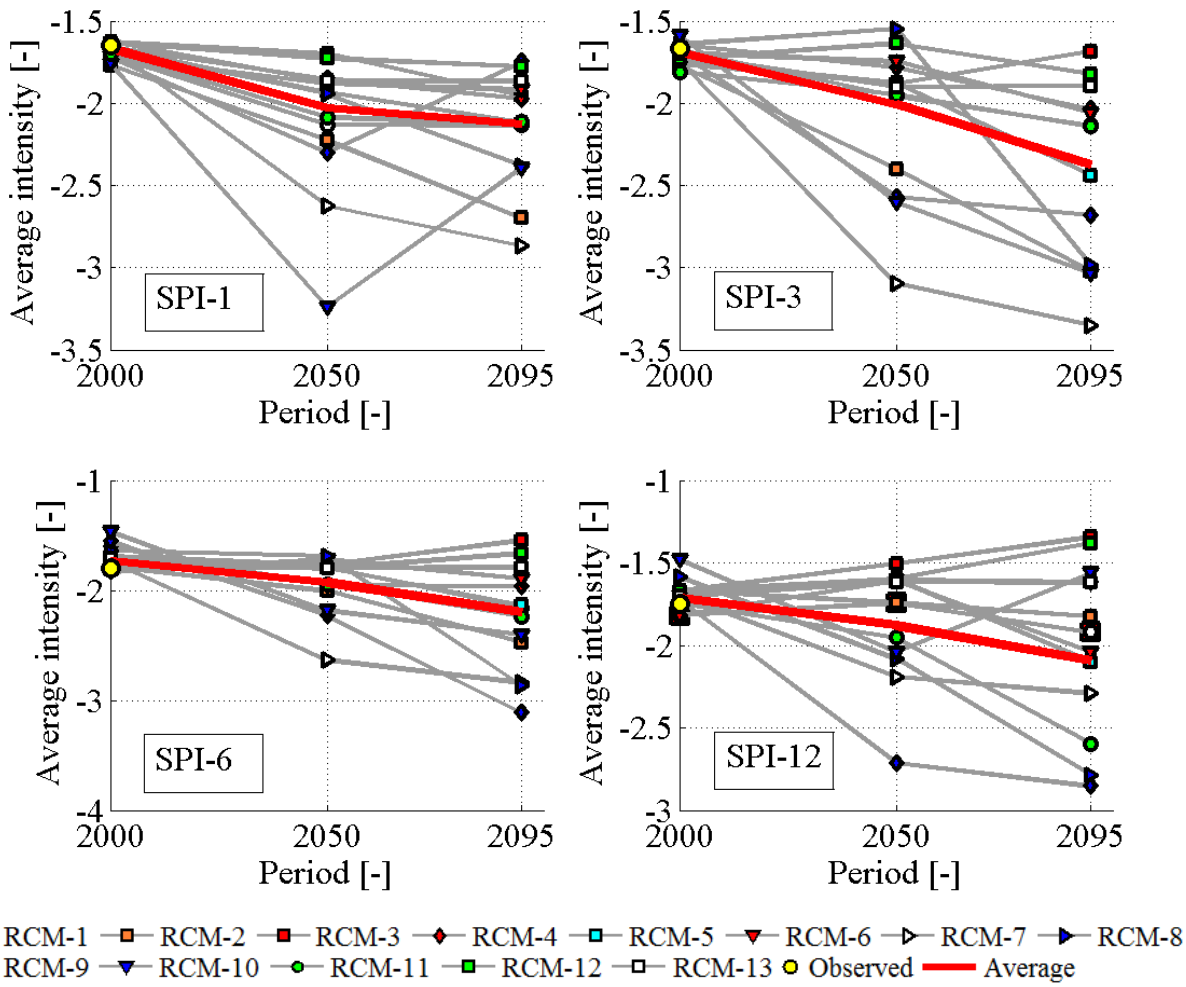

Figure 4-13 Average intensity of drought events, for 2000 (observed and simulated), 2050 (simulated) and 2095 (simulated) with weighted average of simulations.

Figure 4-14 shows the change in standard deviation of the intensity. The standard deviation for each SPI is simulated quite well. The spread in results in the future periods is quite high, but the weighted average shows for all SPIs a considerable increase in the standard deviation of intensity. This implies a more extreme climate: i.e. drought events with a larger variation in intensity. Combined with the projected increase in the average intensity this will result in more events with an extreme intensity. RCM-7 simulates the largest changes for all SPIs.

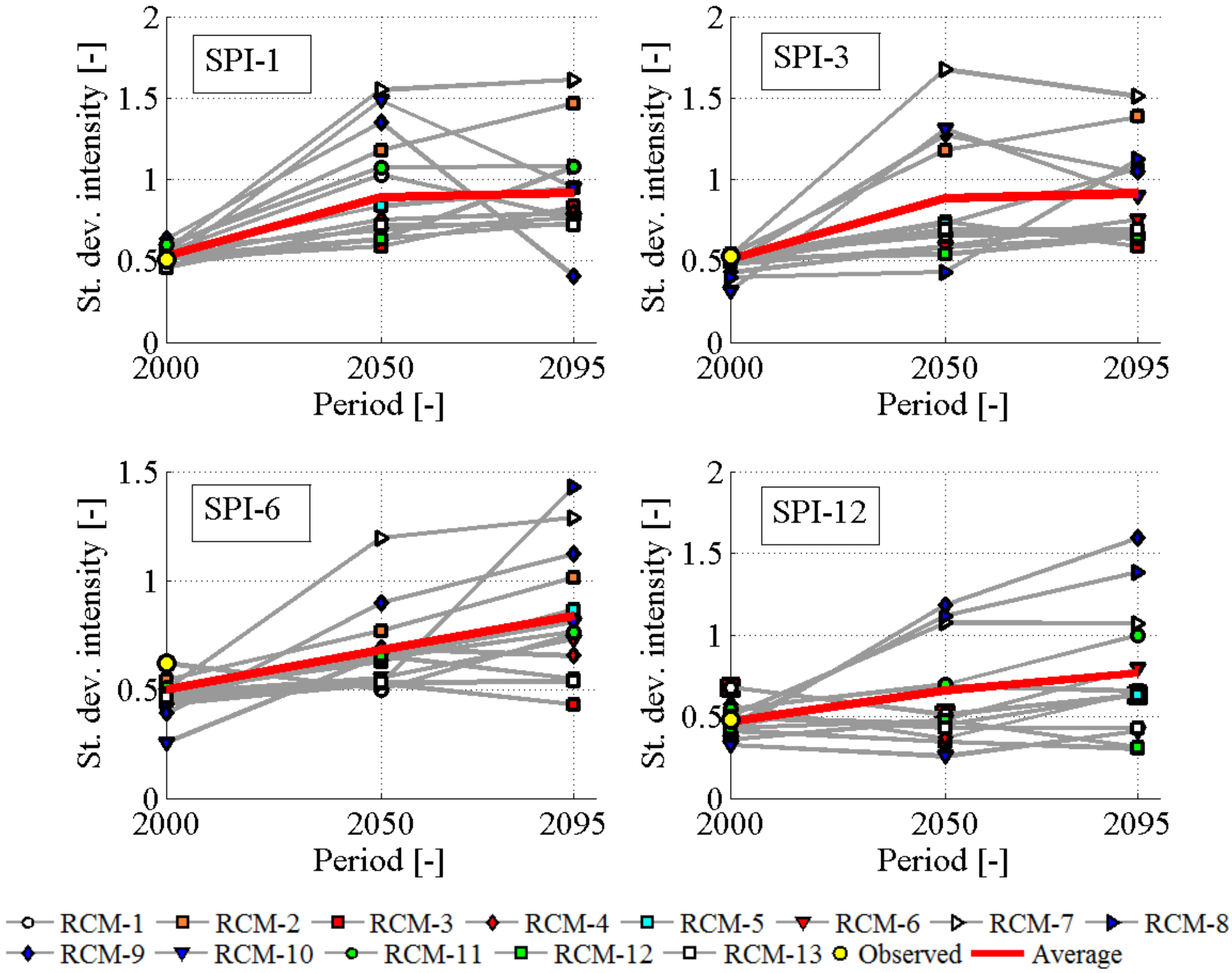

Figure 4-14 Standard deviation of intensity of drought events, for 2000 (observed and simulated), 2050 (simulated) and 2095 (simulated) with weighted average of simulations.

4.3.3 Change in drought frequency basin

The change in basin drought frequency is shown in Figure 4-15. The average is not weighted for this statistic. The average of all RCMs show a slight increase simulated for all SPIs. However the spread in simulations suggest a large uncertainty for the future periods. For SPI-12 (period 2066-2095) there is one RCM (RCM3) that simulates no drought at basin level, while another RCM (RCM11) projects drought around 60% of the time.

Other interesting results are the RCMs with the same GCMs and same or similar RCM. For example the RCMs with ECHAM5-r3 (square) as their driving GCM have overall lower than average drought frequencies in the future periods. The RCMs with ARPEGE (circle) as their driving GCM show the highest change in drought frequency for all SPIs. I.e. the GCM ECHAM5-r3 simulates a wetter climate compared to the weighted average projection, while the GCM ARPEGE simulates a drier climate.

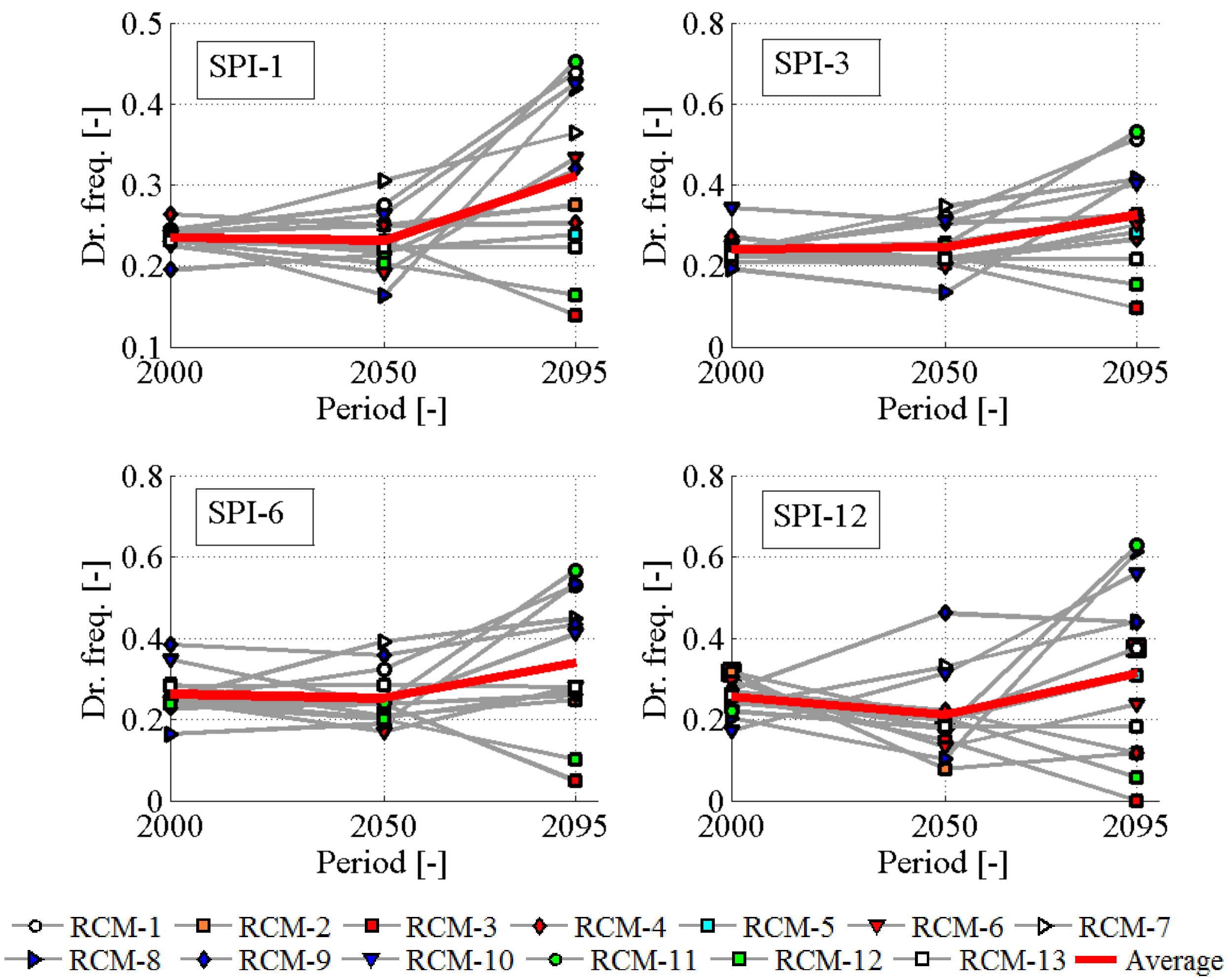

Figure 4-15 Drought frequency of the river basin, for 2000 (simulated), 2050 (simulated) and 2095 (simulated) with average of simulations.

4.3.4 Change in drought frequency pattern

The assessment showed that RCM1 simulated the drought frequency over the basin the best of all RCMs. Figure 4-16 shows the drought frequency for the Meuse basin for the three periods for SPI-1. It is clear that for each future period there is an increase for most part of the basin. This could be expected since the basin average drought frequency changes from 0.244 to 0.275 for 2050 and 0.439 for 2095. An interesting result is the relation with the known relief of the basin; it seems that the higher locations are less drought prone than the less elevated locations. This can be probably largely explained by the RCM-1 projection of more precipitation for higher locations then the lower ones.

Figure 4-17 shows the drought frequency for the basin for the three periods for SPI-3. There is a clear increase in overall drought frequency projected. The basin average changes from 0.235 to 0.321 and 0.514 for 2050 and 2095 respectively. There is a similar spatial pattern visible as for SPI-1; the more elevated the less drought prone the area is.

Figure 4-18 shows the drought frequency for the basin for the three periods for SPI-6. There is a clear spatial pattern simulated for the historical period. This pattern changes to a less clear structure and with more spatial variation. The basin average changes from 0.248 to 0.324 and 0.530 for both future periods. Although it is less obvious for SPI-6 than the smaller time scales, the less elevated areas have higher drought frequencies then the higher elevated areas.

Figure 4-19 shows the drought frequency for the basin for the three periods for SPI-12. There is a clear spatial pattern simulated for the historical period. This pattern changes quite largely to an extremely spatially variable pattern for the period 2050. This changes for the last period (2095) into a spatially correlated pattern with little variation in values. On average for the whole basin the drought frequency changes from 0.315 to 0.198 to 0.375 (see Figure 4-15). This is interesting when combined with the extreme variable pattern for the period 2050; on average there is a decrease which is quite large (from 0.315 to 0.198) while for some parts of the basin there is a strong increase.

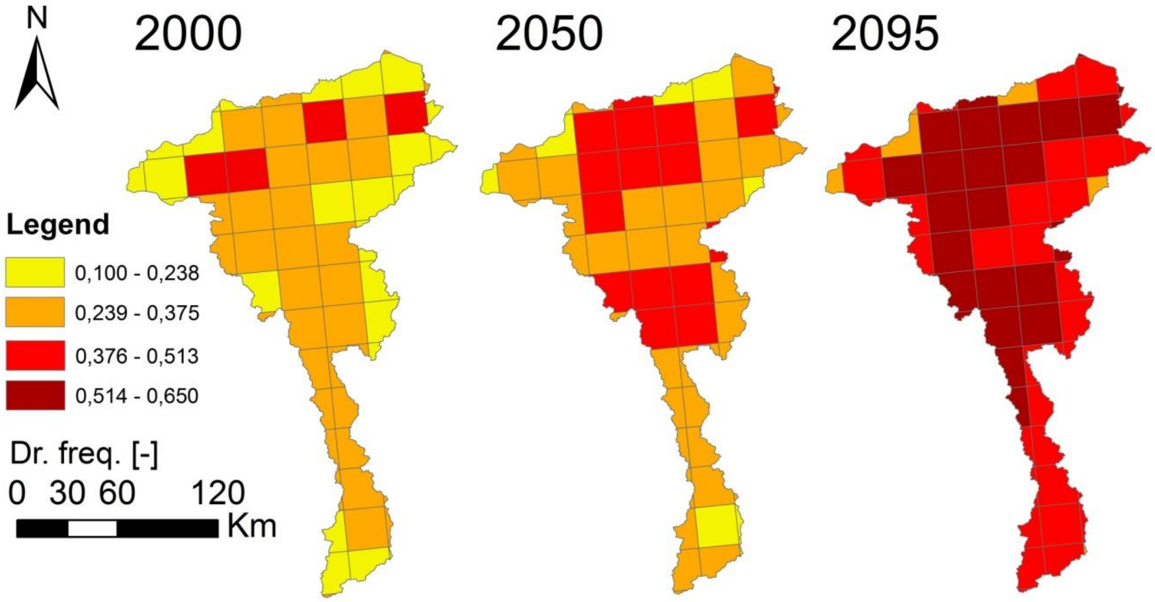

Figure 4-16 Change in drought frequency as simulated by RCM-1 (SPI-1)

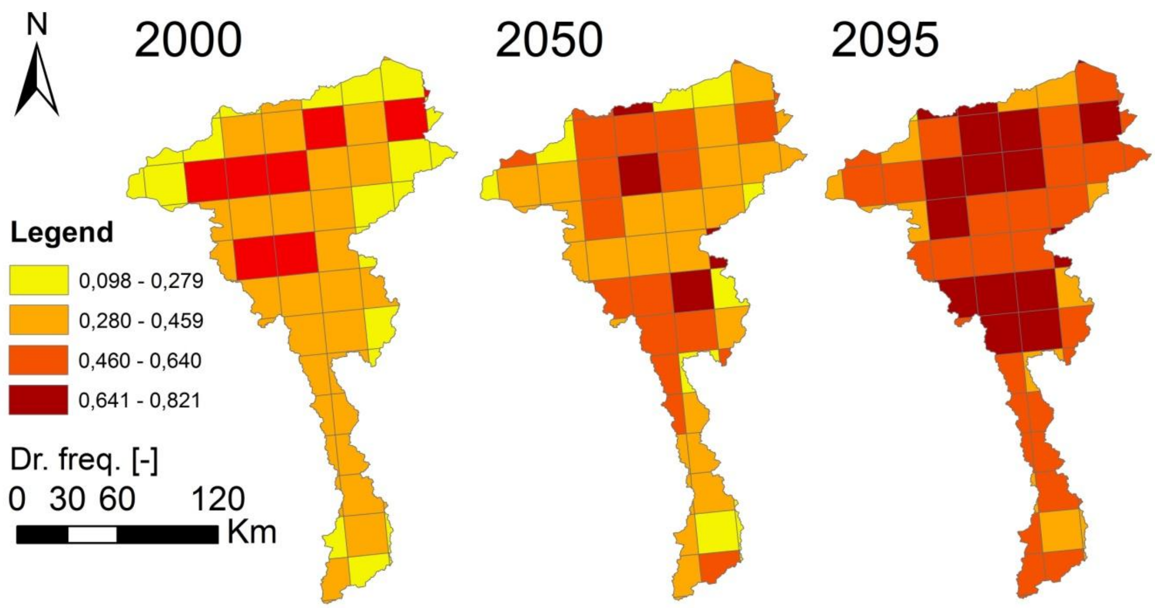

Figure 4-17 Change in drought frequency as simulated by RCM-1 (SPI-3)

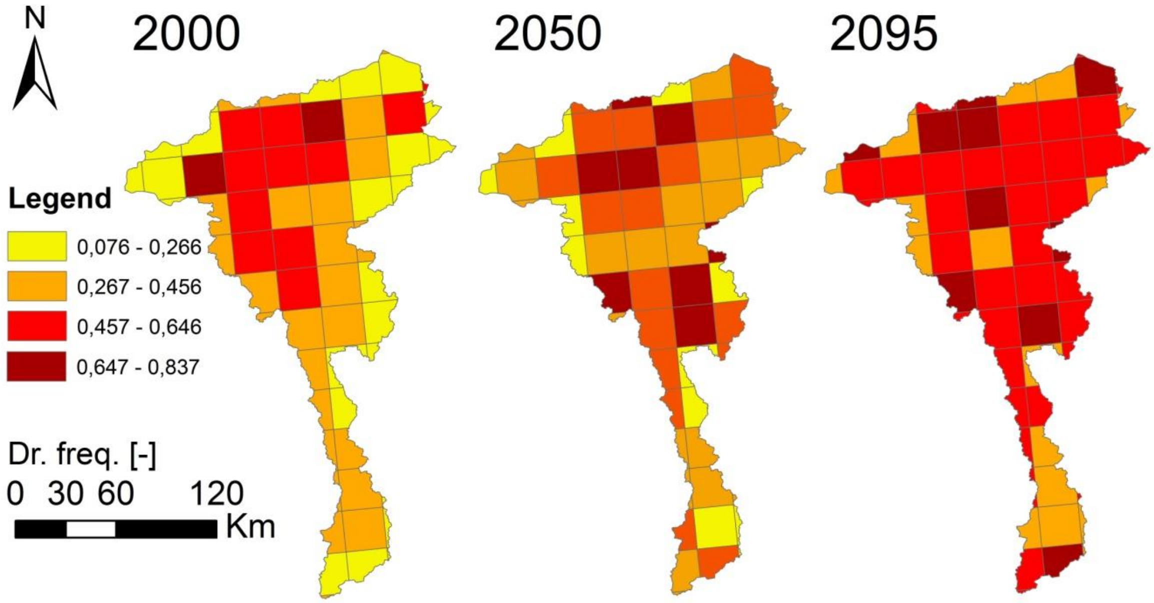

Figure 4-18 Change in drought frequency as simulated by RCM-1 (SPI-6)

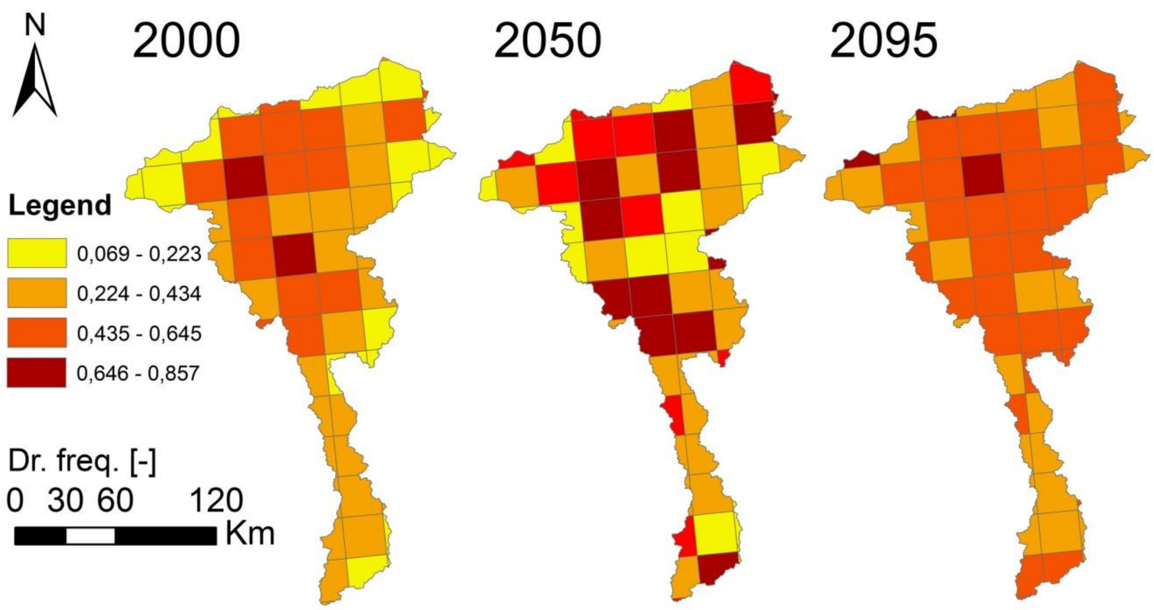

Figure 4-19 Change in drought frequency as simulated by RCM-1 (SPI-12)

4.3.5 Change in deficit-duration relations

Figure 4-20 shows the change in the deficit-duration relationship. For all SPIs the average is decreasing, this indicates a higher deficit for the same duration. For SPI-1 all RCMs simulate a decrease and thus it can be concluded that it is most likely that SPI-1 drought events will become more severe (a higher deficit for the same duration). For SPI-3 drought events a similar observation can be made except that one RCM (RCM-12) simulates no change to a little increase. For SPI-6 and SPI-12 drought events the projection shows for some RCMs an increase, while the average is decreasing. This indicates that there is a bit more uncertainty in the projections than for example SPI-1 where all projections show a decrease. The RCMs with ECHAM5-r3 (square) as their driving GCM show the smallest change in the deficit-duration relation. RCM-7 shows one of the largest changes of all RCMs. RCM-9 shows an outlier for SPI-12 for the period 2095 which could just be the result of particular drought events. As discussed in section 4.2 this statistic is subject of matching drought events for the same duration in both datasets (in this case simulation for the past and future climate). Larger time scales have less drought events and the events have a higher deficit. RCM-10 shows for SPI-1 for the period 2050 an extreme result. Since SPI-1 events are mostly short-lasting and there is not much variation (see section 4.2.1) in deficit it is unlikely that such much change will occur.

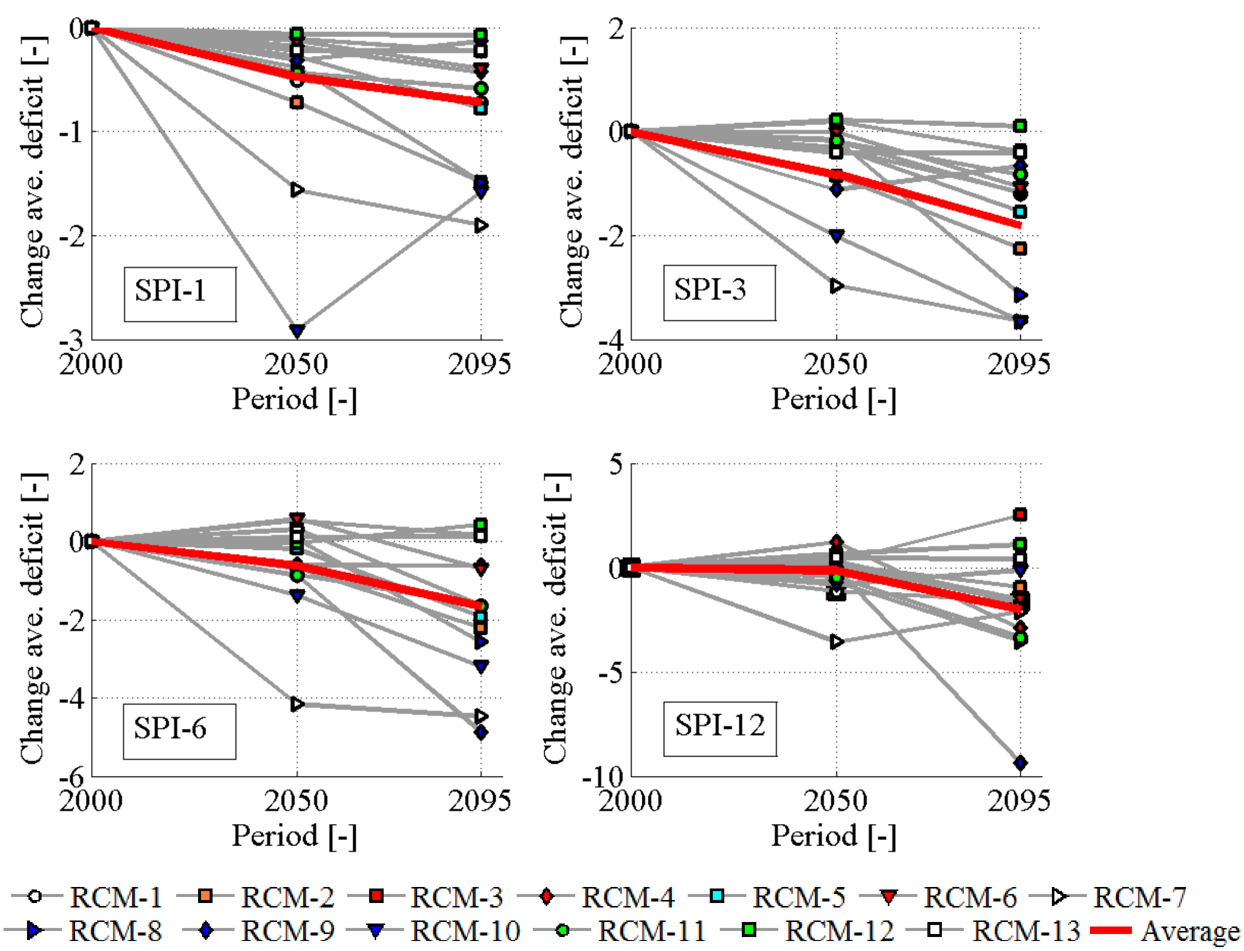

Figure 4-20 Change in the deficit-duration relation of drought events, all SPIs, for 2000 (simulated), 2050 (simulated) and 2095 (simulated) with weighted average of simulations.

4.3.6 Change in temporal correlation

Figure 4-21 shows the change in temporal correlation for the future periods. For SPI-3 the correlation length is well reproduced by quite a lot of RCMs. The weighted average does not show a significant change.

For SPI-6 the RCMs, except for RCM-1, underestimate the correlation length. The weighted average shows a rather large decrease in correlation length.

For SPI-12 the RCMs quite largely underestimate the correlation length. This implies that the projections in the future periods have a relative large uncertainty. The average value in correlation length is slightly decreasing.

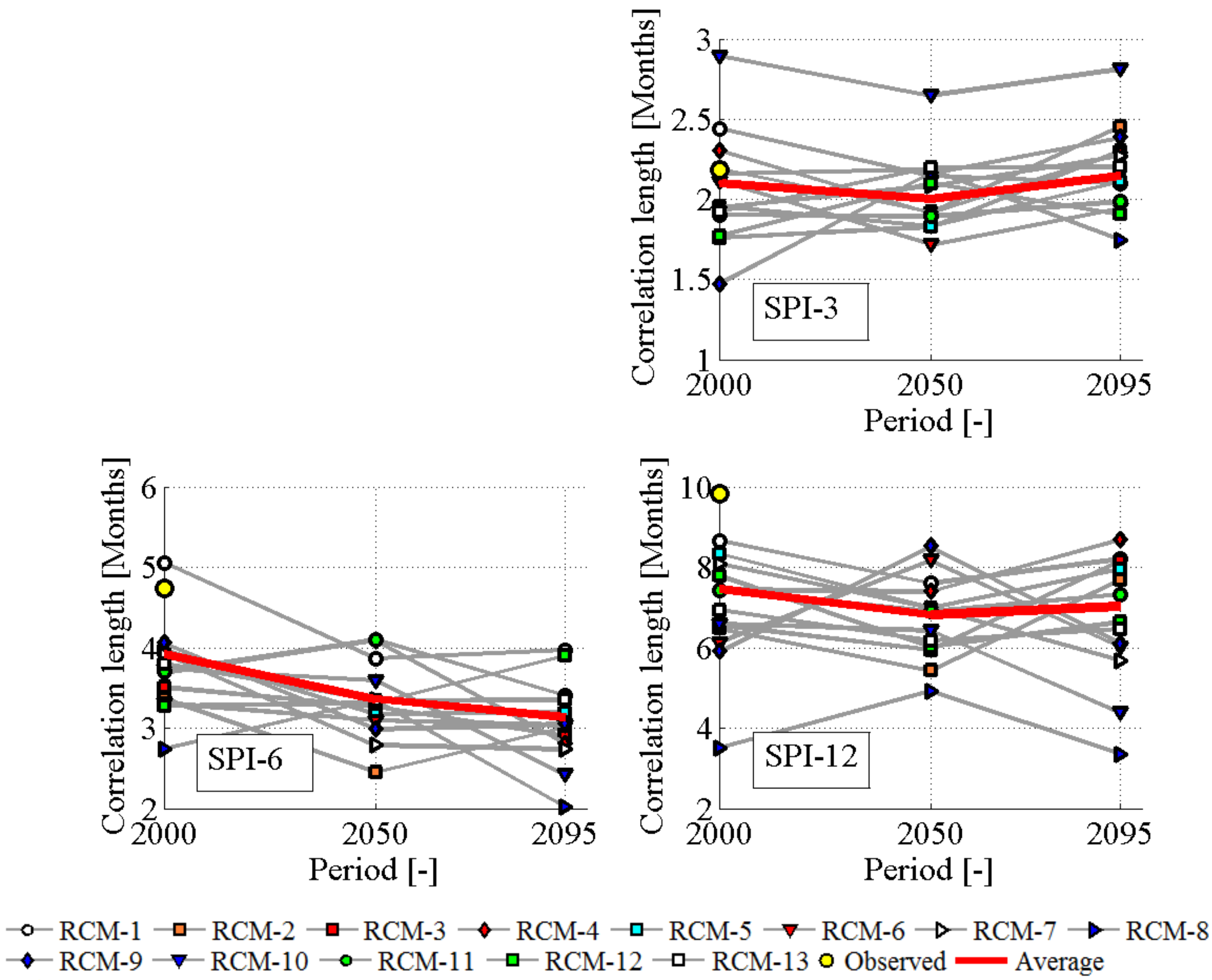

Figure 4-21 Temporal correlation length, for 2000 (observed and simulated), 2050 (simulated) and 2095 (simulated) with weighted average of simulations.

4.3.7 Change in spatial correlation

Figure 4-22 shows the change in spatial correlation. For SPI-1 the spatial correlation length is simulated rather well and the weighted average shows an increase. For SPI-3 the correlation length is simulated quite well by most RCMs. RCM-10 overestimates the value and shows for all SPIs a high value for the period 2050. The average shows a steady increase in correlation length. RCM-11 and 12 (green) show the lowest values for the future periods. For SPI-6 the correlation length is simulated well by most RCMs. On average there is quite a large change in correlation length: from around 800 km up to 1000 km in the period 2095. For SPI-12 the correlation length is simulated quite well by some RCMs. On average the correlation length is projected to increase slightly.

RCM-10 shows an extreme high value for period 2050 for all SPIs. There is on average an increase in correlation length. RCM-11 and 12 (HIRHAM and DMI-HIRHAM as their RCM) show one of the lowest value for both future periods for SPI-1 and SPI-3.

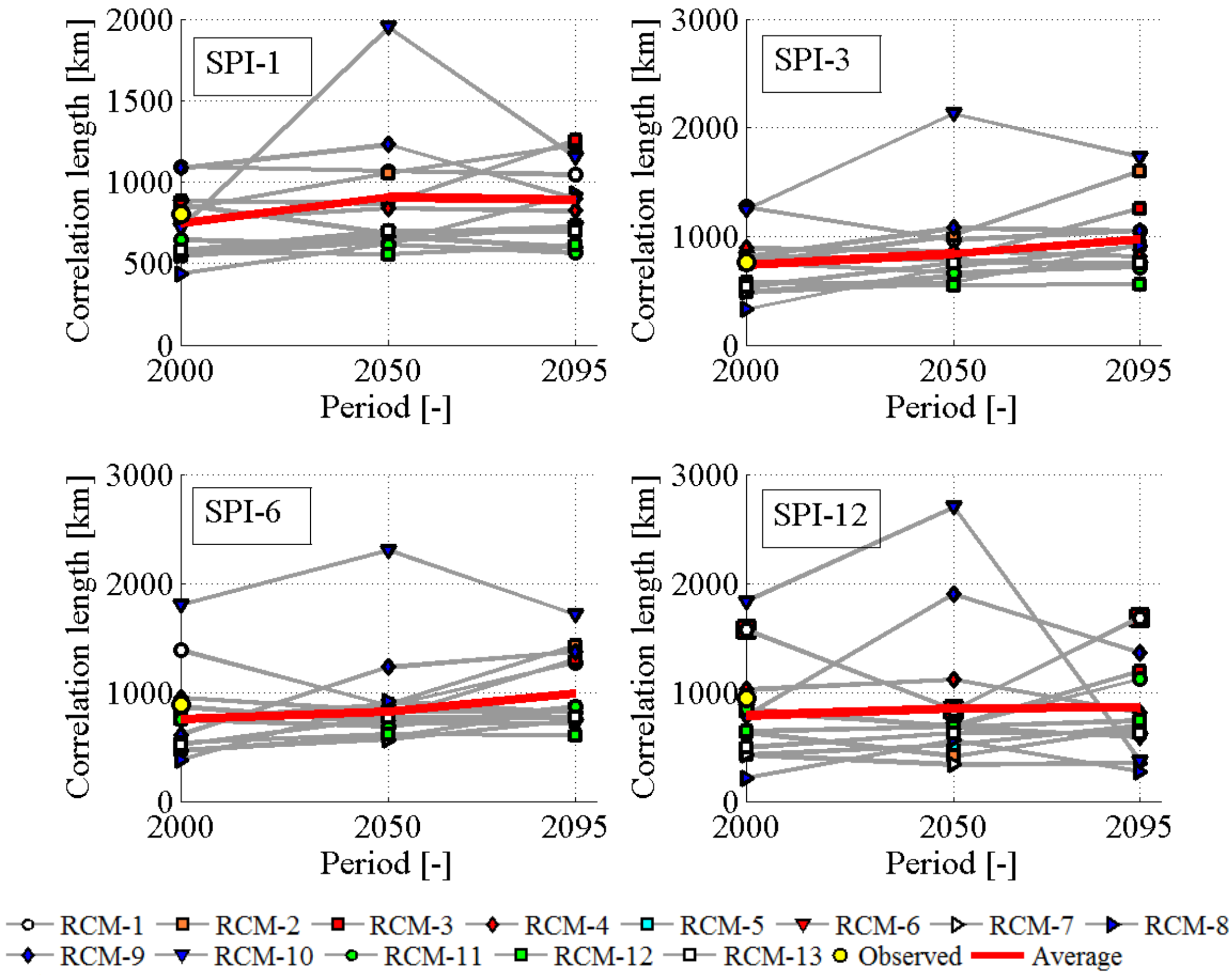

Figure 4-22 Spatial correlation, for 2000 (observed and simulated), 2050 (simulated) and 2095 (simulated) with weighted average of simulations.

4.3.8 Summary of results and discussion

Section 4.3 presents the results of the impact analysis. The results are interpreted for each time scale. Each time scale will relate to a different physical condition in the river basin as discussed in section 3.2.3. This will reveal a more practical application of the results. The statements are based on the average of the projections. The statements concerning the spatial structure are based on RCM-1.

There is no known study done for the Meuse basin concerning the correlation between different time scales and different physical conditions. However for a similar basin (Mosselle, a sub-basin of the Rhine River adjacent to the Meuse basin) the correlation between aggregated precipitation and low-flow has been studied (Demirel et al., 2013). There was some correlation (0.25) found between precipitation (aggregated to around 5 months) and the discharge in that basin. De Wit et al. (2007) found a high correlation between the variance in summer precipitation and the variance in average discharge in the summer for the Meuse basin. This suggests that even small time scales SPI-1 and SPI-3 for this basin are correlated with discharge.

Impact at different time scales

For SPI-1 there is a small increase (7%) in the number of drought events. These events have a higher average duration (11%), higher variation in duration (19%), higher average deficit (40%), higher variation in deficit (79%), higher average intensity (28%) and higher variation in intensity (75%). The basin will have 33% more droughts. The spatial structure of drought will largely remain the same. The spatial correlation length increases with 19%, indicating a significant increase in the area affected by droughts.

For SPI-3 there is a significant increase (29%) in the number of drought events. These events have a higher average duration (14%), higher variation in duration (13%), higher average deficit (50%), higher variation in deficit (56%), higher average intensity (40%) and higher variation in intensity (80%). The basin will have 35% more droughts. The spatial structure of drought will largely remain the same. The temporal correlation does not change largely (+2%). The spatial correlation length increases with 32%, indicating a significant increase in the area affected by droughts.

For SPI-6 there is a significant increase (44%) in the number of drought events. These events have no significant change (+3%) in average duration but a higher variation in duration (21%), higher average deficit (34%), higher variation in deficit (78%), higher average intensity (27%) and higher variation in intensity (68%). The basin will have 29% more droughts. The spatial structure of drought will largely remain the same. The temporal correlation decreases significantly (-20%). The spatial correlation length increases with 31%, indicating a significant increase in the area affected by droughts.

For SPI-12 there is a significant increase (10%) in the number of drought events. These events have a significant higher average duration (12%), higher variation in duration (54%), higher average deficit (40%), higher variation in deficit (123%), higher average intensity (22%) and higher variation in intensity (63%). The basin will have 23% more droughts. The spatial structure of drought will change largely. The temporal correlation decreases but not significantly (-6%). The spatial correlation length increases with 10%, indicating a significant increase in the area affected by droughts.

The main conclusion is that climate change, most likely, has an impact on drought in the Meuse basin. Overall this impact will result in more drought events for most SPIs. For all SPIs the events have on average a higher duration, deficit and intensity. Furthermore the variation in these three drought characteristics increases as well, indicating more extreme events. For most SPIs, except SPI-6, the temporal variability did not seem to change significantly. The temporal variability seems to significantly decrease for SPI-6. For the future periods there are significantly more events with overall more extreme characteristics. The logical explanation for this is the change in climate or more specific the temporal precipitation patterns. The spatial correlation of drought for all time scales increases which indicates that drought events will affect larger areas.

Influence of GCM and RCM on results

Another way of interpreting the results is based on the projections with the same driving GCM or same RCM. Each RCM run has at least one other RCM run with the same RCM or GCM (see table 4-15). Some combinations with similar or clear different results will be discussed.

RCM-7 and RCM-8 (both driven by GCM HadCM3Q0) show similar results regarding the number of drought events and the average duration; both show one of the largest increases in the number of event and an above estimate in average duration. However the similarity seems to stop here. For the other statistics there are no apparent similarities. However RCM-7 shows particular high projections for most SPIs in most drought characteristics statistics. Furthermore the variation in deficit for SPI-12 is particularly high projected by RCM-7 for the two future periods. The assessment of this RCM for this statistic (see section 4.2) shows it was the second worst simulation. This means that the values of this RCM have a weight of 2.9 % on the weighted average (see section 3.4.4). However the particular high value (+400%) for standard deviation in deficit of this RCM compared to the other projections means that it will influence the weighted average largely. However this is not a reason to neglect the results of this RCM. The main reason that this projection is less reliable than most other RCMs is its lack of ability to simulate the observed value for that statistic.

RCM-11 and RCM-12 (same RCM, different GCM) show for the drought frequency basin diverting results; RCM-11 shows for all SPIs one of the highest estimates, and RCM-12 shows for all SPIs one of the lowest. This can only be explained by the difference in driving GCM. This explanation seems logical and furthermore other projections confirm this. For example RCM-1 (same GCM, different RCM than RCM-11) shows also high results, while the RCMs driven by the same GCM as RCM-12 (ECHAM5-r3) shows below average estimates for the drought frequency in the basin. Furthermore this difference was also visible in the number of events and their characteristics; RCM-11 projected consistently more extreme droughts than RCM-12. Interestingly the temporal and spatial correlation was really similar. Based on these statistics it is therefore stated that GCM ECHAM5-r3 shows one of the least extreme climates of all GCMs (there are five RCM runs with this GCM which will be discussed later on) and that GCM ARPEGE shows one of the most extreme climates for the Meuse basin. Since the temporal and spatial correlation was similar it seems that the driving GCM has less influence on this statistic and that the RCM is the main contribution to this. This can be confirmed by focusing on the RCM runs with the same RCM but different driving GCMs. However, based on the RCMs runs with RCA (red marker) or the Hadley RCMs (blue marker) this could not be confirmed. This indicates that both the RCM and the GCM are not dominant when simulating the spatial correlation.

RCM-2, -3, -5, -12 and -13 are all driven by the ECHAM5-r3 (square) and all these projections showed a similar tendency to a less extreme climate change than the weighted average. Most projections showed a below average estimate of the number of drought events. Furthermore the drought characteristics for all these projections were below average. This obviously relates to a below average projection in drought frequency of the basin. Therefore it can be stated that ECHAM5-r3 projects a below average change for the Meuse basin, i.e. a wetter climate than average.

Uncertainty and range of projections

When discussing the results of the impact analysis the uncertainty in these results should be considered as well. The uncertainty of the RCM runs is assessed by calculating the difference between observed and simulated for each individual SPI and statistic. For most statistics the RCMs did not simulate the observed value well. The spread in simulated results and the difference between observed and simulated values indicate the quality of the RCMs. This is the main factor determining the certainty of the projections. Furthermore there was a tendency of higher uncertainty for future periods as well. Both factors give an indication of the uncertainty in the results. Since for each time scale and each statistic there is a different spread and difference, it would be too much to discuss this for each result. Since the weighted average of all these projections give a good estimate of the tendency of all projections and incorporates the uncertainty of these projections, only the average is discussed.

The weighted average is a useful way to analyze the impact of climate change on drought. However the range of the projection is neglected when only focusing on the weighted average. Looking at the RCMs that show the largest increase (more extreme drought) and the smallest increase (or largest decrease; less extreme drought) for each statistic the range in projections is assessed. However for almost each indicator and time scale the smallest change was a small decrease and the largest change was a larger increase. I.e. it is likely that an increase in drought and its characteristics will occur. This is supported by the fact that for most statistics the best performing RCM showed a similar trend as the weighted average. More importantly for most statistics only a few RCMs projected a decrease, i.e. for most statistics most RCMs projected an increase.

Chapter 5 Discussion

The discussion consists of a discussion of the results and the limitations of the applied methods. Furthermore the ability of the applied methods to be used for different cases is discussed.

Results

The results based on the observed dataset showed that different time scales had a clear different temporal variability. This resulted in a clear difference in drought characteristics; higher temporal variability relates with more drought events with less. Komuscu (1999) also found this relation between higher time scales and the number of drought events. The impact analysis showed the impact of climate change on drought and while the temporal variability reduces, the number of events can still increase and its characteristics can be more extreme.

The spatial correlation length was in the range of 1000 km, indicating the low spatial variability of SPI values. As was earlier noted this is a multitude of the river basin itself, i.e. there is a high correlation of the SPI values in the basin. To the authors knowledge this is the first study to show the correlation length of SPI values. Studies concerning spatial correlation or similar phenomena like monthly precipitation values are also not known to the author. The spatial structure based on the observed values showed for most SPIs a clear relation with the elevation in the basin. The spatial structure was not well simulated by most RCMs. This could be expected since some physical processes are active at smaller scales, than incorporated in the RCMs (van der Linden and Mitchell, 2009). The climate model will parameterize these processes using semi-empirical relationships.

Meteorological drought is not only caused by the lack in precipitation; it can also be affected by other factors. The main other factor is evapotranspiration which is largely determined by temperature (Thornthwaite, 1948). The expected result is, since there will be (very likely) an increase in temperature for the 21st century (IPCC, 2012), that the drought events will be even more extreme than projected in this research.

Taylor et al. (2012) showed the importance of using multiple emission scenarios, multiple GCMs and multiple RCMs. This is mainly due to the inherent uncertainty in them and the impact this has on the results. For this impact analysis only one emission scenario (A1B) is used. Therefore the uncertainty and spread in results due to different possible emission scenarios is not included. Thus it can be stated that the impact analysis shows a higher accuracy than there really is.

There was one RCM run (RCM-7 from ETHZ) that projected exceptional large changes in drought characteristics. This can only be explained by the used RCM: CLM. A study by Bachner et al. (2008) evaluates this RCM to simulate daily precipitation characteristics for different areas in Germany. It was found that generally the averages were acceptably simulated. However a significant dry bias was found throughout the summer season. This could partly explain the extreme results this RCM is showing for several drought statistics.

The impact analysis could identify for some RCM runs the significant influence of the driving GCM or the applied RCM on the drought statistics. Van der Linden and Mitchell (2009) already stated the possible influence the driving GCM or RCM has on the output of the RCM run. Van der Linden and Mitchell (2009) found that with a larger climate change, the GCM became more important than the RCM. Therefore the first future period (less climate change than the second future period) it can be expected that the RCM has a larger influence on the result than for the second future period where the GCM will be more important. However in this impact analysis this could not be confirmed.

The RCM assessment found that most ENSEMBLES RCMs tend to underestimate the temporal variability of the SPI in the basin. Nikulen et al. (2011) found that the GCMs in ENSEMBLE all show a complex spatial structure of precipitation for Europe in the historical period. It seems that for most GCMs the precipitation extremes are overestimated for mountains and underestimated over surrounding slopes. The Meuse basin is a relatively small basin with enough elevation to affect the precipitation pattern in the basin. It could be that the GCMs are the reason that precipitation in the historical period is not simulated well for the RCM runs. The focus on similar results based on the same GCM or same RCM suggest that the used GCM and RCM can have influence on the drought statistics. Interestingly for the historical period no strong patterns are found for the drought statistics for RCM runs (with same RCM or same GCM), while strong patterns are identified for the two future periods. For example the GCM ECHAM5-r3 seems to underestimate the extremeness of the impact of climate change (below average projections), but for the historical period this influence of the GCM is not apparent. This should be interpreted as an influence of the emissions in the atmosphere: the main difference between the historical period and the future ones. Apparently the GCMs (see section 4.3.8) react differently to this change in amount of emissions and this difference is reflected in the drought characteristics. This is in line of expectations since each climate model will have a different structure and way of modeling physical processes.

Methods

The relative temporal SPI was introduced by Dubrovsky et al. (2009) and is applied in the research. Based on the different drought statistics it seems that this is a great way to compare different periods of time. Significant changes in the number of drought events and significant changes in the drought characteristics could be quantified. Preliminary results showed that applying the SPI and the relative temporal SPI to the same future period will result in a higher increase in number of events and more extreme characteristics for the relative temporal SPI. The fact that the relative SPI shows a larger change is logical considering the presumed more extreme future climate. The historical variability and mean is used to calculate SPI values when the variability is probably higher and the mean different for the future climate. In other words the relative temporal SPI has a larger range in values than the SPI.

The relative spatial SPI is introduced in this study to make intra basin comparisons. The main question for this modification is what to use as reference point to make the SPI relative. In this research the area-weighted average of the cell parameters are used as a reference point. This was chosen to be more preferred than the parameters of SPI basin or the parameters of one cell. The SPI basin is at a larger spatial scale than a cell, it is therefore likely that there will be a different kind of variability at this scale than at cell level. Therefore the SPI basin parameters are not preferred because the relative spatial SPI is used at cell level. The parameters of one cell are less preferred since this will be less easy to interpret; the basin average will reveal which areas are above or below average for that basin. The main purpose of the relative spatial SPI is to make it possible to identify the spatial variations inside of the basin. The relative spatial SPI for the Meuse basin already showed that the drought frequency (based on the relative spatial SPI) were around the limits of drought frequency (one and zero). In other words it is a possibility that for a basin (with more variation in the basin) the drought frequency based upon relative spatial SPI will show values of one and zero. This would make this statistic less useful. There are other options for the same purpose. Vrochidou et al. (2012) introduced a modification of SPI: SN-SPI (spatially normalized SPI) to compare between areas. The normalization was based on the difference in annual precipitation. Bonaccorsi et al. (2003) utilized the principal component analysis (PCA) to determine the spatial variations in SPI values. The main advantage of the relative spatial SPI is that the spatial variation in drought frequency is determined. There is no normalization based on the annual precipitation needed. The PCA only identifies areas which are spatially related to each other, but it remains unclear how this should be interpreted for drought. However Santos et al. (2010) used the PCA for Portugal and found that the precipitation pattern was closely related with the temporal variability of SPI values over space. In other words it seems that the relative spatial SPI can be a complementary way of assessing the spatial structure of drought.

Spatially aggregating SPI can be different due to using observational stations or a grid based dataset and the option between aggregating precipitation values and aggregating SPI values. Zhai et al. (2010) aggregate monthly SPI series based on grid cells. Jung and Chang (2012) used area-averaged monthly precipitation values to calculate the basin SPI. Fischer et al. (2013) used total precipitation of each basin to calculate the SPI. Based on these studies it seems that there is no preferred way of spatial aggregation. In this research it is done by aggregating SPI series of the cells covering the basin.

In this study the common sample period of 30 years is chosen to analyze the (possible) different climates. However this has implications on the results, on fitting the probability density function to the aggregated data. The SPI values below -2 (and above 2) should be used with care since there is less accuracy for the extremes values (Guttman, 1998). This holds for the normal SPI. The temporal modification causes a shift in the range of SPI values. For the relative temporal SPI the minimum (and maximum) values are still less accurate than the values more close to the average. In case of a more extreme climate the range of SPI values will also increase, due to a larger variation in monthly precipitation values compared to the historical period. This will make the extreme SPI values probably even less accurate.

The drought events based upon cells are sometimes spatially related to each other. When at basin level a drought event is identified, there are probably 63 drought events based on cells. In this study this is not taken into account; the cell events are considered to be independent. This implies that the cell drought events are more related to each other than the results suggests. The drought events based on cells have another issue when describing the basin; there is a large difference in coverage of each cell. This can range from 600 km^2 to only 2 km^2. This difference in 'importance' is not taken into account for these drought events.

The error (and similarly the change) in the deficit-duration relation is analyzed in this study. The error (and change) value can be misleading due to two factors. Firstly for the extreme events (high duration and deficit) there is a high chance that no error is estimated. This will result in an estimate that is probably better than it should be. Secondly the cell based events are probably (spatially) related to each other influencing the error. I.e. multiple similar drought events are simulated, for what actually is one drought event. The weight for calculating the error (or change) will be higher than it should be. The change values have another limitation: an increase for short events can be offset by a decrease for longer event.

Generalization of method

Most drought statistics can be easily applied to different cases. However the possible limitation in applicability of the relative SPIs is already discussed. The number of drought events and their characteristics can be easily applied for different cases. The same holds for the correlation lengths. The main issue is the needed datasets.

For this study the used datasets were at the same spatial resolution (around 25 km) and for most cases (two exceptions) at the same grid (same geographical distribution of basin in cells). The impact analysis is easier to perform when all the datasets are on the same grid; however a simple transformation (as applied in this study) can be applied to overcome this problem. The most important criterion for the datasets is that the same or similar spatial scale is used. This is mainly because the representation of physical processes at different spatial scales is different. The results will be influenced in a way that is difficult to quantify and a transformation is needed. Another limitation is that it is not uncommon that the observed dataset is a point-based datasets with precipitation series of rainfall stations. It is suggested to spatially interpolate these series to the same grid the RCMs are projected for easy comparison.

Chapter 6 Conclusions and recommendations

6.1 Conclusions

The research objective is formulated as:

> *Develop and apply a method to assess the impacts of climate change on drought in the Meuse basin at different time scales*

Three research questions were formulated to reach this objective. A short answer for each research question is presented in this section.

How can drought be assessed in a suitable way for climate impact analysis?

The literature study showed the preference for using RCM projections run with different emission scenarios, GCMs and RCMs. Furthermore for each impact analysis there is the need to assess the quality of the RCM projections by comparing them with an observed dataset. The SPI method is a relatively easy index to identify drought events. One of the findings of this research is that to make the SPI useful for climate impact analysis, the SPI calculations for the future periods should be based on the historical calculations (apply historical probability density functions). In this way the possible difference in climate is taken into account. To assess basin-wide changes the SPI series are spatially aggregated to the basin level. To assess variation of drought in the basin the SPI is modified to a spatially relative SPI. The spatial structure can be investigated with this modified SPI. Temporal and spatial correlograms are made to assess the temporal and spatial correlation of SPI series. The SPI series can be used to identify the number of drought events and to calculate the average and standard deviation of the characteristics (duration, deficit and intensity) of these events. Deficit-duration relationships are investigated.

How well are the climate model simulations in simulating drought?

Multiple criteria were developed to assess how well the simulations simulate the observed drought. These criteria concern the number of drought events, the characteristics (duration, deficit and intensity) of these events, the deficit-duration relation, the temporal and spatial correlation and the spatial structure of drought in the river basin. Not one RCM performs well for all these criteria (and all time scales). Overall there was an underestimation of the temporal variability which relates to more events with less extreme characteristics (duration and deficit). The spatial structure was quite well to poor simulated by one RCM of the thirteen RCM projections. The other projections show a large error in simulating the spatial structure. Overall there was a poor estimation of the spatial correlation, but some RCM runs performed well.

What are the impacts of climate change on drought in the Meuse basin?

Based on the (weighted) average of thirteen RCM projections for two future periods it was shown that for most time scales there will be a significant increase (≥10%) in the number of drought events. For all time scales there was a significant increase in the drought characteristics (duration, deficit and intensity). Especially the variation in intensity increases dramatically for all time scales. Only for SPI-6 (probably related to stream flow) there was a significant change in temporal variability (an increase of 20 %). The spatial variability decreases for all time scales indicating drought events that affect a larger area. However there is inherently uncertainty in these projections and thus these statements. Probably the most important source of uncertainty lies in the lack of using multiple emission scenarios in the impact analysis. Furthermore for most statistics and most RCMs the projection shows a (large) error between the simulated value and the observed one. However this uncertainty could not be further quantified. The RCMs however simulated the average intensity and its standard variation extremely well. So it could be argued that for this statistic the projections have less uncertainty. The spread in projections for the future periods also show how much certainty there is in the average projection.

Objective

Based on the following paragraphs it can be concluded that a method has been developed and applied to assess the impact of climate change on drought in the Meuse basin. The method identifies the number of drought events, its characteristics, temporal variability, spatial variability and spatial distribution of drought in the basin on multiple time scales. Using multiple RCM runs with different GCMs and RCMs a range of possible impacts is provided. The (weighted) average proves to be a useful way to assess the general trend in these projections and to assess the impacts of climate change on drought.

6.2 Recommendations

Based on this study the following is recommended. The drought assessment could be made more comprehensive by applying a hydrological model to the RCM output. In this way the hydrological drought can be appropriately analyzed. Adding and applying possible socio-economical scenarios and using a different drought index, it could be possible to analyze the impact of climate change on socio-economical drought.

The different time scales relate to different physical conditions in this particular river basin. However for this river basin such study has not yet been applied. It would be interesting to establish these relationships (time scale with physical conditions) for this particular basin for a better interpretation of the results in this study. Furthermore the next step could be focusing on particular seasons of interest. For example the growing season in this basin is probably affected by the groundwater level in the basin. Some time scales will relate to this phenomenon and in this way the impact analysis can be more interesting for this particular area of interest. The meteorological drought is caused not only by the lack in precipitation; it can also be affected by other factors. The main other factor is evapotranspiration which is largely determined by temperature. However it is still under debate how to incorporate these factors in the analysis. The obvious and probably one of the easier ways is applying the SPEI method (Vicente-Serrano et al., 2010). In this way the change in temperature, which is a well-established fact, is taken into the impact analysis.

To assess the spatial structure in the basin multiple (complementary) options are found in this research. The relative spatial SPI could also be used to project the lowest relative spatial SPI values over the basin. This will probably reveal a similar pattern to the introduced drought frequencies plots. Another option is plotting the parameter of the used probability density function that describes the standard deviation of the function as a measure of variability in the basin. The temporal variability in the basin is in that way assessed. The application of the relative spatial SPI should be assessed by applying a similar study to a basin with larger spatial variability (for example a similar climate but a larger basin).

Further research and knowledge is needed to assess the spatial extent of each drought event. It remains unknown how the spatial extent could be measured by using the SPI values. For example when there is a drought event: will the neighboring cells with a value between minus one and zero be incorporated in the drought event? Technically these cells are not experiencing drought yet, however it could be well argued that these cells are strongly related to each other.

The relative temporal SPI could also lose its applicability for larger climate changes as discussed in the discussion section. Therefore it is suggested to conduct further research in the applicability of this SPI modification for a different river basin that is subject to larger climate changes.

References

- Agnew, C. T. (2000). *Using the SPI to identify drought.* Drought Network News, 12, 6 – 12
- Bachner, S., Kapala, A., & Simmer, C. (2008). *Evaluation of daily precipitation characteristics in the CLM and their sensitivity to parameterizations.* Meteorologische Zeitschrift, 17(4), 407-419.
- Blenkinsop, S., & Fowler, H. J. (2007). *Changes in European drought characteristics projected by the PRUDENCE regional climate models*. Int. J. Climatol., 27: 1595–1610. doi: 10.1002/joc.1538
- Bonaccorso, B., Bordi, I., Cancelliere, A., Rossi, G., & Sutera, A. (2003). *Spatial variability of drought: an analysis of the SPI in Sicily.* Water resources management, 17(4), 273-296.
- Bussay, A.M., Szinell, C., Hayes, M., Svoboda, M. (1998). *Monitoring drought in Hungary using the standardized precipitation index.* Annales Geophysicae, Supplement 11 to Vol 16, the Abstract Book of 23rd EGS General Assembly, C450. April 1998, Nice; France.
- Christensen, J. H., Carter, T. R., Rummukainen, M., & Amanatidis, G. (2007). *Evaluating the performance and utility of regional climate models: the PRUDENCE project.* Climatic Change, 81(1), 1-6.
- De Wit, M.J.M., van den Hurk, B., Warmerdam, P.M.M., Torfs, P.J.J.F., Roulin, E., & van Deursen, W.P.A. (2007). *Impact of climate change on low-flows in the river Meuse* Climatic Change 82(3-4) 351-372.
- Demirel, M. C., Booij, M. J. & Hoekstra, A. Y. (2013). *Identification of appropriate lags and temporal resolutions for low flow indicators in the River Rhine to forecast low flows with different lead times*. Hydrol. Process., 27: 2742–2758. doi: 10.1002/hyp.9402
- Dubrovsky, M., Svoboda, M.D., Trnka, M., Hayes, M.J., Wilhite, D.A., Zalud, Z., & Hlavinka, P. (2009). *Application of relative drought indices in assessing climate-change impacts on drought conditions in Czechia*. Theoretical and Applied Climatology 96: 155–171
- Edwards, D. C. (1997). *Characteristics of 20th Century drought in the United States at multiple time scales* (No. AFIT-97-051). AIR FORCE INST OF TECH WRIGHT-PATTERSON AFB OH.
- European Environment Agency (1999). *Sustainable water use in Europe* Environmental assessment report No 1 Part 1: Sectoral use of water
- European Environment Agency (2010). *Mapping the impacts of natural hazards and technological accidents in Europe: An overview of the last decade* doi:10.2800/62638
- Feser, F., Rockel, B., von Storch, H., Winterfeldt, J., & Zahn, M. (2011). *Regional climate models add value to global model data: a review and selected examples.* Bulletin of the American Meteorological Society, 92(9), 1181-1192.
- Fischer, T., Gemmer, M., Su, B., & Scholten, T. (2013). *Hydrological long-term dry and wet periods in the Xijiang River basin, South China.* Hydrology and Earth System Sciences, 17(1), 135-148.
- Guttman, N. B. (1998). *Comparing the Palmer Drought Index and the Standardized Precipitation Index.* Journal of the American Water Resources Association, 34, 113-121
- Guttman, N. B. (1999). *Accepting the Standardized Precipitation Index: A calculation algorithm.* J. Amer. Water Resour. Assoc., 35,311–322

- Haan, C., (2002). *Statistical Methods in Hydrology*, 2nd Edition. Blackwell, pp. 496
- Hayes, M. J., Svoboda, M. D., Wilhite, D. A., & Vanyarkho, O. V. (1999). *Monitoring the 1996 drought using the standardized precipitation index*. Bulletin of the American Meteorological Society, 80(3), 429-438.
- Hayes, M., Svoboda, M., Wall, N. and Widhalm, M. (2011). *The Lincoln Declaration on Drought Indices: Universal Meteorological Drought Index Recommended* Bulletin of the American Meteorological Society, 92(4), 485-488.
- Haylock, M. R., Hofstra, N., Klein Tank, A. M. G., Klok, E. J., Jones, P. D., & New, M. (2008). *A European daily high-resolution gridded data set of surface temperature and precipitation for 1950–2006*. Journal of Geophysical Research: Atmospheres (1984–2012), 113(D20).
- IPCC (2007). *Climate Change 2007: Impacts, Adaptation and Vulnerability. Contribution of Working Group II to the Fourth Assessment Report of the Intergovernmental Panel on Climate Change* [M.L. Parry, O.F. Canziani, J.P. Palutikof, P.J. van der Linden and C.E. Hanson (eds.)], Cambridge, United Kingdom and New York, NY, USA, Cambridge University Press.
- IPCC (2012). *Managing the Risks of Extreme Events and Disasters to Advance Climate Change Adaptation.* A Special Report of Working Groups I and II of the Intergovernmental Panel on Climate Change [Field, C.B., V. Barros, T.F. Stocker,D. Qin, D.J. Dokken, K.L. Ebi, M.D. Mastrandrea, K.J. Mach, G.-K. Plattner, S.K. Allen, M. Tignor, and P.M. Midgley (eds.)]. Cambridge University Press, Cambridge, UK, and New York, NY, USA
- Jung, I. W., & Chang, H. (2012). *Climate change impacts on spatial patterns in drought risk in the Willamette River Basin, Oregon, USA.* Theoretical and Applied Climatology, 108(3-4), 355-371.
- Kjellström, E., Nikulin, G., Hansson, U., Strandberg, G., & Ullerstig, A. (2011). *21st century changes in the European climate: uncertainties derived from an ensemble of regional climate model simulations.* Tellus A, 63(1), 24-40.
- Komuscu, A. U. (1999). *Using the SPI to analyze spatial and temporal patterns of drought in Turkey.* Drought Network News, 11(1), 7-13.
- Lee, J.H. and Kim, C.J. (2012). *A multimodel assessment of the climate change effect on the drought severity–duration–frequency relationship.* Hydrol. Process.. doi: 10.1002/hyp.9390
- Lenderink, G., Van Ulden, A., Van den Hurk, B., & Van Meijgaard, E. (2007). *Summertime inter-annual temperature variability in an ensemble of regional model simulations: analysis of the surface energy budget.* Climatic Change,81(1), 233-247.
- Liu, L., Hong, Y., Bednarczyk, C.N., Yong. B., Shafer, M.A.,Riley, R. and Hocker, J.E. (2012). *Hydro-Climatological Drought Analyses and Projections Using Meteorological and Hydrological Drought Indices: A Case Study in Blue River Basin, Oklahoma,* Springer Science+Business Media B.V. 2012
- Livada, I., & Assimakopoulos, V. D. (2007). *Spatial and temporal analysis of drought in Greece using the Standardized Precipitation Index (SPI).* Theoretical and applied climatology, 89(3-4), 143-153.
- Lloyd-Hughes, B. and Saunders, M.A. (2002). *A drought climatology for Europe* International journal of climatology Int. J. Climatol. 22: 1571 – 1592

- Maule, C. F., Thejll, P., Christensen, J. H., Svendsen, S. H., & Hannaford, J. (2013). *Improved confidence in regional climate model simulations of precipitation evaluated using drought statistics from the ENSEMBLES models.* Climate Dynamics, 40(1-2), 155-173.
- McKee, T. B., Doesken, N. J. and Kleist, J. (1993). *The relationship of drought frequency and duration to time scales.* Eighth Conference on Applied Climatology, 17-22 January 1993, Anaheim, California Department of Atmospheric Science, Colorado State University.
- Min, S. K., Kwon, W. T., Park, E., & Choi, Y. (2003). *Spatial and temporal comparisons of droughts over Korea with East Asia.* International Journal of Climatology, 23(2), 223-233.
- Myronidis, D., Stathis, D., Ioannou, K., & Fotakis, D. (2012). *An Integration of Statistics Temporal Methods to Track the Effect of Drought in a Shallow Mediterranean Lake*. Water Resources Management, 26(15), 4587-4605.
- Nikulin, G., Kjellström, E., Hansson, U. L. F., Strandberg, G., & Ullerstig, A. (2011). *Evaluation and future projections of temperature, precipitation and wind extremes over Europe in an ensemble of regional climate simulations.* Tellus A,63(1), 41-55.
- Palmer, W. C. (1965). *Meteorological drought* (p. 58). Washington, DC, USA: US Department of Commerce, Weather Bureau.
- Paulo, R. D., Rosa and L. S. Pereira (2012). *Climate trends and behaviour of drought indices based on precipitation and evapotranspiration in Portugal.* Published by Copernicus Publications on behalf of the European Geosciences Union
- Pfister, L., Kwadijk, J., Musy, A., Bronstert, A., & Hoffmann, L. (2004). *Climate change, land use change and runoff prediction in the Rhine–Meuse basins.* River Research and Applications, 20(3), 229-241.
- Santos, J. F., Pulido-Calvo, I., & Portela, M. M. (2010). *Spatial and temporal variability of droughts in Portugal. Water Resources Research, 46(3), W03503.*
- Schär, C., Vidale, P.L., Lüthi, D., Frei, C., Häberli, C., Liniger, M.A. and Appenzeller, C. (2004). *The role of increasing temperature variability for European summer heat waves.* Nature, 427, 332-336; doi:10.1038/nature02300 (also published on January 11, 2004, as Advance Online Publication)
- Sheffield, J., Andreadis, K. M., Wood, E. F., & Lettenmaier, D. P. (2009). *Global and continental drought in the second half of the twentieth century: Severity-area-duration analysis and temporal variability of large-scale events.* Journal of Climate, 22(8), 1962-1981.
- Sienz, F., Bothe, O., and Fraedrich, K. (2012). *Monitoring and quantifying future climate projections of dryness and wetness extremes: SPI bias,* Hydrol. Earth Syst. Sci. Discuss., 8, 10635–10677, doi:10.5194/hessd-8-10635-2011
- Szalai S and Szinell C. (2000). *Comparison of two drought indices for drought monitoring in Hungary — a case study.* In Drought and Drought Mitigation in Europe, Vogt JV, Somma F (eds). Kluwer: Dordrecht; 161–166
- Taylor, I.H., Burke, E., McColl, L., Falloon, P., Harris, G.R. and McNeall, D. (2012). *Contributions to uncertainty in projections of future drought under climate change scenarios* doi:10.5194/hessd-9-12613-2012

- Thom, H. C. S. (1966). *Some methods of climatological analysis*. Secretariat of the World Meteorological Organization.
- Thornthwaite, C. W., (1948). *An Approach toward a Rational Classification of Climate Geographical Review*, Vol. 38, No. 1. (Jan., 1948), pp. 55-94
- Trenberth, K. E., Dai, A., Rasmussen, R. M. & Parsons, D. (2003). *The Changing Character of Precipitation*. Bulletin of the American Meteorological Society, 84, 1205-1217.
- Van Der Linden P., and J.F.B. Mitchell (eds.) (2009). *ENSEMBLES: Climate Change and its Impacts: Summary of research and results from the ENSEMBLES project.* Met Office Hadley Centre, FitzRoy Road, Exeter EX1 3PB, UK. 160pp.
- Vicente-Serrano S.M., Beguería S. and López-Moreno J.I. (2010). *A Multi-scalar drought index sensitive to global warming: The Standardized Precipitation Evapotranspiration Index – SPEI.* Journal of Climate 23(7), 1696-1718, DOI: 10.1175/2009JCLI2909.1
- Vrochidou, A. E., Tsanis, I. K., Grillakis, M. G., & Koutroulis, A. G. (2012). *The impact of climate change on hydrometeorological droughts at a basin scale.* Journal of Hydrology.
- Wang, D., Hejazi, M., Cai, X. and Valocchi, A. (2011). *Climate change impact on meteorological, agricultural, and hydrological drought in central Illinois* WATER RESOURCES RESEARCH, VOL. 47, W09527,doi :10.1029/2010WR009845
- Wilhite, D. A. (2011). *National Drought Policies: Addressing Impacts and Societal Vulnerability.* In TOWARDS A COMPENDIUM ON NATIONAL DROUGHT POLICY PROCEEDINGS OF AN EXPERT MEETING (p. 13).
- World Meteorological Organization (2012). *Standardized Precipitation Index User Guide* (M. Svoboda, M. Hayes and D. Wood). (WMO-No. 1090), Geneva
- Wu, H., Hayes, M.J., Wilhite, D.A., & Svoboda, M.D. (2005). *The effect of the length of record on the standardized precipitation index calculation*. International Journal of Climatology 25: 505–520.
- Zhai, J. Q., Liu, B., Hartmann, H., Da Su, B., Jiang, T., & Fraedrich, K. (2010*). Dryness/wetness variations in ten large river basins of China during the first 50 years of the 21st century.* Quaternary International, 226(1), 101-111.

Appendices

A. SPI calculation

The full computational procedure as presented by Edwards (1997) is described below. The gamma distribution is defined by its probability density function:

$$g(x) = \frac{1}{\beta^{\alpha}\Gamma(\alpha)} x^{\alpha-1} e^{-x/\beta} \; for \; x > 0 \qquad \text{Eq. (A.1)}$$

$$\begin{array}{ll} \alpha > 0 & \alpha : shape\ parameter \\ \beta > 0 & \beta : scale\ parameter \\ x > 0 & x : precipitation\ amount \end{array}$$

$$\Gamma(\alpha) = \int_0^{\infty} y^{\alpha-1} e^{-y} dy \quad \Gamma(\alpha) : gamma\ function \qquad \text{Eq. (A.2)}$$

Where y is the real value representing the aggregated precipitation values. This probability density function will be fitted to a frequency distribution of precipitation totals. Thom (1966) provides the maximum likelihood solution to estimate $\hat{\alpha}$ and$\hat{\beta}$:

$$\hat{\alpha} = \frac{1}{4A}\left[1 + \sqrt{1 + \frac{4A}{3}}\right] \qquad \text{Eq. (A.3)}$$

$$\hat{\beta} = \frac{\bar{x}}{\hat{\alpha}} \qquad \text{Eq. (A.4)}$$

Where

$$A = \ln(\bar{x}) - \frac{\sum \ln(x)}{n} \qquad \text{Eq. (A.5)}$$

$$\bar{x} = mean\ precipitation\ amount$$

$$x = precipitation\ amount$$

$$n = number\ of\ precipitation\ observations$$

The SPI values in this research are calculated with the software package Matlab (2012a) where the best estimates are calculated by the so-called *gamfit* function. This function provides the parameters with the most likely estimate. The parameters ($\hat{\alpha}\ and\ \hat{\beta}$) are used to find the cumulative probability of monthly precipitation. The cumulative probability is given by:

$$G(x) = \int_0^{x} g(x)dx = \frac{1}{\hat{\beta}^{\hat{\alpha}}\Gamma(\hat{\alpha})}\int_0^{x} x^{\hat{\alpha}-1}\ e^{-x/\hat{\beta}} dx \qquad \text{Eq. (A.6)}$$

Letting $t = x/\hat{\beta}$ the equation above becomes the incomplete gamma function:

$$G(x) = \frac{1}{\Gamma(\hat{\alpha})} \int_0^x t^{\hat{\alpha}-1} \;\; e^{-t} dt$$ Eq. (A.7)

The gamma function in Matlab (2012a) is described by the function *gamcdf* which uses the same formulas as described. The gamma function is undefined for x = 0, therefore the cumulative probability becomes:

$$H(x) = q + (1 - q)G(x)$$ Eq. (A.8)

where q is the probability of a zero. Thom (1966) stated that q can be estimated by dividing the number of zeros in the precipitation series by the number of precipitation values. This estimate is used in this research. The cumulative probability ($H(x)$) is transformed to the standard normal random variable Z with mean zero and a variance of one.

B. R-squared and F values

For the temporal and spatial fits the goodness-of-fit is assessed by the r^2value and the significance of the fit is based on the F-value.

Temporal correlation

Historical period

r^2	SPI-3	SPI-6	SPI-12
EOBS	0.95	0.87	0.93
RCM1	0.90	0.88	**0.70**
RCM2	0.95	**0.69**	0.81
RCM3	0.94	0.89	0.84
RCM4	0.94	0.80	**0.76**
RCM5	0.97	0.91	0.87
RCM6	0.95	0.86	0.80
RCM7	0.97	0.90	0.82
RCM8	0.96	0.86	**0.79**
RCM9	**0.79**	0.81	0.82
RCM10	0.83	**0.74**	**0.64**
RCM11	0.86	0.82	0.80
RCM12	0.91	0.85	0.84
RCM13	0.96	0.87	0.84

Table B-1 The r^2 values, bold values are below 0.8. Temporal correlation (2000)

F	SPI-3	SPI-6	SPI-12
EOBS	89.02	104.72	195.78
RCM1	60.85	38.46	10.49
RCM2	14.16	**4.42**	18.36
RCM3	10.50	20.82	27.99
RCM4	12.47	**8.70**	16.10
RCM5	23.26	25.80	188.67
RCM6	14.21	11.54	20.30
RCM7	22.65	23.09	147.63
RCM8	21.07	**7.23**	**8.92**
RCM9	**2.19**	**6.96**	15.03
RCM10	**5.62**	**4.04**	**5.42**
RCM11	11.38	18.91	19.52
RCM12	**7.11**	13.07	33.02
RCM13	17.10	17.03	28.53

Table B-2 The F values, bold values are below 9.5. Temporal correlation (2000)

Future period 2050

r^2	SPI-3	SPI-6	SPI-12
RCM1	0.95	0.81	0.81
RCM2	0.92	0.84	0.96
RCM3	0.98	0.93	0.82
RCM4	0.95	0.88	0.81
RCM5	0.97	**0.72**	0.84
RCM6	0.88	0.94	**0.71**
RCM7	0.94	0.86	0.84
RCM8	**0.79**	0.90	**0.71**
RCM9	0.93	**0.68**	0.90
RCM10	0.94	0.86	**0.73**
RCM11	**0.75**	0.89	0.82
RCM12	0.97	0.83	0.85
RCM13	0.95	0.82	**0.74**

Table B-3 The r^2 values, bold values are below 0.8. Temporal correlation (2050)

F	SPI-3	SPI-6	SPI-12
RCM1	15.66	9.59	22.38
RCM2	**8.05**	**5.91**	159.84
RCM3	36.16	29.15	21.45
RCM4	13.59	18.34	20.09
RCM5	22.84	**5.39**	27.03
RCM6	**4.73**	34.08	15.34
RCM7	11.65	**7.69**	30.02
RCM8	**4.16**	12.45	**5.80**
RCM9	**9.46**	**3.12**	66.78
RCM10	12.33	**7.30**	11.10
RCM11	**3.25**	20.41	20.67
RCM12	26.16	11.03	21.88
RCM13	14.32	**7.70**	13.10

Table B-4 The F values, bold values are below 9.5. Temporal correlation (2050)

Future period 2095

r^2	SPI-3	SPI-6	SPI-12
RCM1	0.80	0.85	**0.61**
RCM2	0.89	0.81	**0.75**
RCM3	0.93	**0.58**	0.80
RCM4	0.93	**0.67**	0.95
RCM5	0.91	0.81	**0.80**
RCM6	0.92	0.84	0.84
RCM7	0.94	**0.80**	0.97
RCM8	0.88	**0.80**	0.91
RCM9	0.80	**0.65**	0.84
RCM10	0.92	**0.55**	**0.47**
RCM11	0.95	0.91	0.85
RCM12	0.98	0.91	**0.73**
RCM13	0.95	0.82	0.85

Table B-5 The r^2 values, bold values are below 0.8. Temporal correlation (2095)

F	SPI-3	SPI-6	SPI-12
RCM1	**4.58**	13.31	53.67
RCM2	**5.56**	**4.74**	17.00
RCM3	9.54	**1.96**	22.21
RCM4	9.68	**2.96**	468.47
RCM5	**7.40**	**6.87**	91.68
RCM6	**8.68**	**9.18**	21.57
RCM7	11.42	**4.28**	293.26
RCM8	**4.81**	**4.37**	51.05
RCM9	**4.42**	**2.59**	20.02
RCM10	**7.94**	**1.15**	32.06
RCM11	16.36	24.95	30.10
RCM12	48.47	25.19	12.73
RCM13	14.32	**7.68**	27.18

Table B-6 The F values, bold values are below 9.5. Temporal correlation (2095)

	SPI-3	SPI-6	SPI-12
n_0	358	355	349
p	2	2	2
$F_{1-\alpha,p-1,n_0-p}$ sig. level of 0.90	9.50	9.50	9.50
$F_{1-\alpha,p-1,n_0-p}$ sig. level of 0.96	24.5	24.5	24.5
$F_{1-\alpha,p-1,n_0-p}$ sig. level of 0.99	99.5	99.5	99.5

Table B-7 F threshold values. Based on n_0= 120 since Haan (2002) has no higher value: F threshold values could be expected to be a bit higher for a higher n_0

Spatial correlation

Historical period

r^2	SPI-1	SPI-3	SPI-6	SPI-12
EOBS	0.90	0.83	**0.66**	**0.60**
RCM1	0.84	**0.79**	**0.70**	**0.71**
RCM2	0.95	0.93	0.88	0.86
RCM3	0.95	0.91	0.89	0.89
RCM4	0.94	0.92	0.90	0.82
RCM5	0.83	**0.74**	**0.74**	**0.70**
RCM6	0.91	0.89	0.89	0.81
RCM7	0.83	**0.73**	**0.73**	**0.69**
RCM8	**0.65**	**0.60**	**0.69**	**0.50**
RCM9	0.84	0.80	0.85	**0.60**
RCM10	**0.79**	**0.59**	**0.46**	**0.28**
RCM11	0.91	0.86	0.81	**0.71**
RCM12	0.83	0.80	0.80	**0.77**
RCM13	0.81	0.83	**0.77**	**0.73**

Table B-8 The r^2 values, bold values are below 0.8. Spatial correlation (2000)

F	SPI-1	SPI-3	SPI-6	SPI-12
EOBS	16635	9519	5048	3906
RCM1	8976	6594	4257	4127
RCM2	29841	20523	9888	7532
RCM3	28711	15327	11134	11978
RCM4	23898	16629	14850	6718
RCM5	12963	7895	6433	4826
RCM6	16645	12078	13351	8232
RCM7	12989	7815	6260	4687
RCM8	2266	1677	2405	761
RCM9	9529	7028	8625	2250
RCM10	5597	2610	1793	1125
RCM11	18302	12834	8135	4800
RCM12	8835	8471	7534	5852
RCM13	10336	9510	5549	4272

Table B-9 The F values, spatial correlation (2000)

Future period 2050

r^2	SPI-1	SPI-3	SPI-6	SPI-12
RCM1	0.90	0.88	0.86	0.81
RCM2	0.89	0.82	**0.79**	**0.69**
RCM3	0.93	0.92	0.91	0.90
RCM4	0.93	0.91	0.88	0.85
RCM5	0.86	**0.78**	**0.67**	**0.58**
RCM6	0.89	0.90	0.89	0.81
RCM7	**0.79**	**0.69**	**0.69**	**0.55**
RCM8	0.85	0.84	0.85	**0.64**
RCM9	0.88	0.85	**0.72**	**0.62**
RCM10	**0.79**	**0.68**	**0.42**	**0.40**
RCM11	0.90	0.82	**0.74**	**0.71**
RCM12	0.87	0.84	**0.80**	**0.68**
RCM13	**0.72**	**0.69**	**0.76**	0.81

Table B-10 The r^2 values, bold values are below 0.8. Spatial correlation (2050)

F	SPI-1	SPI-3	SPI-6	SPI-12
RCM1	14278	11282	9266	6011
RCM2	14800	7753	6156	3426
RCM3	21207	17678	14855	11766
RCM4	19074	15724	11201	9629
RCM5	15012	9794	6516	4316
RCM6	11338	15981	13508	7187
RCM7	9628	5807	5148	3238
RCM8	7252	6794	7632	2066
RCM9	13520	8559	4099	2604
RCM10	7044	3827	1644	1926
RCM11	19026	9819	5985	4839
RCM12	11050	8169	6495	4160
RCM13	6996	6476	7445	7936

Table B-11 The F values, spatial correlation (2050)

Future period 2095

r^2	SPI-1	SPI-3	SPI-6	SPI-12
RCM1	0.90	0.89	0.87	**0.74**
RCM2	0.86	0.90	0.84	0.80
RCM3	0.84	**0.56**	**0.49**	**0.79**
RCM4	0.93	0.88	0.88	0.85
RCM5	0.90	0.85	0.85	0.81
RCM6	0.89	0.86	0.87	0.86
RCM7	0.89	**0.78**	**0.62**	**0.41**
RCM8	0.86	0.89	0.85	**0.61**
RCM9	**0.78**	**0.77**	**0.67**	**0.57**
RCM10	0.81	**0.77**	**0.72**	**0.52**
RCM11	0.82	0.88	0.81	**0.74**
RCM12	0.87	0.84	**0.79**	**0.73**
RCM13	**0.71**	**0.69**	**0.76**	0.81

Table B-12 The r^2 values, bold values are below 0.8. Spatial correlation (2095)

F	SPI-1	SPI-3	SPI-6	SPI-12
RCM1	13208	10991	9441	5944
RCM2	9481	12742	6657	4541
RCM3	11386	3862	2764	6658
RCM4	21944	11395	10159	8028
RCM5	21663	14596	11981	6382
RCM6	12104	8868	9513	7914
RCM7	14480	9154	5636	2930
RCM8	8338	9774	6249	1071
RCM9	6466	5073	3262	2247
RCM10	4831	4153	3127	774
RCM11	11886	15368	9809	7206
RCM12	11836	9571	7839	5454
RCM13	6988	6466	7443	7928

Table B-13 The F values, spatial correlation (2095)

	All SPIs
n_0	1953
p	2
$F_{1-\alpha,p-1,n_0-p}$ sig. level of 0.90	9.50
$F_{1-\alpha,p-1,n_0-p}$ sig. level of 0.96	24.5
$F_{1-\alpha,p-1,n_0-p}$ sig. level of 0.99	99.5

Table B-14 F threshold values. Based on n_0= 120 since Haan (2002) presents no higher value.F threshold values could be expected to be a bit higher for a higher n_0

C. All temporal and spatial correlograms

This appendix presents the correlograms (temporal and spatial) of all RCMs and the SPIs with its exponential fit. The choice of no temporal correlogram and fit for SPI-1 is presented and discussed.

No temporal length for SPI-1

The SPI-1 is not selected to be fitted with an exponential fit. This is based on the observed SPI-1 dataset. The correlation value of SPI-1 on lag 1 is near zero and negative, which indicates that there is no correlation on this lag. From a physical point of view it seems not logical that a significant correlation value will occur; if on lag 1 there is no correlation the other lags are just derivatives of this lack in correlation. Figure C-1 shows how SPI-1 is correlated on larger lags. It seems like a correlogram of a random dataset. Furthermore the fit is based on negative values and this seems not logical since the positive correlation length is an indication of how the positive temporal correlation is. This last point of discussion is the main reason and a solid one to reject the SPI-1 for calculation of a temporal correlation length.

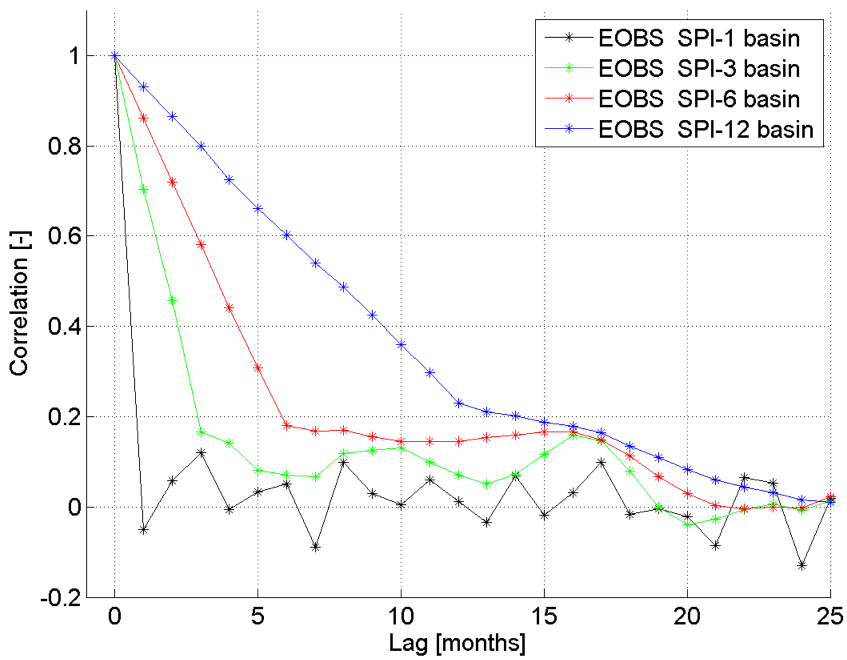

Figure C-1 All the correlation values up to lag 25 for the observed dataset

Temporal correlograms

Historical period

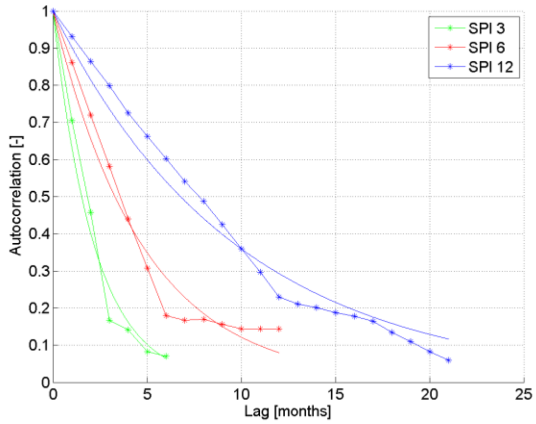

EOBS

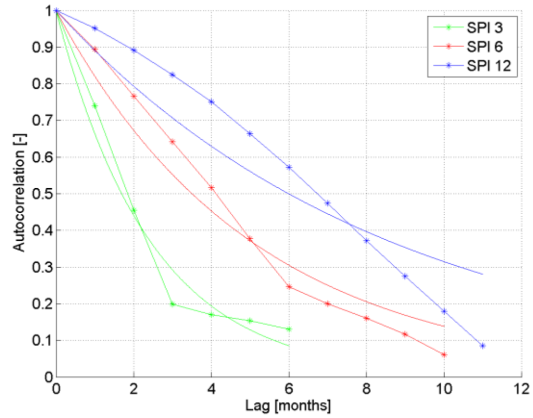

RCM1

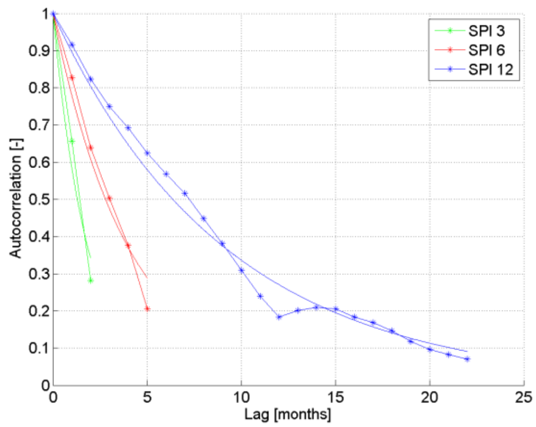

RCM2

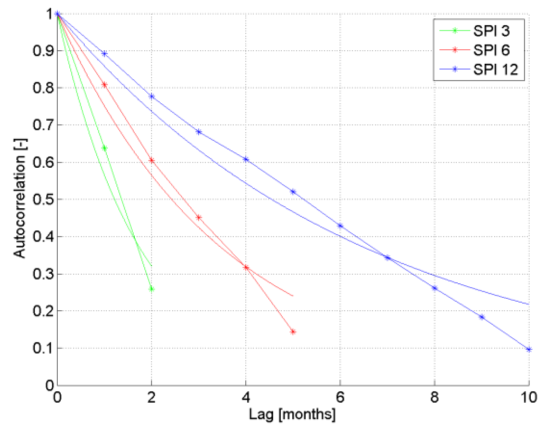

RCM3

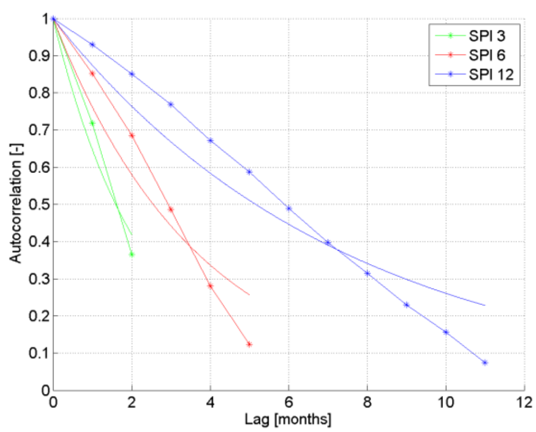

RCM4

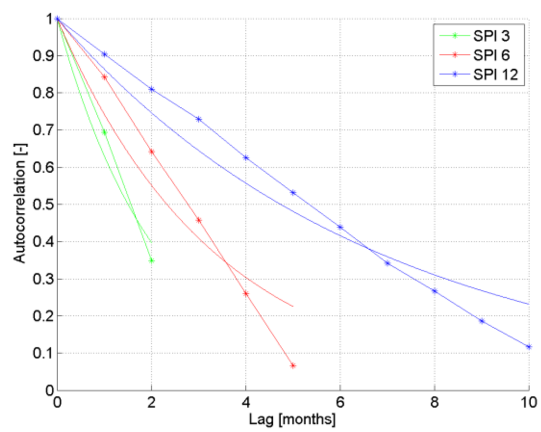

RCM5

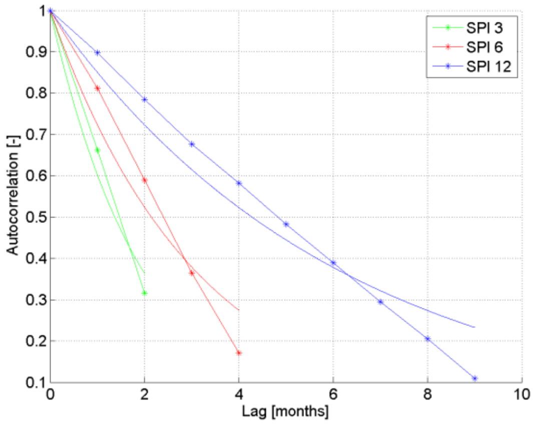

RCM6

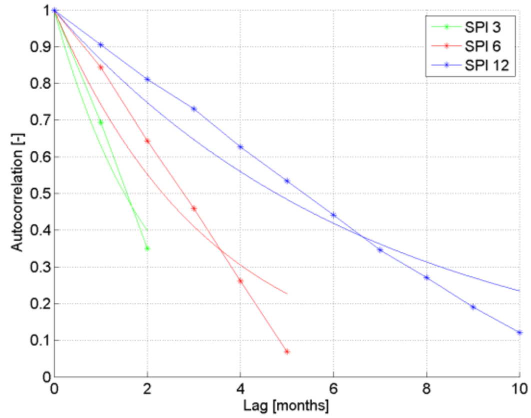

RCM7

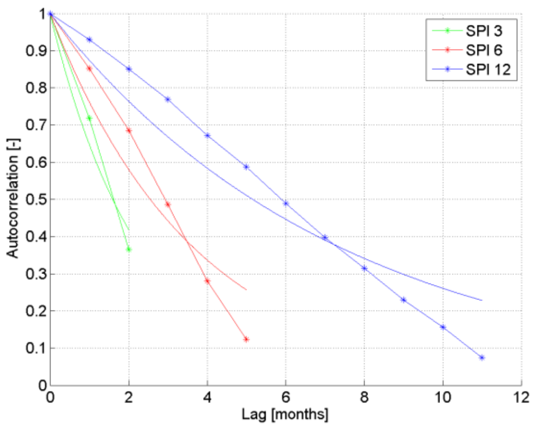

RCM8

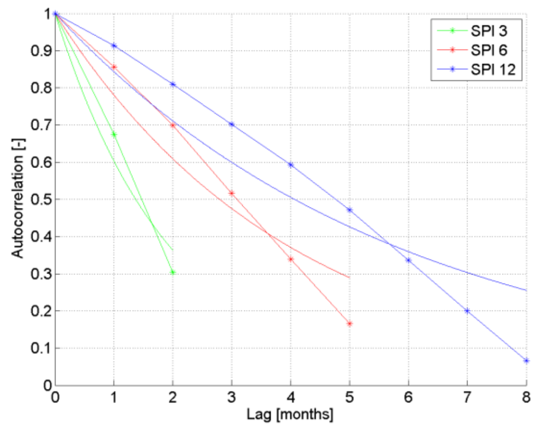

RCM9

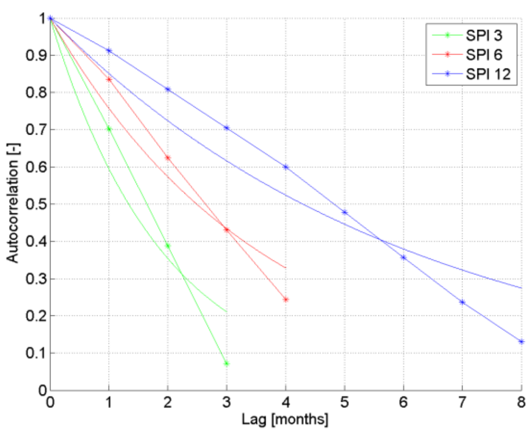

RCM10

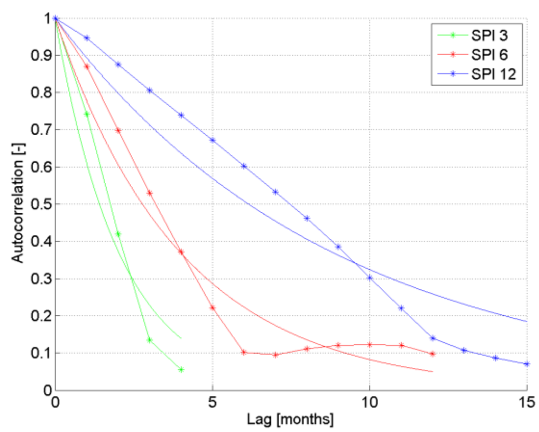

RCM11

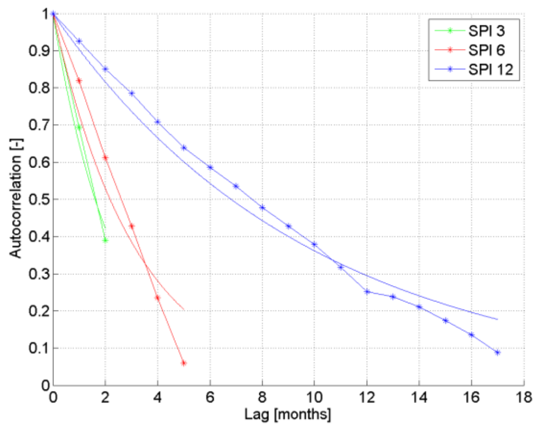

RCM12

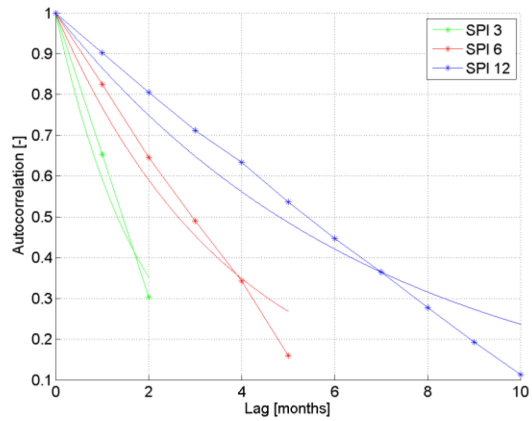

RCM13

Figure C-2 All temporal fits and the data points the fits are based on. (2000)

Future period 2050

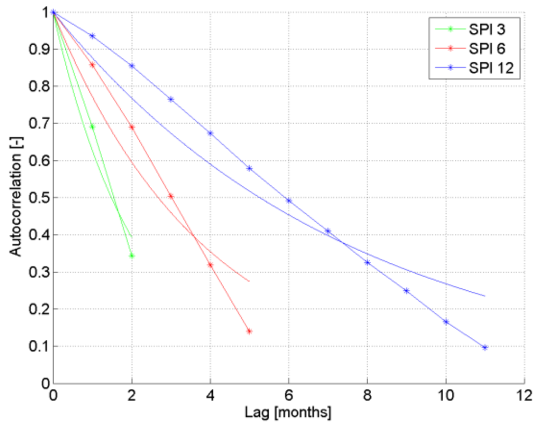

RCM1

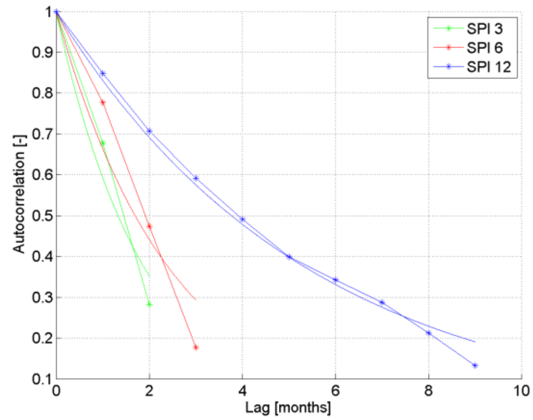

RCM2

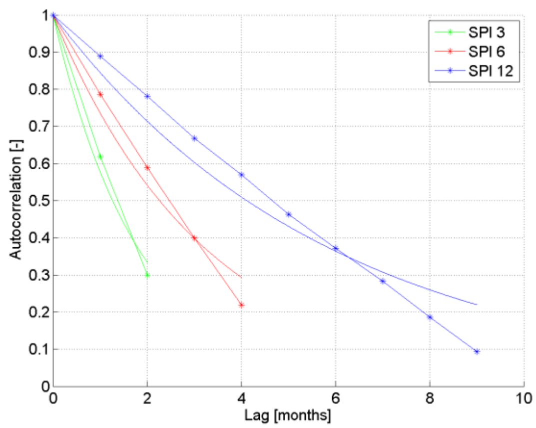

RCM3

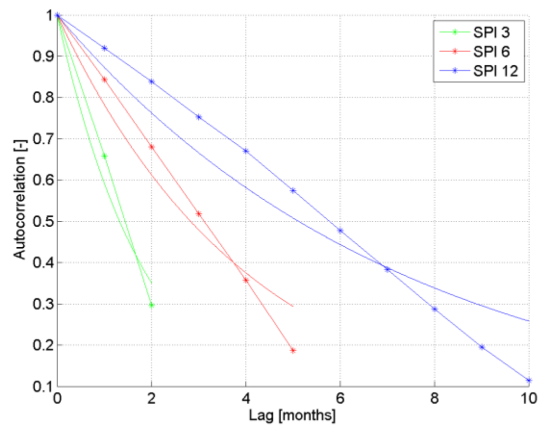

RCM4

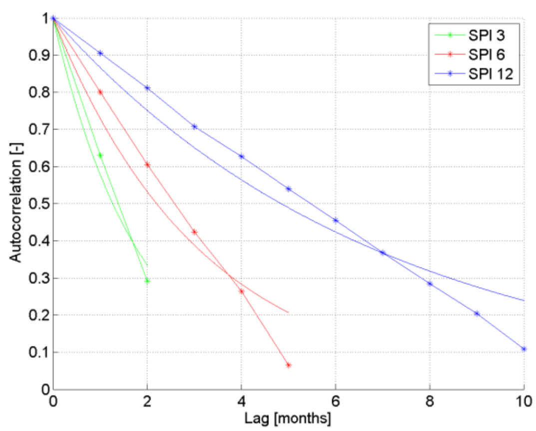

RCM5

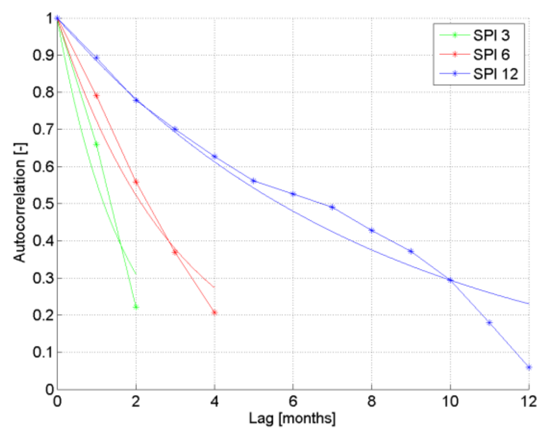

RCM6

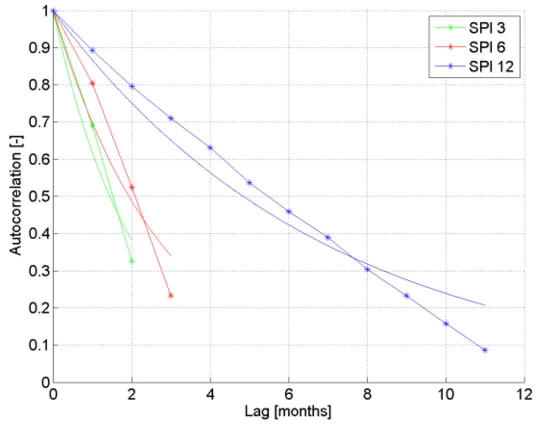

RCM7

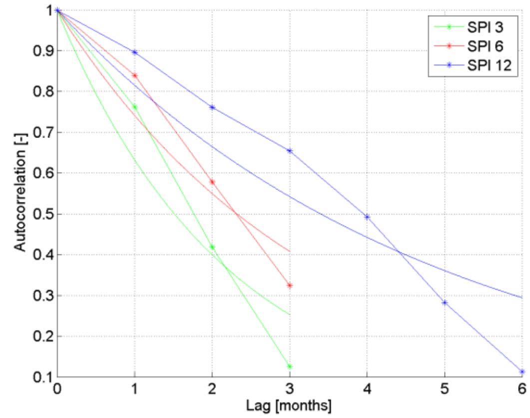

RCM8

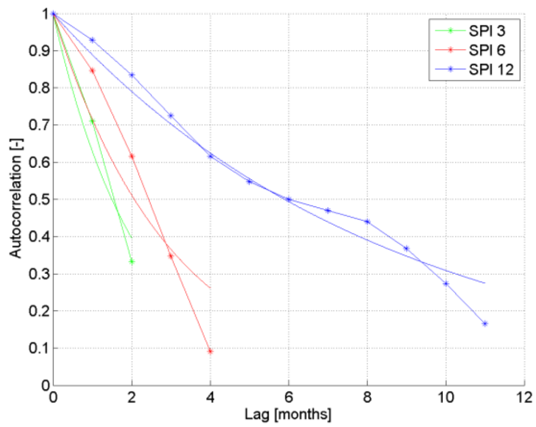

RCM9

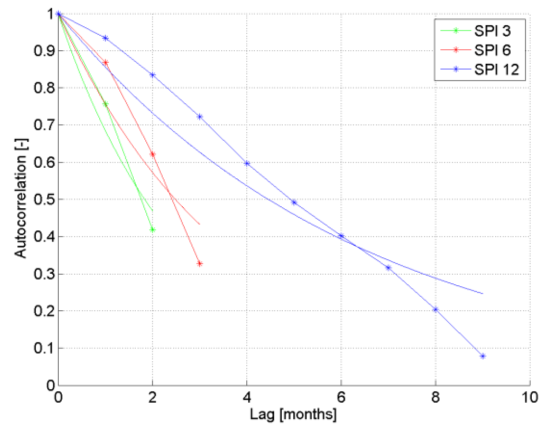

RCM10

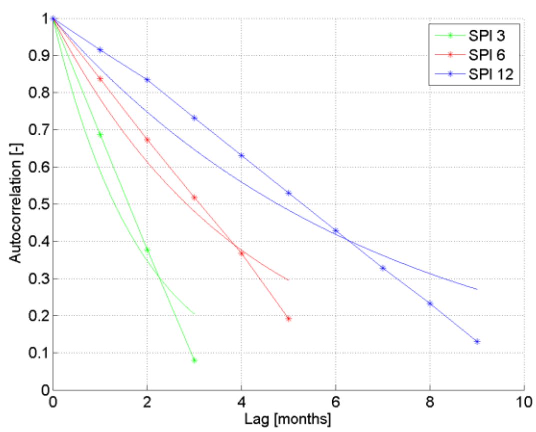

RCM11

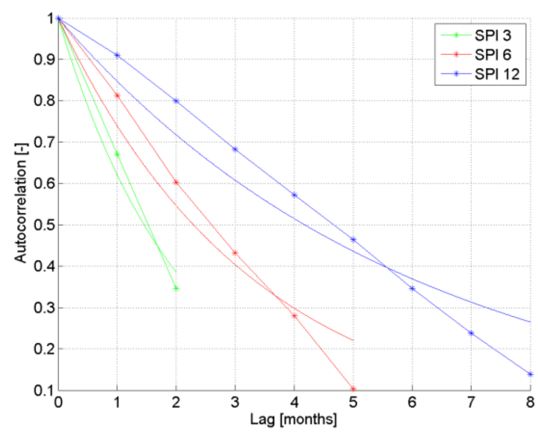

RCM12

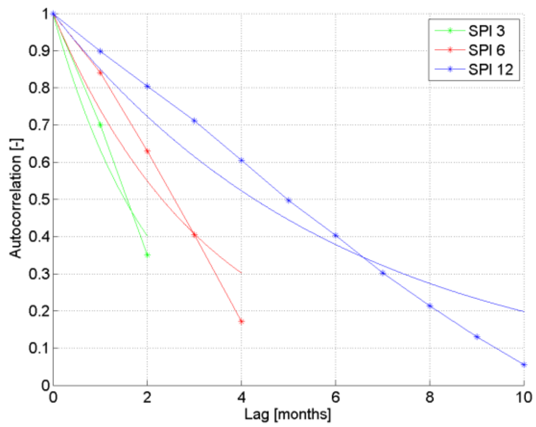

RCM13

Figure C-3 All temporal fits and the data points the fits are based on. (2050)

Future period 2095

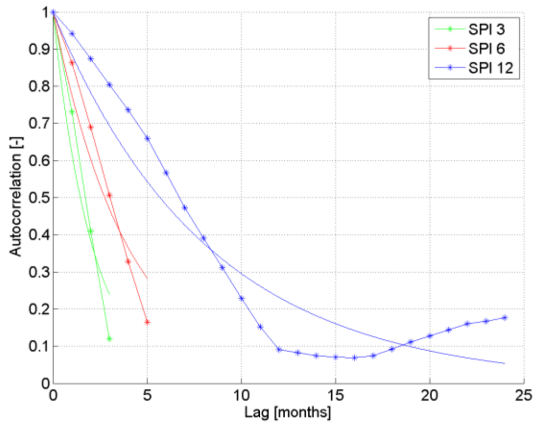

RCM1

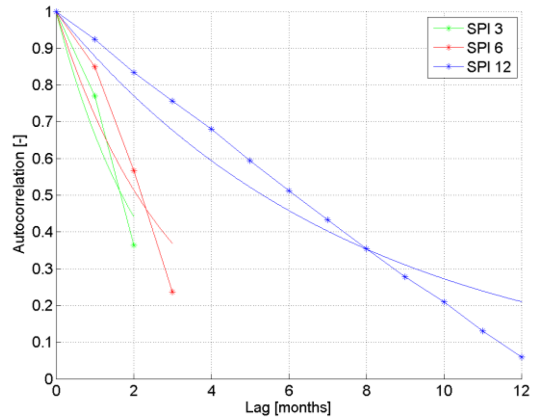

RCM2

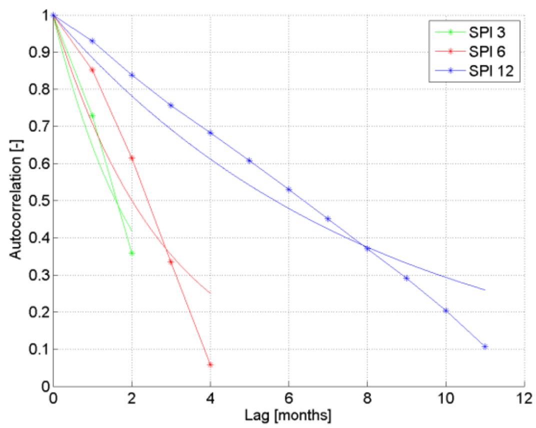

RCM3

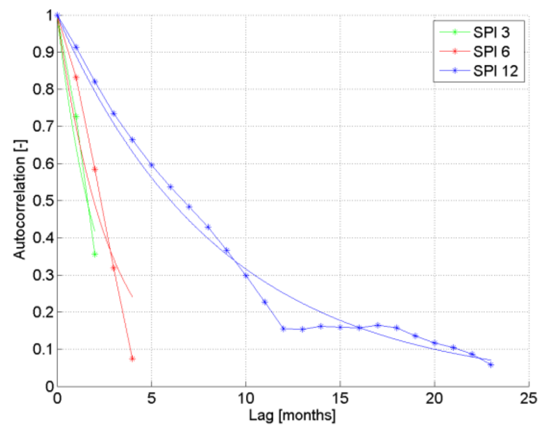

RCM4

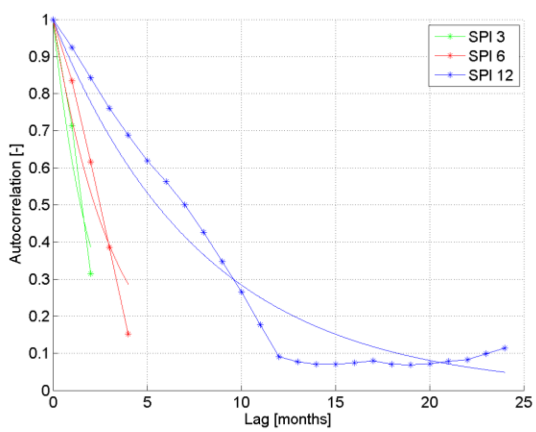

RCM5

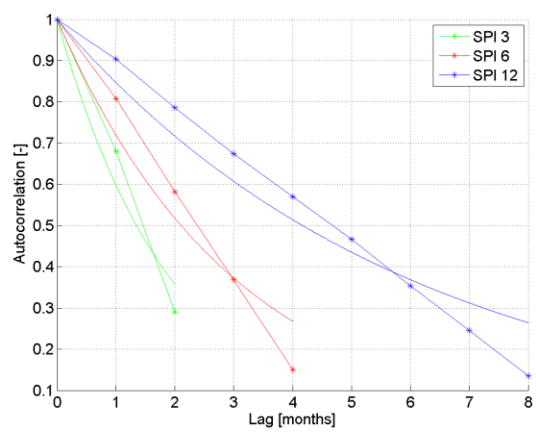

RCM6

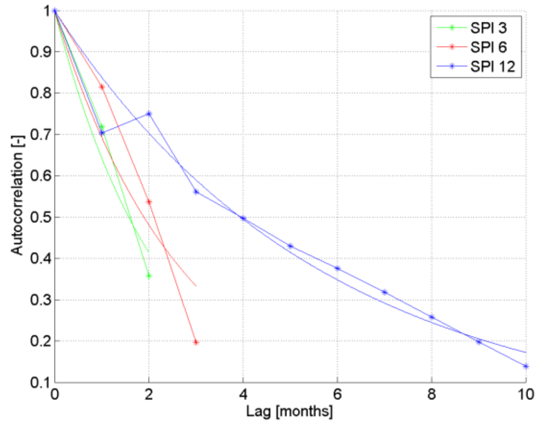

RCM7

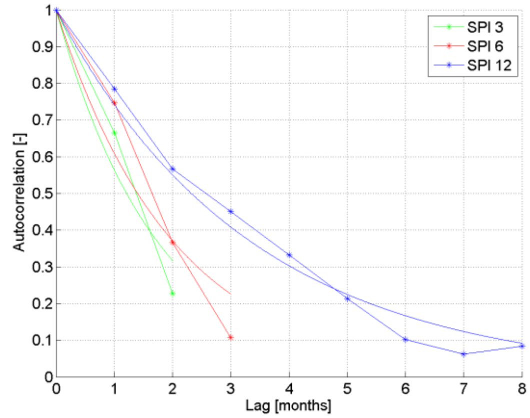

RCM8

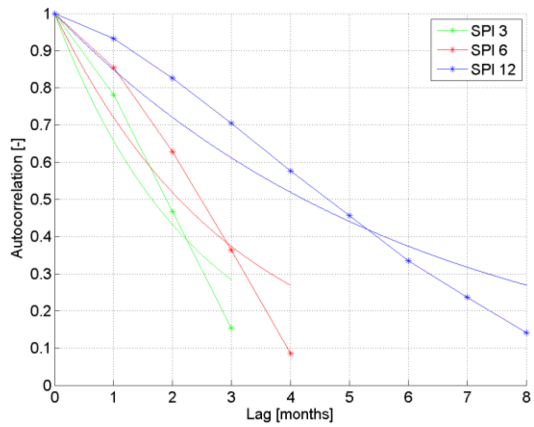

RCM9

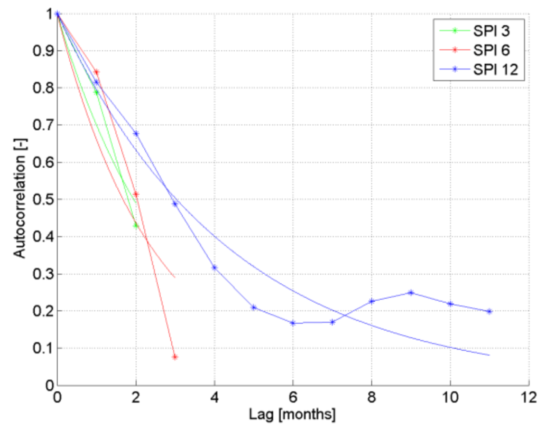

RCM10

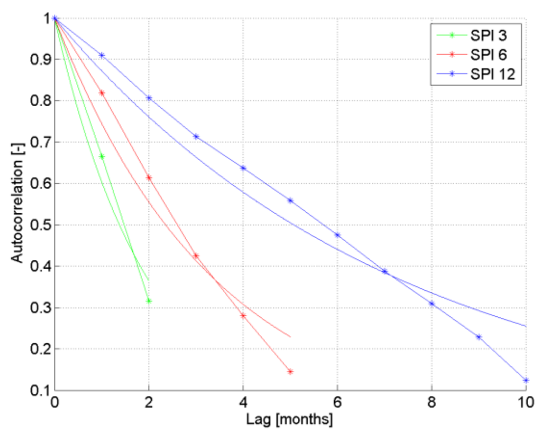

RCM11

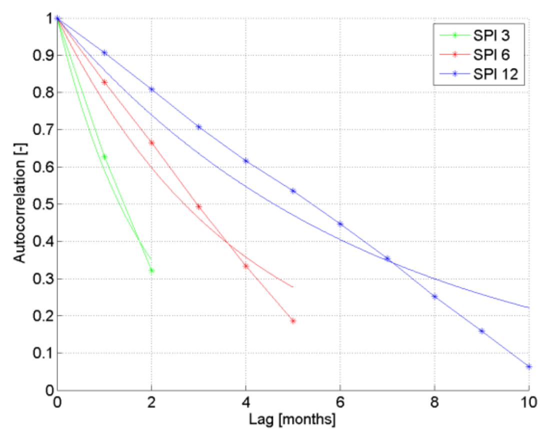

RCM12

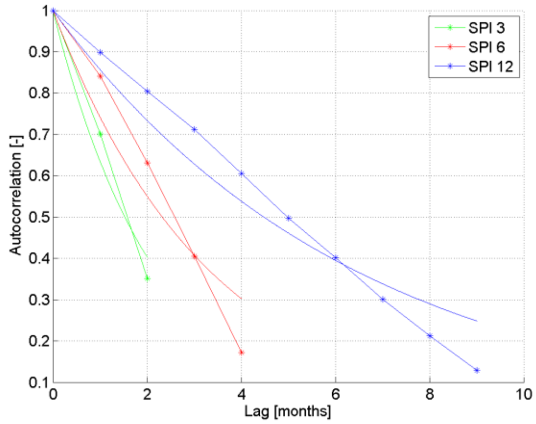

RCM13

Figure C-4 All temporal fits and the data points the fits are based on. (2095)

Spatial correlograms

For each RCM there are four plots. The EOBS spatial fits are presented in chapter 4. Since there are 13 RCMS, three periods and 4 plots for each period, there are 156 correlograms that could be shown. Therefore only the best and worst fits (based on the r^2 value) will be shown, for each period and SPI.

Historical period

SPI-1

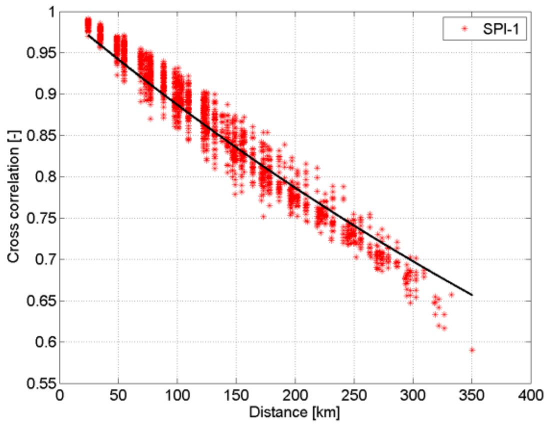

Best RCM-2

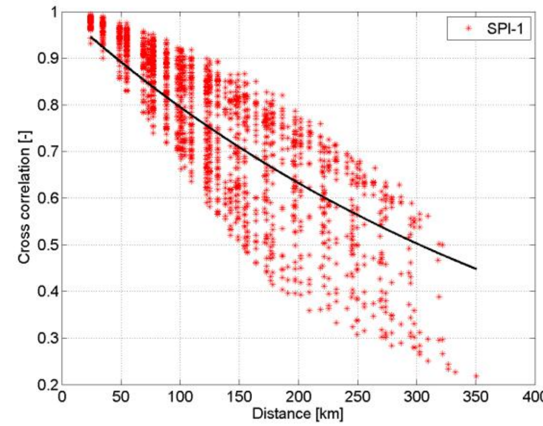

Worst RCM-8

SPI-3

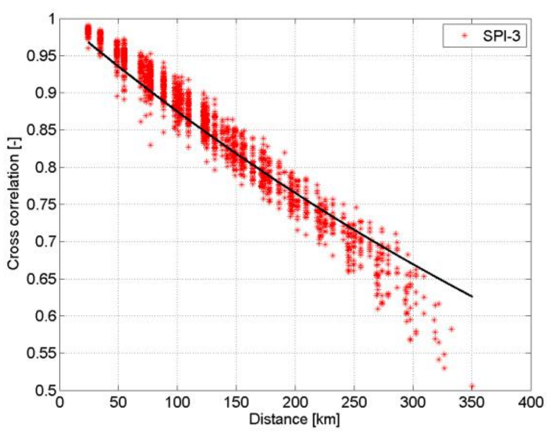

Best RCM-2

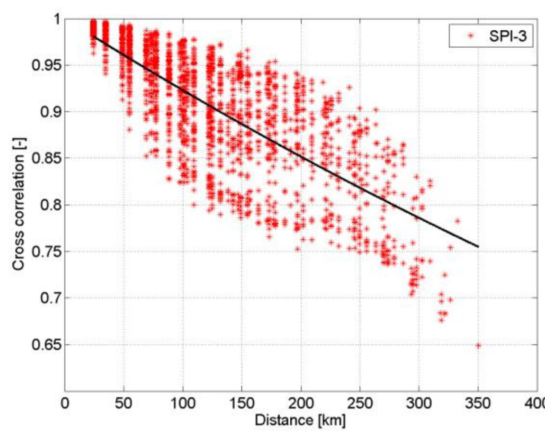

Worst RCM-10

SPI-6

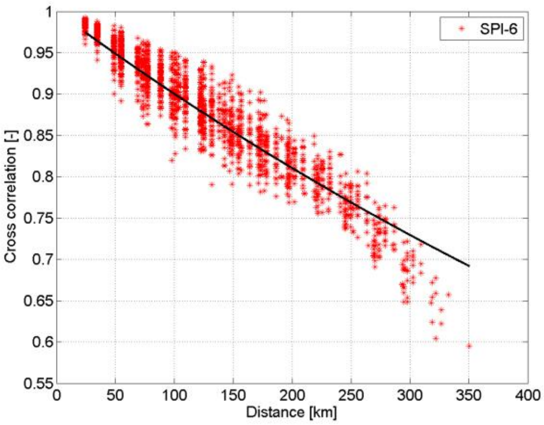

Best RCM-4

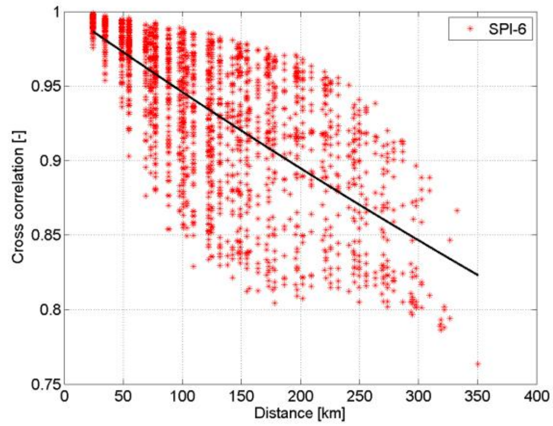

Worst RCM-10

SPI-12

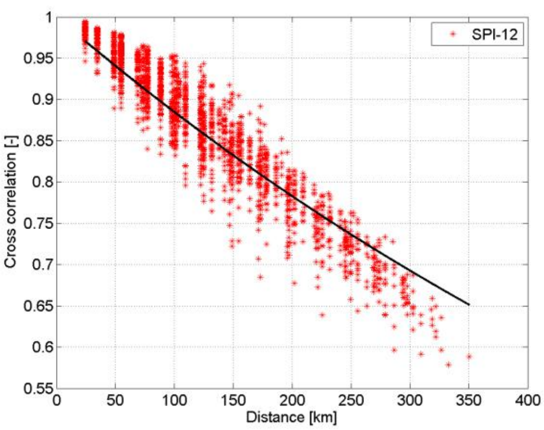

Best RCM-3

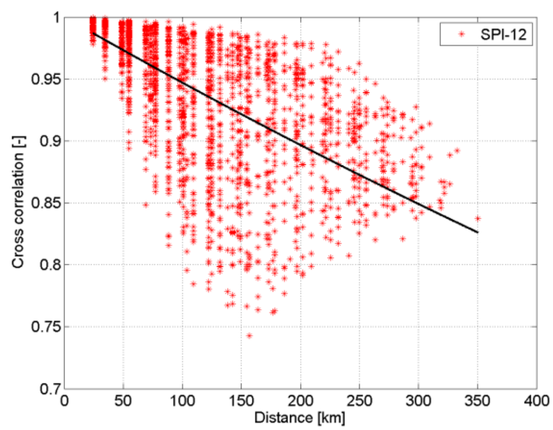

Worst RCM-10

Figure C-5 All best and worst fits (2000)

Future period 2050

SPI-1

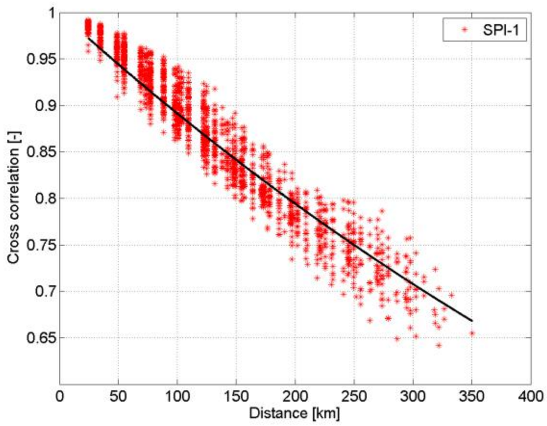

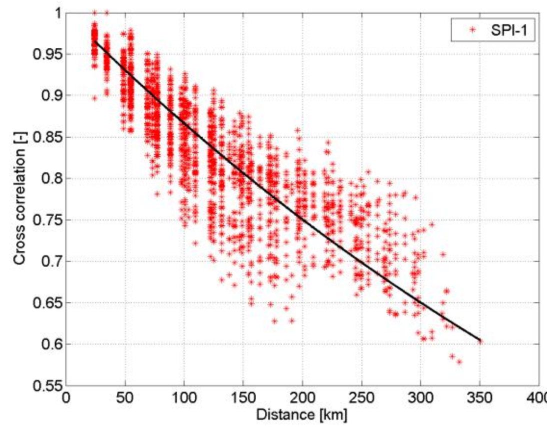

Best RCM-3

Worst RCM-13

SPI-3

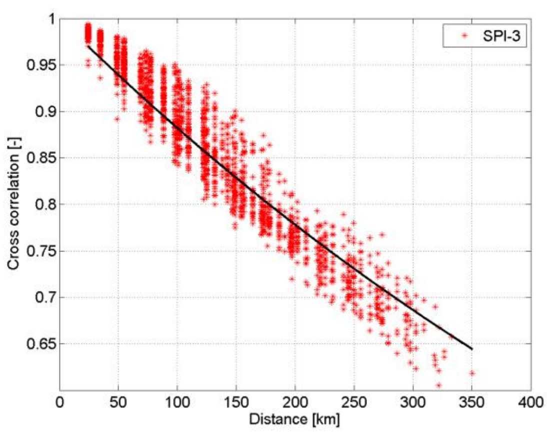

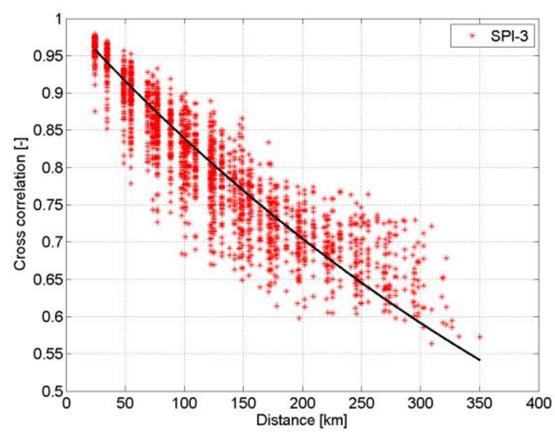

Best RCM-3

Worst RCM-5

SPI-6

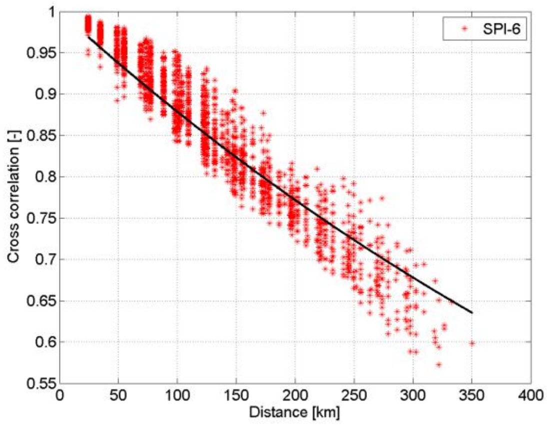

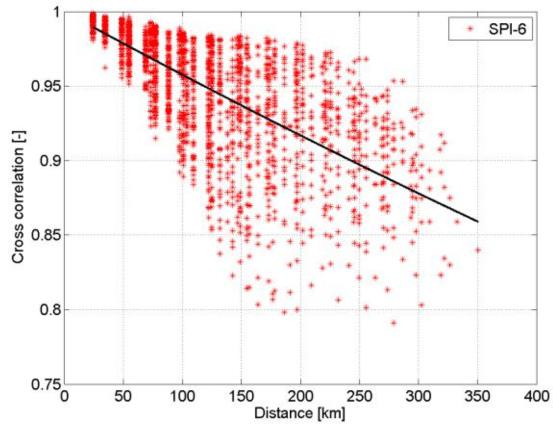

Best RCM-3

Worst RCM-10

SPI-12

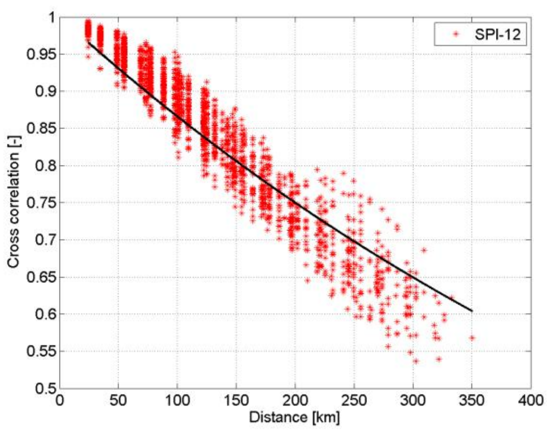

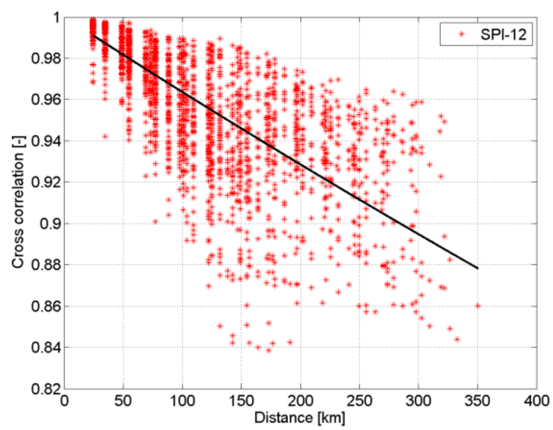

Best RCM-3

Worst RCM-10

Figure C-6 All best and worst fits (2050)

Future period 2095

SPI-1

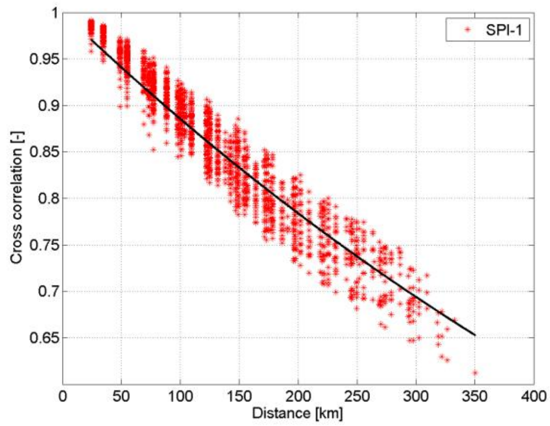

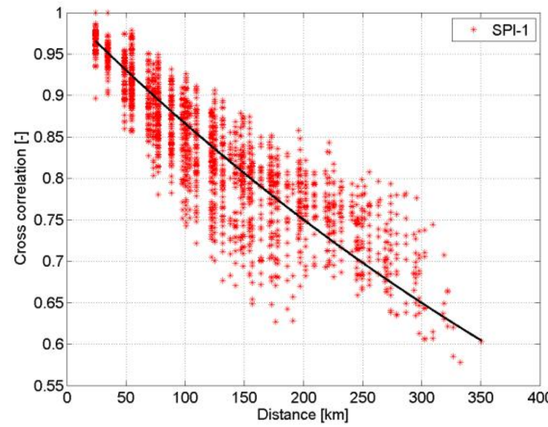

Best RCM-4

Worst RCM-13

SPI-3

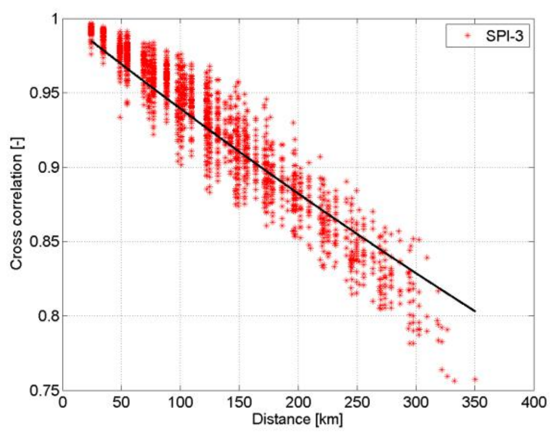

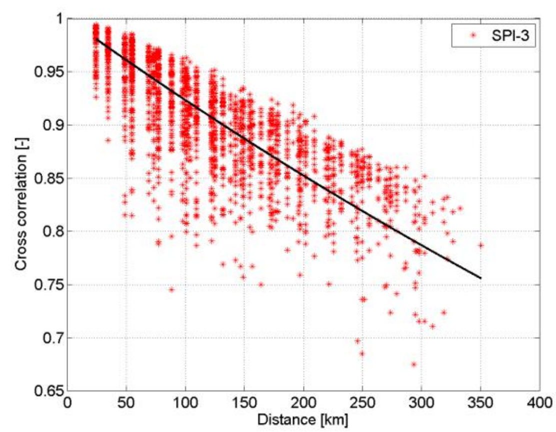

Best RCM-2

Worst RCM-3

SPI-6

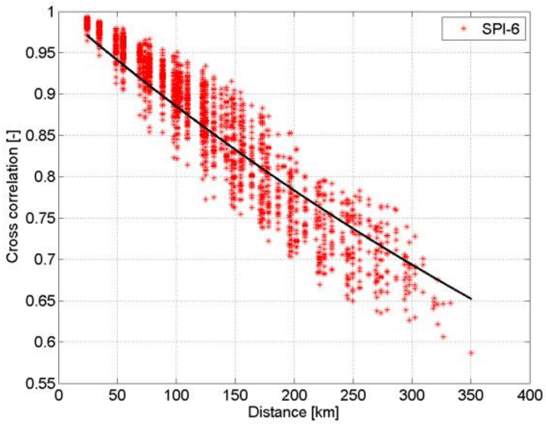

Best RCM-4

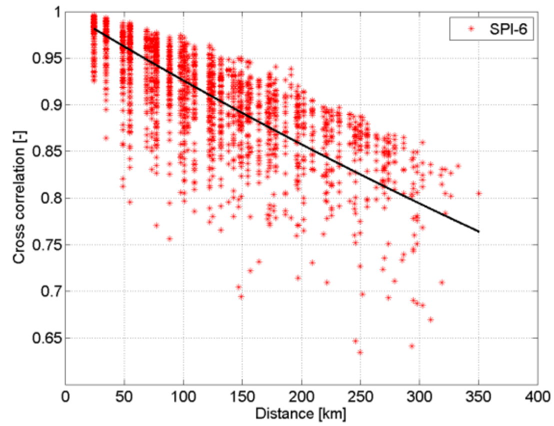

Worst RCM-3

SPI-12

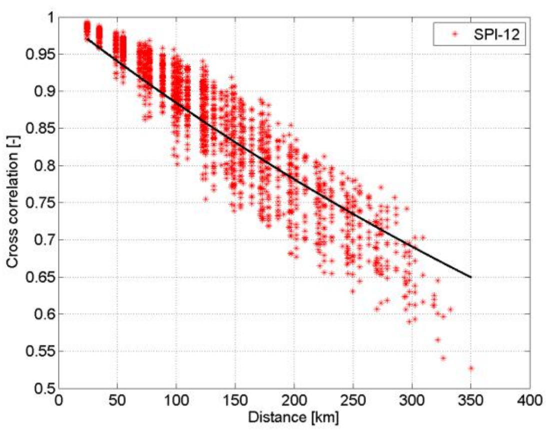

Best RCM-4

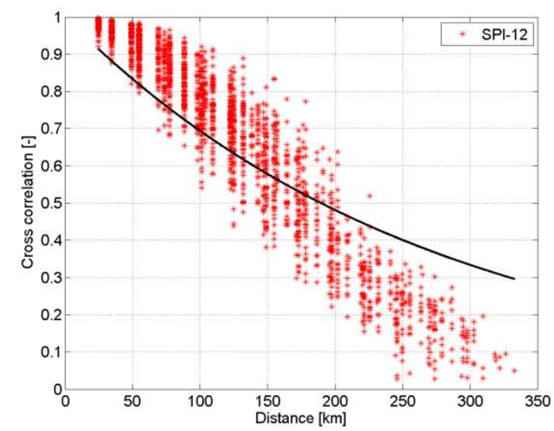

Worst RCM-8

Figure C-7 All best and worst fits (2095)

D. Example deficit-duration error plot

To get a better understanding of the how the relative errors are calculated the following plots are shown. The absolute error for each duration value (only when possible) is calculated and plotted in Figure D-1. The total relative error is plotted in the figure; this value summarizes the plot to one value. This are the values used to assess the RCMs. The table below shows the amount of events outside of the range of the plot (these are events that could not be analyzed). The change is calculated similarly; the mean error (blue line) can however become negative.

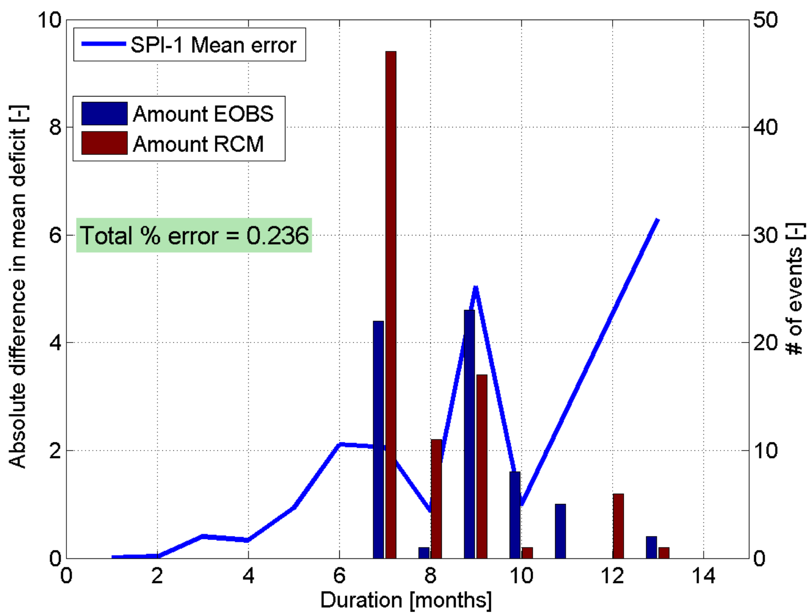

Figure D-1 RCM1 the absolute error (blue line) and for the last duration values the amount of events the absolute error is based on. For example for duration 11 there is no RCM event simulated and thus no absolute error calculated

Table D-1 The drought events out of range of the deficit-duration plots. These events could not be compared with each other since the event had a different duration.

	# drought events above max duration	Mean duration	Mean deficit
E-OBS	0	0	0
RCM	8	14	-18.19

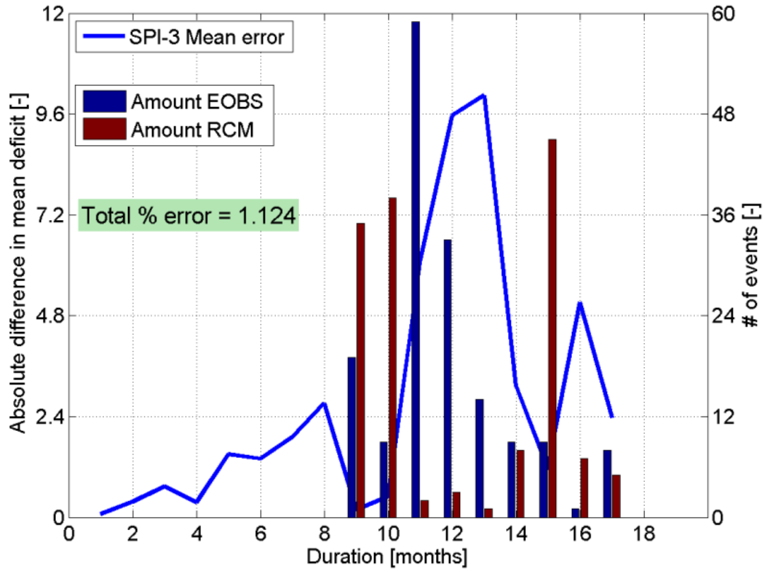

Figure D-2 RCM1 the absolute error (blue line) and for the last duration values the amount of events the absolute error is based on. For example for duration 11 there is no RCM event simulated and thus no absolute error calculated

Table D-2 The drought events out of range of the deficit-duration plots. These events could not be compared with each other since a different duration value.

	# drought events above max duration	Mean duration	Mean deficit
E-OBS	28	22.07	-20.18
RCM	0	0	0

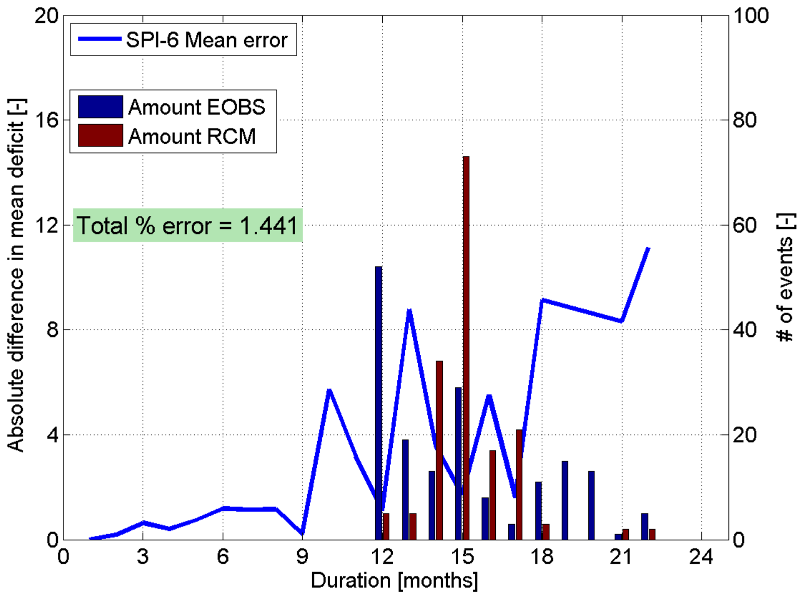

Figure D-3 RCM1 the absolute error (blue line) and for the last duration values the amount of events the absolute error is based on. For example for duration 11 there is no RCM event simulated and thus no absolute error calculated

Table D-3 The drought events out of range of the deficit-duration plots. These events could not be compared with each other since a different duration value.

	# drought events above max duration	Mean duration	Mean deficit
E-OBS	9	48.56	-58.22
RCM	43	27.93	-35.47

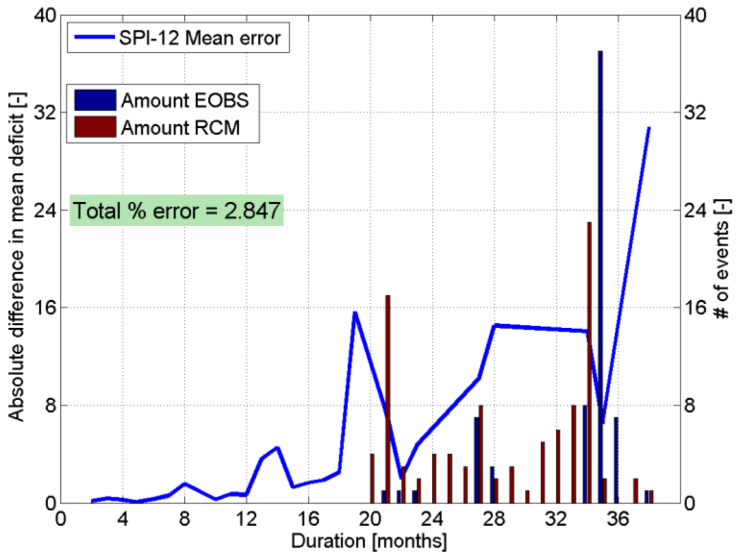

Figure D-4 RCM1 the absolute error (blue line) and for the last duration values the amount of events the absolute error is based on. For example for duration 11 there is no RCM event simulated and thus no absolute error calculated

Table D-4 The drought events out of range of the deficit-duration plots. These events could not be compared with each other since a different duration value.

	# drought events above max duration	Mean duration	Mean deficit
E-OBS	8	88.63	-105.24
RCM	0	0	0

E. All available ENSEMBLES RCM runs

Table E-1 All ENSEMBLES RCMs runs available (http://ensemblesrt3.dmi.dk/extended_table.html)

Institute	Scenario	Driving GCM	Model	Resolution
C4I	A2	ECHAM5	RCA3	25km
CNRM	A1B	ARPEGE	Aladin	25km
	A1B	ARPEGE_RM5.1 New ens.mb. to 2100	Aladin	25km
KNMI	A1B	ECHAM5-r3	RACMO	25km
	A1B	ECHAM5-r1	RACMO	50km
	A1B	ECHAM5-r2	RACMO	50km
	A1B	ECHAM5-r3	RACMO	50km
	A1B	MIROC	RACMO	50km
OURANOS	A1B	CGCM3	CRCM	25km
SMHI	A1B	ECHAM5-r3	RCA	50km
	A1B	BCM	RCA	25km
	A1B	ECHAM5-r3	RCA	25km
	A1B	HadCM3Q3	RCA	25km
MPI	A1B	ECHAM5-r3	REMO	25km
METNO	A1B	BCM	HIRHAM	25km
	A1B	HadCM3Q0	HIRHAM	25km
C4I	A1B	HadCM3Q16	RCA3	25km
UCLM	A1B	HadCM3Q0	PROMES	25km
ETHZ	A1B	HadCM3Q0	CLM	25km
HC	A1B	HadCM3Q0	HadRM3Q0	25km
	A1B	HadCM3Q3	HadRM3Q3	25km
	A1B	HadCM3Q16	HadRM3Q16	25km
DMI	A1B	ARPEGE	HIRHAM	25km
	A1B	ECHAM5-r3	DMI-HIRHAM5	25km
	A1B	BCM	DMI-HIRHAM5	25km
ICTP	A1B	ECHAM5-r3	RegCM	25km
VMGO	A1B	HadCM3Q0	RRCM	25km
GKSS	A1B	IPSL	CLM	25km